



LUND UNIVERSITY

Ischemic QRS Prolongation as a Biomarker of Severe Myocardial Ischemia

Almer, Jakob

2018

Document Version:

Publisher's PDF, also known as Version of record

[Link to publication](#)

Citation for published version (APA):

Almer, J. (2018). *Ischemic QRS Prolongation as a Biomarker of Severe Myocardial Ischemia*. [Doctoral Thesis (compilation), Department of Clinical Sciences, Lund]. Lund University: Faculty of Medicine.

Total number of authors:

1

General rights

Unless other specific re-use rights are stated the following general rights apply:

Copyright and moral rights for the publications made accessible in the public portal are retained by the authors and/or other copyright owners and it is a condition of accessing publications that users recognise and abide by the legal requirements associated with these rights.

- Users may download and print one copy of any publication from the public portal for the purpose of private study or research.
- You may not further distribute the material or use it for any profit-making activity or commercial gain
- You may freely distribute the URL identifying the publication in the public portal

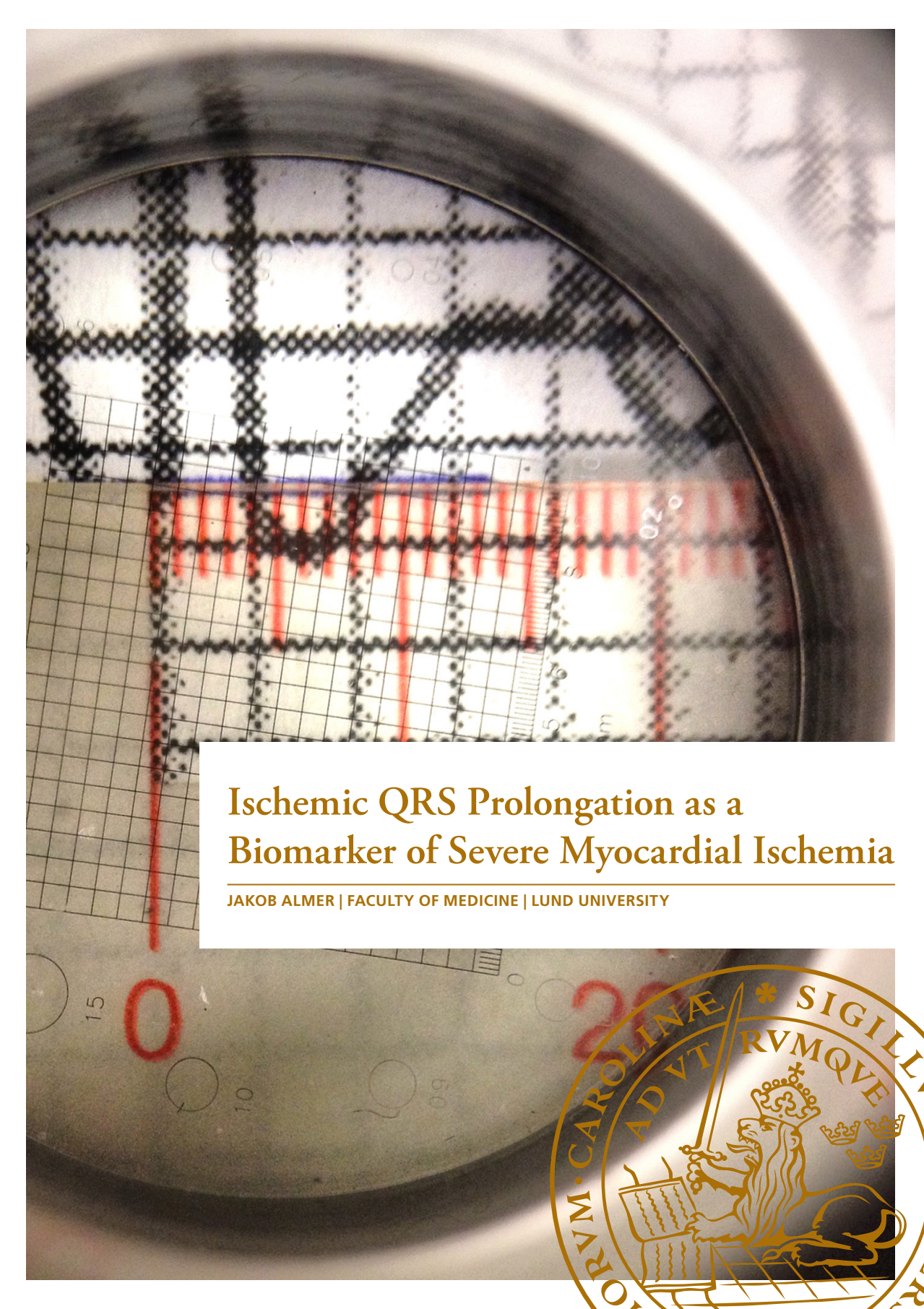
Read more about Creative commons licenses: <https://creativecommons.org/licenses/>

Take down policy

If you believe that this document breaches copyright please contact us providing details, and we will remove access to the work immediately and investigate your claim.

LUND UNIVERSITY

PO Box 117
221 00 Lund
+46 46-222 00 00

The background of the slide is a close-up photograph of an ECG tracing on a circular grid. A red QRS complex is highlighted with a red box. The grid is black and white, with a red vertical line and a red horizontal line intersecting at the QRS complex. The text is overlaid on a white rectangular box in the lower right quadrant.

Ischemic QRS Prolongation as a Biomarker of Severe Myocardial Ischemia

JAKOB ALMER | FACULTY OF MEDICINE | LUND UNIVERSITY



Ischemic QRS Prolongation as a Biomarker of Severe Myocardial Ischemia



Ischemic QRS Prolongation as a Biomarker of Severe Myocardial Ischemia

Jakob Almer



LUND
UNIVERSITY

Thesis for the degree of Doctor of Philosophy
Thesis advisor: Assoc. Prof. Henrik Engblom
Faculty opponent: Assoc. Prof. Ljuba Bacharova

To be presented for public criticism in Föreläsningssal 1, Blocket, Skånes Universitetssjukhus i Lund on
Saturday, 24th of November 2018 at 09:00.

Organization LUND UNIVERSITY	Document name DOCTORAL DISSERTATION	
	Date of issue	
	Sponsoring organization	
Author(s) Jakob Almer		
Title and subtitle Ischemic QRS Prolongation as a Biomarker of Severe Myocardial Ischemia		
<p>Abstract</p> <p>Acute myocardial ischemia, due to an acute coronary occlusion (ACO), and its possible subsequent complications is one of the most common causes of death in the western world. If not treated with removal of the coronary occlusion in a timely manner, the acute myocardial ischemia will develop into an acute myocardial infarction (AMI). Furthermore, malignant arrhythmias, such as ventricular fibrillation (VF), may arise during ischemia or even at reperfusion of the ischemic myocardium, potentially causing a cardiac arrest (CA). Early diagnosis and treatment is, therefore, paramount in this patient group. The predominant method of diagnosing these patients today is by the use of the 12-lead ECG. Acute myocardial ischemia is visualized on the ECG as ST-segment elevation. However, when the myocardial ischemia is more severe, patients may not only have ST-segment changes but can also develop concurrent changes in the QRS complex, termed 'terminal QRS distortion', which has been linked to measures of ischemia severity and poorer outcome. There is, however, no clinically viable method for detecting these changes on the ECG, in order to change patient management and/or treatment, in use today.</p> <p>Paper I 1) introduces a novel method for quantifying terminal QRS distortion, termed ischemic QRS prolongation (IQP), 2) establishes the correlation between IQP and collateral flow during acute ischemia in an experimental dog model and 3) prove that the same pattern of IQP occurs in patients with coronary artery disease (CAD) undergoing prolonged, elective angioplasty balloon inflation.</p> <p>Paper II develops the initial one-lead method of IQP measurement to 12-leads and eliminates the need for a pre-occlusion baseline measurement.</p> <p>Paper III demonstrates that IQP is predictive of impending reperfusion VF in an experimental canine model undergoing coronary occlusion and, thus, acute ischemia.</p> <p>Paper IV compares IQP with measures of myocardial injury by cardiac magnetic resonance imaging (CMR) showing that IQP does not correlate to the amount of myocardial injury in stable first time ST elevation myocardial infarction (STEMI) patients.</p> <p>Paper V shows that IQP, in the context of an acute coronary occlusion and STEMI, is associated with out-of-hospital cardiac arrest (OHCA).</p> <p>In summary, IQP shows promising correlations to ischemia severity and malignant arrhythmias, displaying its potential for identifying of STEMI patients at risk of poor outcome and/or impending CA.</p>		
Key words: Acute coronary occlusion, Ischemia, Acute myocardial infarction, Electrophysiology, Electrocardiography, Arrhythmia, Cardiac arrest		
Classification system and/or index terms (if any):		
Supplementary bibliographical information:		Language
ISSN and key title: 1652-8220		ISBN 978-91-7619-700-4
Recipient's notes	Number of pages 102	Price
	Security classification	

Distribution by (name and address)

I, the undersigned, being the copyright owner of the abstract of the above-mentioned dissertation, hereby grant to all reference sources permission to publish and disseminate the abstract of the above-mentioned dissertation.

Signature _____

Date 2018-10-22 _____

Ischemic QRS Prolongation as a Biomarker of Severe Myocardial Ischemia

Jakob Almer



LUND
UNIVERSITY

Faculty Opponent

Assoc. Prof. Ljuba Bacharova
International Laser Center &
Institute of Pathological Physiology, Comenius University
Bratislava, Slovakia

Evaluation Committee

Prof. Jan Engvall
Linköping University
Linköping, Sweden

Assoc. Prof. Johan Brandt
Lund University
Lund, Sweden

Assoc. Prof. Sandra Lindstedt Ingemansson
Lund University
Lund, Sweden

Cover: Photograph of canine ECG through a loupe. Credit: Jakob Almer

© Jakob Almer 2018

Faculty of Medicine, Department of Clinical Physiology

ISBN: 978-91-7619-700-4 (print)

ISSN: 1652-8220

Printed in Sweden by Media-Tryck, Lund University, Lund 2018



To the love of my life

Veronica

Contents

List of publications	iii
Abstract	v
Populärvetenskaplig sammanfattning	vii
Abbreviations	ix
Acknowledgements	xi
1 Research Context	
1 Introduction	1
1.1 Acute Myocardial Ischemia	2
1.2 Cardiac Electrophysiology	8
1.3 Visualizing Ischemia with ECG	13
2 Aims	29
3 Materials and Methods	31
3.1 Experimental Canine Model	31
3.2 Human Study Populations	32
3.3 Electrocardiography	33
3.4 Magnetic Resonance Imaging	37
3.5 Statistical Methods	38
4 Results and Discussion	41
4.1 IQP and Ischemia Severity	41
4.2 IQP and Malignant Arrhythmias	47
4.3 Clinical Significance	54

5	Conclusions	55
5.1	Compiled Conclusion and Future Directions	56
	References	56

II Research Papers

Author contributions

Paper I: Ischemic QRS prolongation as a biomarker of severe myocardial ischemia

Paper II: A 12-lead ECG-method for quantifying ischemia-induced QRS prolongation to estimate the severity of the acute myocardial event

Paper III: Ischemic QRS prolongation as a predictor of ventricular fibrillation in a canine model

Paper IV: Ischemic QRS prolongation as a biomarker of myocardial injury in STEMI patients

Paper V: Ischemic QRS prolongation associated with out-of-hospital cardiac arrest

List of publications

This thesis is based on the following publications:

- I **Ischemic QRS prolongation as a biomarker of severe myocardial ischemia**
J. Almer, R. B. Jennings, A. C. Maan, M. Ringborn, C. Maynard, O. Pahlm, H. Arheden, G. S. Wagner, H. Engblom
Journal of Electrocardiology, 49(2):139-147 (2016)
- II **A 12-lead ECG-method for quantifying ischemia-induced QRS prolongation to estimate the severity of the acute myocardial event**
V. Elmberg, J. Almer, O. Pahlm, G. S. Wagner, H. Engblom, M. Ringborn
Journal of Electrocardiology, 49(3):272-277 (2016)
- III **Ischemic QRS prolongation as a predictor of ventricular fibrillation in a canine model**
J. Almer, R. B. Jennings, M. Ringborn, H. Engblom
Scandinavian Cardiovascular Journal, 52(6):1-6 (2018)
- IV **Ischemic QRS prolongation as a biomarker of myocardial injury in STEMI patients**
J. Almer, V. Elmberg, J. Bränsvik, D. Nordlund, A. Khoshnood, M. Ringborn, M. Carlsson, U. Ekelund, H. Engblom
Annals of Noninvasive Electrocardiology, 2018;e12601.
- V **Ischemic QRS prolongation associated with out-of-hospital cardiac arrest**
J. Almer, J. Dankiewicz, V. Elmberg, A. Khoshnood, M. Ringborn, U. Ekelund, N. Nielsen, H. Engblom
Submitted manuscript

Abstract

Acute myocardial ischemia, due to an acute coronary occlusion (ACO), and its possible subsequent complications is one of the most common causes of death in the western world. If not treated with removal of the coronary occlusion in a timely manner, the acute myocardial ischemia will develop into an acute myocardial infarction (AMI). Furthermore, malignant arrhythmias, such as ventricular fibrillation (VF), may arise during ischemia or even at reperfusion of the ischemic myocardium, potentially causing a cardiac arrest (CA). Early diagnosis and treatment is, therefore, paramount in this patient group. The predominant method of diagnosing these patients today is by the use of the 12-lead ECG. Acute myocardial ischemia is visualized on the ECG as ST-segment elevation. However, when the myocardial ischemia is more severe, patients may not only have ST-segment changes but can also develop concurrent changes in the QRS complex, termed ‘terminal QRS distortion’, which has been linked to measures of ischemia severity and poorer outcome. There is, however, no clinically viable method for detecting these changes on the ECG, in order to change patient management and/or treatment, in use today.

Paper I 1) introduces a novel method for quantifying terminal QRS distortion, termed ischemic QRS prolongation (IQP), 2) establishes the correlation between IQP and collateral flow during acute ischemia in an experimental dog model and 3) prove that the same pattern of IQP occurs in patients with coronary artery disease (CAD) undergoing prolonged, elective angioplasty balloon inflation.

Paper II develops the initial one-lead method of IQP measurement to 12-leads and eliminates the need for a pre-occlusion baseline measurement.

Paper III demonstrates that IQP is predictive of impending reperfusion VF in an experimental canine model undergoing coronary occlusion and, thus, acute ischemia.

Paper IV compares IQP with measures of myocardial injury by cardiac magnetic resonance imaging (CMR) showing that IQP does not correlate to the amount of myocardial injury in stable first time ST elevation myocardial infarction (STEMI) patients.

Paper V shows that IQP, in the context of an acute coronary occlusion and STEMI, is

associated with out-of-hospital cardiac arrest (OHCA).

In summary, IQP shows promising correlations to ischemia severity and malignant arrhythmias, displaying its potential for identification of STEMI patients at risk of poor outcome and/or impending CA.

Populärvetenskaplig sammanfattning

Akut hjärtinfarkt och kranskärslsjukdom är en av de vanligaste orsakerna till död och sjuklighet i västvärlden idag. En hjärtinfarkt beror oftast på att det, pga. en blodpropp, har blivit stopp i ett av de kärl som försörjer hjärtat med blod (kranskärl). Eftersom blodet försörjer hjärtmuskeln med syre så uppstår det därför en akut syrebrist (ischemi) i det drabbade området om inte blodproppen kan avlägsnas inom rimlig tid. Förutom att syrebristen på sikt leder till att hjärtcellerna dör (hjärtinfarkt) så kan ischemin i sig leda till farliga rytmrubbningar (arytmier) som i sin tur kan orsaka ett hjärtstopp. Även när man tar bort blodproppen och hjärtat återfår tillgång till syrerikt blod kan det uppstå farliga arytmier. Tidig upptäckt och behandling är därför av yttersta vikt i denna patientgrupp. Den huvudsakliga metoden för att diagnostisera dessa patienter idag är med EKG. Vågorna på EKG:et består av P vågen, QRS komplexet och T vågen. Ischemin syns på EKG:et som en höjning av sträckan mellan QRS komplexet och T vågen. Dock så kan en allvarigare ischemi också visa sig som förändringar av QRS komplexet. Denna förändring har i tidigare studier kopplats till allvarlig ischemi och sämre prognos. Trots detta så finns det idag ingen kliniskt användbar metod för att mäta och upptäcka dessa förändringar av QRS komplexet, och därmed styra behandlingen av dessa patienter på ett bättre sätt.

Arbete I 1) introducerar en ny metod för att mäta QRS förvrängningen, kallad 'ischemic QRS prolongation' (IQP; ischemisk QRS förlängning), 2) etablerar kopplingen mellan IQP och allvarlig syrebrist i hundexperiment och 3) bevisar att IQP även uppträder i människor på ett liknande vis.

Arbete II utvecklar den ursprungliga metoden introducerad i arbete I.

Arbete III visar att IQP har en förmåga att förutsäga om hundar får allvarliga rytmrubbningar när de återfår normalt blodflöde efter 15 minuters ischemi.

Arbete IV demonstrerar att IQP inte är kopplat till hjärtskada, mätt med magnetkamera (MR), hos stabila patienter som genomgår en hjärtinfarkt för första gången.

Arbete V visar att ökat IQP är kopplat till hjärtstopp i patienter med akut hjärtinfarkt.

Sammanfattningsvis så visar IQP kopplingar till ischemins allvarlighetsgrad och farliga rytmrubbningar och har därmed potential att identifiera hjärtinfarktspatienter med dålig prognos och som har hög risk att drabbas av ett hjärtstopp.

Abbreviations

ACO	Acute coronary occlusion
aIQP	Absolute ischemic QRS prolongation
AMI	Acute myocardial infarction
AP	Action potential
ATP	Adenosine triphosphate
AUC	Area under the curve
AVN	Atrioventricular node
BBB	Bundle branch block
CA	Cardiac arrest
CABG	Coronary artery bypass grafting
CAD	Coronary artery disease
CI	Confidence interval
CMR	Cardiac magnetic resonance imaging
ECG	Electrocardiogram
ED	End diastole
ES	End systole
ETC	Electron transport chain
IQP	Ischemic QRS prolongation
IS	Infarct size
LAD	Left anterior descending artery
LCX	Left circumflex artery
LGE	Late gadolinium enhancement
LVEF	Left ventricle ejection fraction
MaR	Myocardium at risk
MSI	Myocardial salvage index
NSTEMI	Non ST segment elevation myocardial infarction
OHCA	Out-of-hospital cardiac arrest
OR	Odds ratio
PCI	Percutaneous coronary intervention
QRSd	QRS duration
QRSd _{cg}	Computer generated QRS duration

QRSd_{m,STD}	QRS duration at maximum ST-deviation
QRSd_r	Reference QRS duration
RCA	Right coronary artery
rIQP	Relative ischemic QRS prolongation
ROC	Receiver operating characteristic
ROSC	Return of spontaneous circulation
SAN	Sinoatrial node
SCD	Sudden cardiac death
SOCCER	Supplemental oxygen in catheterized coronary emergency reperfusion
STD	ST-segment deviation
STE	ST-segment elevation
STEMI	ST-segment elevation myocardial infarction
TTM	Target temperature management trial
VF	Ventricular fibrillation
VT	Ventricular tachycardia
WCT	Wilson's central terminal

Acknowledgements

The thesis in your hand would not have been possible without the collaboration and help from a great number of people. Here follow some special considerations:

Veronica, I am forever in your debt, for all the hard work, sacrifices and enormous amount of support that you have given me. This thesis, as romantic as theses are, is dedicated to you and would not have been possible without you by my side.

The late Dr. **Galen S. Wagner** (1939-2016) was very much the instigator to both the current thesis and my entire academic career. During my time working with Galen I experienced some of the most difficult moments in my academic career, however, it was also the most enriching period in my life regarding personal, academic and philosophic development. I feel very fortunate to have had the privilege of undergoing Galen's 'school of research', especially at location in Durham with Galen as mentor, chauffeur and friend. He is missed.

Henrik Engblom, thank you for taking me on as a bachelor, master and PhD student, for guiding me through difficult moments across the globe and editing numerous iterations of manuscripts, thanks for being my supervisor. **Robert Jennings**, you are the one who actually performed the experiments on the canine population over 35 years ago, and half of the thesis would not have any data to support it without you, it has been an absolute pleasure to work with you. **Viktor Elmberg**, thank you for the engagement into IQP and the absolutely essential development of the method, as well as our many skype sessions debating every ECG in detail. Thanks, **Michael Ringborn**, for your support and input. **Josef Bränsvik**, thank you for taking on a really big project for your bachelor degree and joining me on my very first Tesla ride. Thank you, **Ardavan Khoshnood**, for a wonderful job proofreading the thesis, for being the fastest to answer any communications and, mostly, for your kindness and wit. **Ulf Ekelund**, thank you for letting me use the data you worked so hard to collect. **Josef Dankiewicz**, thanks for your support and guidance through the OHCA jungle. I also want to thank **Niklas Nielsen** and the rest of the **TTM-study group** for letting me use your data to achieve the most significant results in the thesis. Thank

you, **David Nordlund**, for your countless hours analyzing CMR data. **Marcus Carlsson**, thank you for your essential feedback and critique, thereby, improving and elevating my work in ways I hadn't thought of. Thank you **Håkan Arheden**, for your discussions, encouragement and strength. Thank you, **Arie C Maan**, for your technical expertise, skype sessions, and being the key-master of the STAFF-III ECG vault. **Olle Pahlm**, thank you for manuscript feedback, spelling and grammar expertise and interesting discussions. **Chuck Maynard**, for your help with statistical methods. Thank you, **Sebastian Bidhult**, for the technical and statistical expertise in paper I. I would also like to send a special thanks to **Per Arvidsson** for always wondering how it's going and his latex expertise. A great thanks to the rest of the **Cardiac MR-group**, fellow PhD-Students, engineers and administrative personnel, in Lund for all your support and feedback. I would also like to highlight the main **funding bodies** behind my research, Hjärt-Lungfonden, the Faculty of Medicine at Lunds University, the Department of Clinical Physiology and Nuclear Medicine at Skåne University Hospital, Region Skåne.

I also want to thank the student group that worked in Galen's office the fall of 2014, **Siri, Roderick, Laura, Thomas and Irene**, for your indispensable company in 'Galen's school of research'. **Robbert Zusterzeel**, thank you for being very nice to a young student embarking on research for the very first time. **Louise Markert**, I will always associate my time in Durham with your hospitality, chilled red wine and car rides, thanks for taking me into your home. **Claire and Benoit Almer** for being the perfect toastmasters as well as phenomenal cousins, thank you for your support, conversations and laughs.

Thank you, **Anna-Karin Thuvesholmen Almer** and **Andreas Almer** for your support and encouragement.

Harry & Viola, you are the joy of my life.

Östraby, 18 October 2018

Part I

Research Context

Chapter 1

Introduction

Based on previous studies, it is known that patients suffering from a presumed heart attack and a certain tombstone-like morphology on their electrocardiogram (ECG) have a worse outcome. In the following chapters the underlying electrophysiology of the heart that produces this pattern in a situation of total coronary occlusion will be discussed, the concept of ischemic QRS prolongation (IQP) will be introduced and its potential role in future healthcare will be explained. First, however, a discussion on the role of cardiovascular disease in today's society.

Acute myocardial infarction (AMI) is the leading cause of death in the western world.^[1] In 2016, 25 700 people suffered from an AMI in Sweden, one- and 28-day mortality was 17% and 25% respectively.^[2] Sometimes an AMI or even its precursor, the acute coronary occlusion (ACO) with subsequent acute myocardial ischemia, will cause a cardiac arrest (CA). When the CA lead to death, it is defined as a sudden cardiac death (SCD). Indeed, 80% of SCDs have disease in their coronary arteries,^[3] which is the precursor to ACO, and 57% had a thrombus, disrupted plaque or both in one or more coronary arteries causing an ACO.^[4] However, if the patient survives the immediate ramifications of a CA outside of a hospital setting it is defined as an out-of-hospital cardiac arrest (OHCA). OHCA is also a leading cause of mortality in the world,^[5, 6] with a very poor prognosis of only 10.5% surviving to hospital discharge in Europe.^[7] An OHCA is caused either by a cardiac or non-cardiac cause,^[8] with a cardiac cause being more frequent.^[9, 10] In an angiographic study, 50% of OHCA survivors were found to have an ACO.^[11] Thus, a very common cause for OHCA seems to be ACO and acute myocardial ischemia with or without AMI. Therefore, there is much to be gained by improving the identification and management of these patients.

1.1 Acute Myocardial Ischemia

Both AMI and the majority of OHcAs are preceded by an ACO, loss of blood flow to the affected myocardium, impaired oxygen delivery and subsequent acute myocardial ischemia. The term ischemia does not indicate or include infarction, however, it will lead to cell death if the myocardium is not reperfused in a timely manner.

1.1.1 Pathophysiology

Atherosclerosis

The pathophysiology of acute myocardial ischemia is multifactorial. However, the basis of an ACO is often atherosclerosis,^[12] and the rupture of a sclerotic plaque. Atherosclerosis is the gradual buildup of plaques in the intima layer of the arterial wall over decades.^[13] Risk factors for atherosclerosis are the following:^[14]

- | | | |
|-----------------------|----------------------|--------------------------|
| a) Diabetes | b) Dyslipidemia | c) Smoking |
| d) Trans fats | e) Abdominal obesity | f) Western pattern diet |
| g) Insulin resistance | h) Hypertension | i) Advanced age |
| j) Male gender | k) Family history | l) Genetic abnormalities |

The process of atherosclerosis is characterized by inflammation in the arterial walls. Lipoproteins are accumulated in the intima of the vessel wall which, when subjected to oxidative stress, induce leukocyte migration. The macrophages are signaled, due to the oxidative stress, to consume the lipoproteins. Thus, over time the macrophages become laden with cholesterol products, particularly LDL within the vessel wall and develop into so called 'foam cells'. As the macrophages die the foam core remains and form the basis of the plaque. Concurrently smooth muscle cells are signaled to migrate from the media layer of the vessel wall to the intima. They stabilize the intima by secreting extracellular matrix forming a fibrous capsule around the lipid core. The core and the fibrous capsule makes up what we call the sclerotic plaque. The strength of the fibrous capsule governs the propensity for the plaque to rupture,^[15] and inflammation can weaken the capsule and destabilize the plaque. When the plaque is weakened by this process it may rupture and trigger the formation of a thrombus in the coronary vessel. This is due to the thrombogenic contents of the plaque, causing platelet activation, initiation of the coagulation cascade, mural thrombus formation, and embolization. Furthermore, this hypercoagulable state can cause a chain reaction and initiate the rupture of other at-risk plaques, causing more than one culprit lesion.^[16]

Thus, the formation of a thrombus due to a ruptured plaque, is the cause of the ACO, in turn leading to obstructed blood flow downstream of the lesion and initiation of the ischemic cascade.^[17]

Cell Respiration

The healthy and normal myocyte is supplied, via a coronary artery and subsequent capillary, with glucose and oxygen (Figure 1.1). At the same time waste products from the metabolism is released into the blood stream and removed from the cell. Glucose is the main energy substrate and is broken down in the cell through glycolysis, in which pyruvate and a small amount of adenosine tri-phosphate (ATP) are produced. ATP is the main energy currency within the cell and is used for an abundant amount of different processes. [18] Pyruvate is in turn metabolized through Kreb's cycle into NADH and additional ATP. [19, 20] However, the main ATP production occurs in the mitochondria through a process known as the mitochondrial electron transport chain (ETC). [21, 22] NADH carries a proton (H^+) which generates a proton gradient over the inner membrane of the mitochondria. To fuel this process oxygen is needed, which helps move the proton against the gradient. The passive movement of protons along the gradient subsequently powers the production of ATP.

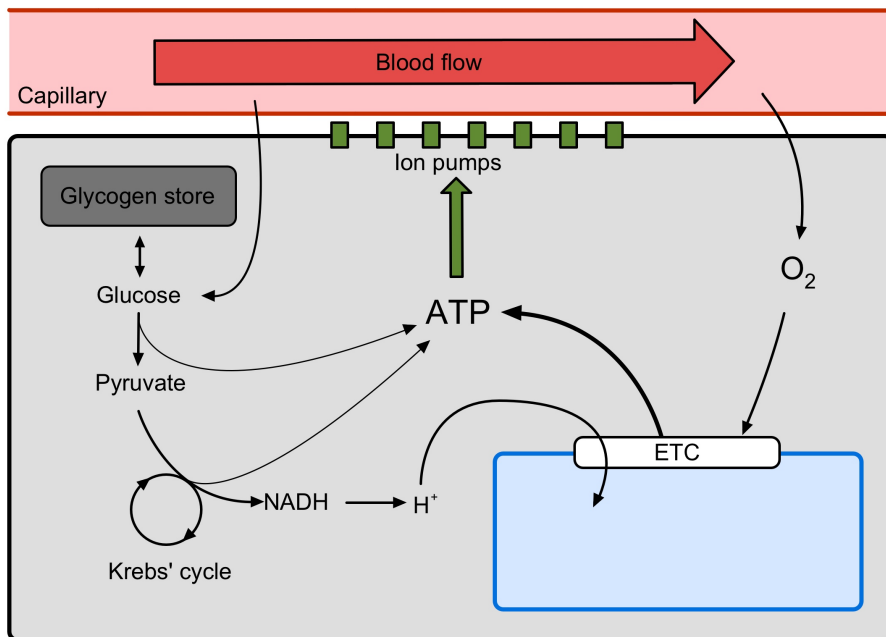


Figure 1.1: Normal cell respiration. Glucose and oxygen is supplied via the bloodstream. Through glycolysis, glucose is broken down into pyruvate and a small amount of adenosine tri-phosphate (ATP). Pyruvate is in turn metabolized through Kreb's cycle into NADH and additional ATP. The main ATP production occurs in the mitochondria through the electron transport chain (ETC). A proton gradient is maintained over the inner membrane of the mitochondria with the use of oxygen. Passive movement of protons along the gradient subsequently powers the production of ATP.

When the supplying artery is closed, due to an ACO, ischemia ensues and suspends the processes discussed above (Figure 1.2). When the oxygen supply dwindles, the ETC is halted and the proton gradient becomes impaired.[23] Thus, the cell quickly switch to anaerobic respiration and relies on glycolysis alone, turning glucose molecules into lactate instead of pyruvate, for ATP production.[24] This causes acidosis within the cell. The glucose supply will also dwindle since it is mainly supplied via the bloodstream, however, the cell does have glycogen reserves which can readily be converted into glucose, although these are finite. Thus, they are depleted quickly and the ATP consumption surpasses the production leading to an immediate energy shortage.[23, 25, 26] Furthermore, protons from NADH are accumulated in the cell since there is no oxygen to uphold the proton gradient in the mitochondria,[27] causing further intracellular acidosis.[28] The cell will try to reverse the acidosis but by doing so destabilize the membrane potential further.[29] Furthermore, as ischemia continues, catabolites are accumulated and as ATP levels fall there is not enough energy to uphold the membrane potential, ultimately signaling the initiation of apoptosis.[24] Membrane potential and effects on ion gradients will be discussed in detail in section 1.2.

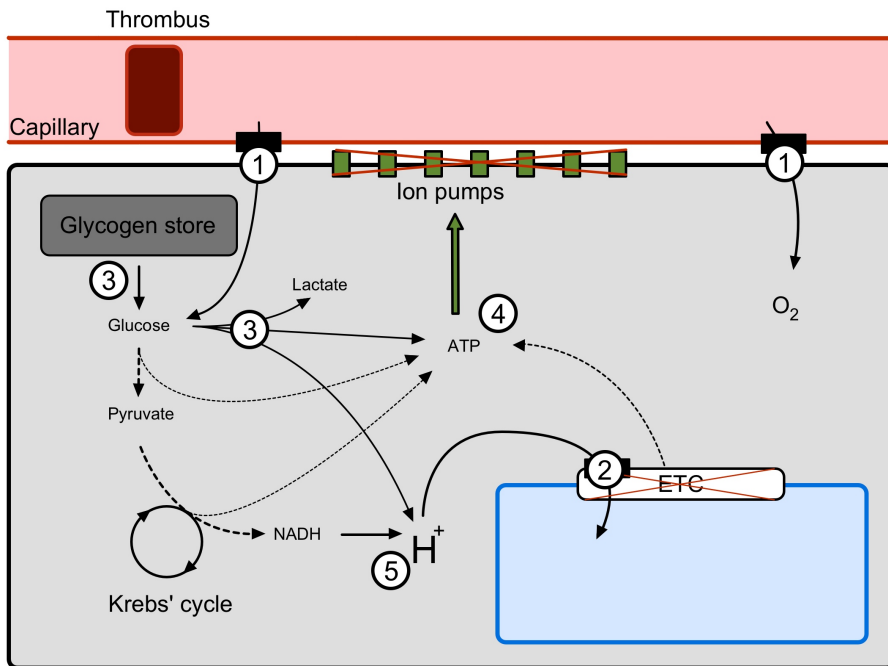


Figure 1.2: Ischemic cell respiration. 1) Due to the occluding thrombus, glucose and oxygen supply is drastically deprived. 2) The ETC is halted and the proton gradient becomes impaired. 3) The cell switch to anaerobic respiration and relies on glycolysis alone, turning glucose molecules into lactate instead of pyruvate, for ATP production. 4) The ATP consumption surpasses the production leading to an immediate energy shortage. 5) The halted processes together lead to a mounting acidosis.

The Ischemic Cascade

The last step of the ischemic cascade is cell death and infarction but, before this terminal fate, several alterations in the myocardium can be observed; diastolic dysfunction, systolic dysfunction, ECG changes and angina pectoris.[17]

Diastolic dysfunction is defined as impaired relaxation of the heart. It is the most energy demanding process and is therefore affected first. During diastole, Ca^{2+} is moved from the intracellular space extracellularly or into the sarcoplasmic reticulum, a process which uses membrane pumps and requires energy (ATP). As described above, during ischemia the myocardial cells goes from aerobic to anaerobic respiration and within 30 seconds there is an imbalance in ATP production and consumption.[26] Therefore, there is a decline in Ca^{2+} moving against the concentration gradient during diastole resulting in an impaired relaxation and also repolarization before the next action potential (AP)(see section 1.2).

Systolic dysfunction follows due to the accumulation of Ca^{2+} intracellularly, thus, becoming acidic and rich in phosphate.[30, 31] This causes decreased regional contractility within a few beats and dyskinesia within 1 minute. since the global contractility is affected negatively, left ventricle (LV) end-diastolic pressure rises and systolic blood pressure drops,[24] affecting cardiac output and stroke volume as well. These hemodynamic affects depend on the severity (subsection 1.1.2) and extent of ischemia.

ECG changes is the third step in the ischemic cascade and will be considered in detail in section 1.3. The accumulation of metabolites eventually causes angina pectoris,[32] but this usually is the last sign of ischemia before irreversible cell injury. The patient can experience chest pain, with possible radiation to arms, neck, jaw, shoulder or back. The heart is innervated diffusely and merge with nerves from the respective pain areas causing the pain radiation.

The ultimate step in the ischemic cascade, as mentioned above, is irreversible cell injury (cell death) and, thus, AMI. If ischemia is allowed to persist the infarction will spread in a wavefront manner from endo- to epicardium.[33] Finally, the infarct will become transmural (covering the full thickness of the ventricle wall) and no ischemic cells remain. Thus, the duration of ischemia is paramount for patient prognosis.

AMI Classification

Although the thesis does not consider AMI in detail but rather the precursor, acute myocardial ischemia, it is of value to describe the different sub classifications of AMI. The main classification is that of occurrence of an ST-segment elevation (STE) on the presenting ECG or not (The pathophysiology and electrophysiology of the ECG and ST-segment will be covered in section 1.3):

- **ST-segment elevation myocardial infarction (STEMI)**. An elevated ST-segment signifies, predominantly, transmural ischemia due to an ACO. The STEMI term is

therefore contradictory since, in large proportion of STEMI cases, the myocardium has not actually infarcted yet. The recommended therapy is, therefore, immediate reperfusion of the ischemic region in order to minimize the myocardial injury.[34]

- **Non ST-segment elevation myocardial infarction (NSTEMI).** NSTEMI is defined as ischemia and infarction without STE. Clinical evaluation, anamnesis and chemical markers of myocardial cell death are used to differentiate NSTEMI from other cardiac and non-cardiac diseases.[35]

1.1.2 Severity of Ischemia and Collateral Flow

During myocardial ischemia the affected myocardial cells are deprived of oxygen and glucose (as discussed above). However, it is not an immediate cessation of supply, thus, the rate at which the ischemic area develops into infarction varies.[36] This window of time, from ACO to necrosis and, thus, infarction, depends on several factors and ranges from 2-6 h.[37] Furthermore, Hedström *et al.* reports a mean time of 290 minutes from pain onset to 50% infarction of the myocardial region at-risk.[38] This multifactorial rate variation of the infarct evolution is compundly termed the ‘severity of ischemia’. Factors affecting the severity of ischemia include; presence of collaterals,[39] artery spasm with intermittent occlusion, the sensitivity of the myocytes to ischemia, pre-conditioning,[40] and individual demand for oxygen and nutrients.[41, 42]

Measuring the severity of ischemia is challenging. One surrogate is the quantification of collateral arterial flow, which is closely related to the time course of irreversible myocyte injury.[24, 43] Collateral arterial flow can be measured by radioactive substances,[44] but also indirectly assessed by cardiac magnetic resonance imaging (CMR) and angiography.[45] It has been correlated to infarction size, left ventricular function, mortality and the amount of at-risk myocardium that does not infarct on CMR.[38, 46, 47]

Collaterals are vessels that interconnect the main coronary arteries, and in case of an ACO, partly supplies the ischemic myocardium with blood and oxygen apart from the culprit vessel.[48] However, collaterals are normally only able to allocate less then 10% of the normal blood flow in case of an ACO,[24] and are non-functioning otherwise.[49] Pre-conditioning, ischemic heart disease (IHD) and coronary artery disease (CAD) promotes arteriogenesis due to mild repeated hypoxia over a long period of time in the affected area, opening up the unused collaterals.[49] Thus, patients with recruitable collaterals have a lower cardiovascular event rate and improved survival.[43] In fact, a collateral flow of 30% of the resting flow value can protect and prevent infarction in patients with ischemia for longer than 1 hour.[50]

Patients without or with only a restricted amount of collaterals, therefore, tend to suffer from more severe ischemia, have a faster infarct rate and move through the ischemic cascade quicker.

1.1.3 Therapy

The aim of therapy in ACO and acute myocardial ischemia is to restore blood flow to the ischemic myocardium through fast reperfusion and is the absolute recommended therapy, in both the US and Europe.[51–53] Furthermore, faster reperfusion correlates to smaller infarct size and lower mortality.[54] There are two fundamentally different methods of achieving reperfusion; mechanical (percutaneous coronary intervention [PCI] and coronary artery bypass grafting [CABG]) and pharmacological (fibrinolysis).

PCI

Current guidelines for treatment of STEMI recommend primary PCI as therapy if a PCI center is available, and the intervention can be completed within 120 min from first medical contact.[42, 51–53, 55–60] During PCI the affected coronary artery is, usually, accessed from the radial or femoral artery through catheterization and visualized using real-time x-ray imaging (angiography). Coronary angioplasty is performed to open up the occluded artery via inflation of a balloon catheter at the stenosis, often with the insertion of a stent in order to keep the artery open. Stent placement is preferred over balloon angioplasty alone as it decreases target vessel revascularization and subsequent myocardial infarction.[61, 62] Progressive delay between pain onset and PCI increase in-hospital and long-term mortality and a 30-minute delay in treatment increases risk ratio (RR) of 1-year mortality by 8%.[51, 63]

CABG

The CABG procedure consists of opening up the chest cavity, accessing the heart and grafting veins, extracted from the patient's own shank, bypassing the occluded or stenotic part of the culprit artery(ies). It should be noted that the procedure is a major surgery with potentially serious complications attached to it. CABG is preferred over PCI in patients with multi-vessel disease. However, in an acute setting, angiography with or without PCI is usually performed for diagnostic purposes and to alleviate the immediate coronary occlusion causing symptoms. Thus, although primary PCI is the standard revascularization technique for STEMI patients, CABG could benefit those who do not respond to PCI.[53] In NSTEMI patients, however, CABG is a more common occurrence due to, foremost, multivessel disease.[64, 65]

Fibrinolysis

Fibrinolysis is an alternative treatment therapy to PCI or CABG aimed at dissolving the thrombus pharmacologically. Thrombolytics induce the conversion of plasminogen to plasmin which lyse the fibrin and dissolves the thrombus,[66, 67] resulting in a reduced mortality by 29% compared to placebo.[68, 69] However, it has been shown that PCI is preferable over fibrinolysis in the acute stage (<120 min from medical contact),[59, 70] which reduces

short-term major adverse cardiac and cerebrovascular events (8% vs 14%; $p < 0.0001$). [71] Furthermore, fibrinolysis is only 33–60% successful in restoring arterial flow in STEMI patients. [69] In more than 50% with persistent STE after fibrinolysis rescue PCI is necessary due to complications and uncomplete reperfusion. [51, 53] However, the treatment has a purpose in situations in which intervention within the 120 min time limit is difficult or impossible to achieve. In this situation, Liu *et al.* shows that PCI after fibrinolysis show similar results to primary PCI and is better compared to late PCI (>120 min from first medical contact). [56] Furthermore, Renard *et al.* showed in an retrospective study that OHCA patients treated with fibrinolysis in ambulance had a higher chance of arriving at hospital alive. [72] OHCA (as discussed above) is often due to severe myocardial ischemia, which have poorer outcome compared to stable STEMI patients. [8]

1.2 Cardiac Electrophysiology

The normal electrophysiology of the myocardium including the membrane potential, the action potential (AP) and the cardiac conduction system followed by the changes that occurs during acute myocardial ischemia will be described.

1.2.1 The Membrane Potential

Every single eukaryotic cell have a cell membrane and across it an electric potential of -40 to -90 mV. [73] This electrical charge is paramount for cell survival and function. The membrane potential is maintained by ion channel pumps, fueled by ATP, moving ions across the membrane against their concentration gradient. The membrane potential of ventricular cells is around -90 mV. The main ions involved in the maintenance of the membrane potential are sodium (Na^+), chloride (Cl^-), calcium (Ca^{2+}) and potassium (K^+). [74] Concentration of Na^+ , Cl^- and Ca^{2+} are higher extracellularly while K^+ concentration is higher intracellularly. [74] Examples of ion channel pumps are the Na-K pump which move three Na^+ out of the cell for two K^+ into the cell and the Na-Ca exchanger which removes one Ca^{2+} from the cell for three Na^+ . [75] Potassium can travel freely over the membrane through diffusion and the resulting equilibrium determines the resting potential. [76]

Myocardial cells are electrically excitable and use the membrane potential for transmitting signals between different parts of the cell. The signal is transmitted via local changes in the membrane potential spreading to adjacent or more distant parts of the membrane which in turn activates distant ion channels to the source. Thus, reproducing the signal. Furthermore, all myocardial muscle cells are linked by gap junctions, which allows the electric charge to propagate from one cell to the next, [77] forming a network across all myocytes that is particularly important for the electric propagation in the heart and cardiac pump functionality.

1.2.2 The Action Potential

An AP causes a total cell depolarization where the membrane potential changes its polarity from negative (-90 mV) to positive (50 mV). Certain voltage gated ion channels, when activated, induces the AP, which spreads throughout the cell. [78] It is the AP that propagates the electrical activation of the heart leading to myocardial contraction. APs vary within the heart due to the varying setups of ion channels. An AP in a cardiac muscle cell go through the following cycle (Figure 1.3):

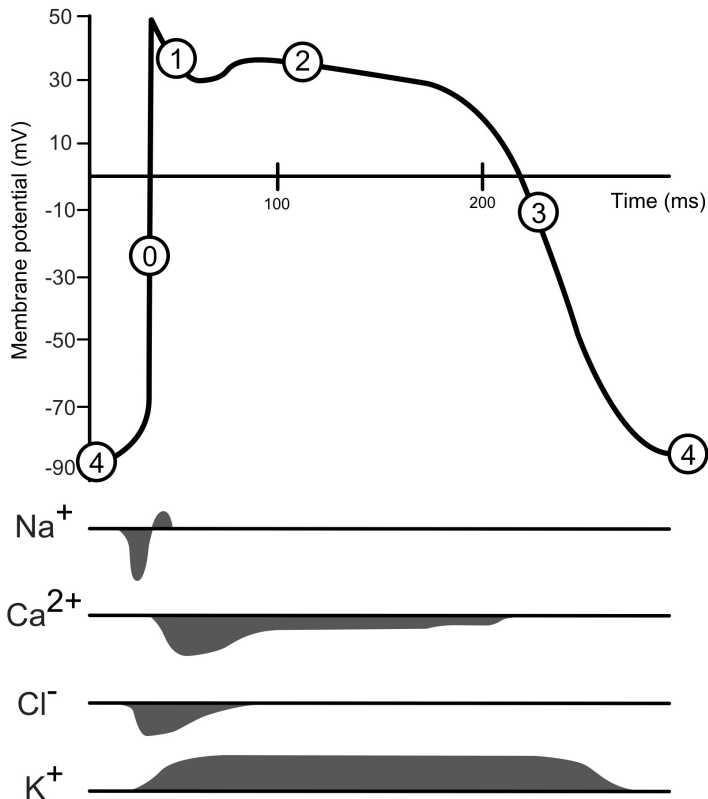


Figure 1.3: Action potential (AP) of a myocardial muscle cell. The numbers indicate the AP phases on the waveform. Below, the main ion movement is shown. A positive deflection from the line indicates efflux while a negative deflection signifies influx.

Phase 4

Phase 4 is the resting phase between APs when the potential of the membrane is roughly -90 mV. [74] As described above, the resting potential depends on the ion gradients over

the cell membrane which is upheld by ion pumps and channels.

Phase 0

The AP begins with a rapid influx, along the gradient, of mainly Na^+ ions through voltage gated channels in the cell membrane. The channels are activated by an AP arriving from a neighboring cell through gap junctions. The neighboring AP raises the membrane potential near the gap junctions above the threshold potential (about -70 mV) which causes the Na^+ -channels to open. The AP spreads across the cell and causes the immediate (in less than 2 ms) depolarization and reversed polarity of the entire membrane potential, reaching a potential of about 50 mV.[79]

Phase 1

During phase 1 the voltage gated Na^+ channels inactivate, due to the new positive membrane potential, trapping sodium inside the cell, thus, reversing its concentration gradient. Concurrently other channels open allowing a limited amount of sodium to leave the cell, along its new gradient, resulting in a net loss of positive ions intracellularly, which results in the notch of the AP (Figure 1.3).[74]

Phase 2

Phase 2 is known as the plateau phase. The membrane potential remains constant due to the balanced ion movements across the membrane. K^+ move extracellularly since there is a deficit of positive ions there, while Ca^{2+} flow in (along its gradient) through L-type channels activated by the sodium influx. The calcium performs positive feedback and opens additional calcium channels in the sarcoplasmic reticulum increasing the calcium concentration further intracellularly.[80] The increase in Ca^{2+} concentration activates the contraction of the myocyte. Furthermore, it opens channels for Cl^- influx. The net charge difference of these ion movements is close to neutral and the membrane potential remains constant.[76]

Phase 3

Phase 3 is the repolarization phase. Calcium channels close while potassium channels remain open. Thus, the net flow is of positive ions out of the cell, lowering the membrane potential, in turn opening more K^+ channels. These channels stand for the majority of the repolarization and the potassium channels does not close until a membrane potential of -85 mV to -90 mV is achieved. Concurrently, the Na-K pump and the Na-Ca exchanger restore the pre-AP steady state. The calcium is, thus, removed from the intracellular space and contraction stops. Then, L-type calcium channels close at the end of phase 3.

1.2.3 The Electrical Conduction System of the Heart

The conduction system of the heart consists of and propagate the electrical activation signal (AP) in the following order; the sinoatrial node (SAN), the atria, the atrioventricular node (AVN), His bundle, the right and left bundle branch, the purkinje fibers and the ventricle myocytes (Figure 1.4). [78] All these structures, except the myocytes of the both atria and ventricles, are made up of so called pacemaker cells. A pacemaker cell will spontaneously generate an AP at given intervals if not prematurely activated from an external AP, compared to the myocardial muscle cells which simply conduct the AP. Based on their setup and variety of ion channels these different pacemaker cells have each a different AP waveform morphology and frequency. The SAN produce the highest amount of APs per minute (60-100), which propagates through the electrical conduction system, activating the other pacemaker cells prematurely of their own frequency. Thus, the resulting heart rate is that of the SAN in a healthy heart.

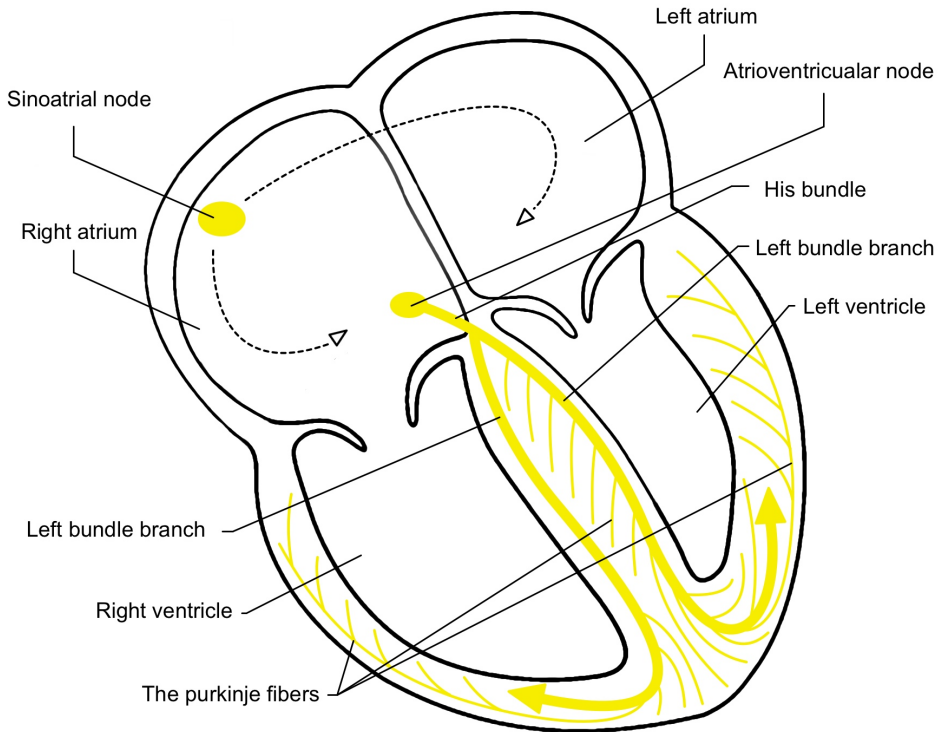


Figure 1.4: The electrical conduction system of the heart. The electrical signal transmits through step by step activation of the different structures, starting with the sinoatrial node (the pacemaker) then activating the atria, the atrioventricular node, His bundle, the right and left bundle branch, the purkinje fibers, the septum and finally the ventricle myocytes.

The AP of a pacemaker cell is different from a ventricle myocyte and its cycle is described below (Figure 1.5):

Phase 4

The resting phase is what sets the pacemaker cells apart since a pacemaker cells membrane potential is never static. During phase 4 the membrane potential of pacemaker cells (known as the pacemaker potential) gradually becomes more positive until it reaches the threshold potential (around -40 mV), initiating the firing of an AP.[78] The channels thought to be behind the pacemaker potential are called hyperpolarisation-activated cyclic nucleotide-gated channels,[81] which open at negative voltages and allow potassium and sodium ions into the cell. This flow of ions is referred to as the funny current.[82] Another hypothesis for the pacemaker potential is the so called 'calcium clock'. Calcium is thought to leak from the SR, activating the sodium/calcium exchanger, causing a slow net raise of the positively charged ions intracellularly.[83]

Phase 0

In contrast to the myocardial muscle cells, which relies on fast sodium channels for the main AP spike, pacemaker cells have voltage gated calcium channels. These channels are activated by the pacemaker potential reaching the threshold value (phase 4). The Ca^{2+} channels are slower than the Na^+ channels and, therefore, the depolarization spike has a flatter upslope.[74] The depolarization spike has its peak at about 10 mV.

Phase 1 & 2

There is no apparent phase 1 and 2 in pacemaker cells.

Phase 3

As in myocardial muscle cells, phase 3 is the repolarization phase and encompasses the closure of calcium channels and opening of voltage gated L-type potassium leak channels.[84] Concurrently sodium permeability into the cell decreases. These ion flows, together with the ongoing processes of the Na-Ca exchanger and Na-K pump, cause a slow repolarization to the second (negative) peak in membrane potential of -60 mV. At the end of phase 3 the voltage gated calcium channels close and phase 4 ensues.

Thus, the ion channel and pump setup of the different pacemaker cells is what determines the rate at which the pacemaker potential depolarizes and, thereby, the frequency of the APs. As noted earlier, the SAN has the highest frequency of about 60-100 Hz, AVN 40-60 Hz and the purkinje fibers 20-40 Hz.

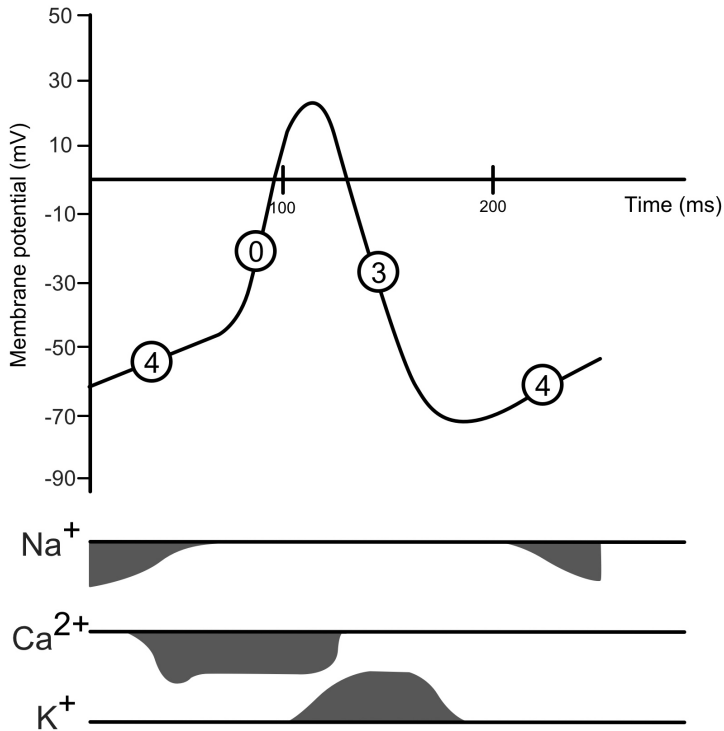


Figure 1.5: Action potential (AP) of a myocardial muscle cell. The numbers indicate the AP phases on the waveform. Below, the main ion movement is shown. A positive deflection from the line indicates efflux while a negative deflection signifies influx.

1.3 Visualizing Ischemia with ECG

The standard 12-lead ECG is still the most common cardiac diagnostic examination used today due to several reasons. [85] Foremost, it is very inexpensive and only takes a few seconds for the actual recording. It is also widely available in almost all parts of the world and, lastly, there is a strong collective experience within the medical field of interpreting the ECG waveforms.

1.3.1 A Brief History of the ECG

The first practical electrocardiograph was invented in 1902 in Leiden, the Netherlands, by Willem Einthoven. [86] It was a string galvanometer, an improvement over the original galvanometer invented by Clément Ader, a French engineer, in 1897. [87] Einthoven's version was capable of detecting very weak currents. There are, however, precursors leading up to Einthoven's invention. In 1878 John Burden Sanderson recorded electrical currents

in a frog heart, [88] and in 1887 Augustus Waller recorded the first human ECG with a Lippmann capillary electrometer which produced a trace of the heartbeat in real time. [89] However, in 1895 Einthoven assigned the letters P, Q, R, S and T to the theoretical waveforms created by equations from Waller's capillary electrometer. [90, 91] When the more precise waveforms were obtained from his own string galvanometer in 1902 the letters were kept and are still in use today. The initial ECGs used only limb electrodes and leads. In 1906 Einthoven published his first report on normal and pathologic ECG recordings including premature beats, atrial flutter, and AV block among others. [92] Einthoven continued to describe the ECG features of a number of cardiovascular disorders and received the Nobel prize in 1924 for his work and discovery. [93]

In 1920 the first ECG in a patient with acute myocardial ischemia was recorded and published by Harold Pardee. [94]

In 1927, General Electric developed a portable device without the use of the string galvanometer, but rather internals from a radio.

In 1934, the Wilson central terminal (WCT) was first described by Wilson and coworkers. [95] The WCT is essential for the recording of leads V_1 - V_6 and is described in detail below. In short, the WCT is a compound of the recordings from the limb leads, providing a negative pole or electrode to the chest electrodes. The leads were given the prefix V due to the voltage recorded at the positive electrode. A standardization of leads V_1 - V_6 was published in 1938 and describes the placement of the electrodes on the chest. [96]

With the WCT three other new leads were also introduced, VR, VL and VF, with the WCT as negative pole and the right arm, left arm and left foot electrode as positives. However, in 1942 Emanuel Goldberger proposed an improvements on the new leads called the augmented leads; aVR, aVL and aVF (explained in detail below), which had higher amplitude than the previous versions. [97]

1.3.2 Theory

Cardiac Electric Field Generation

The depolarization of the heart moves as a wavefront through the atria, AVN, His bundle, bundle branches, purkinje fibers, septum and the ventricles, conducting, propagating and initiating an AP in each cell. During depolarization the cells gain a reversed polarity (described above) and will be net positive. As the AP spreads, across the mentioned structures but especially the myocardial muscle cells (the ventricles), it forms an activation wavefront. The activated depolarized cells will be positively charged while the distal cells, which have not been activated yet, retains its negative charge. This difference in charge across the wavefront generates an electric field. [98] The electric field can be represented by the cardiac vector with a certain direction and magnitude in every instant that changes continuously as the wavefront propagates (Figure 1.6).

Since, all myocardial muscle cells have similar duration of depolarization, the repolarization wavefront will start with the cells that depolarized first and travel in the same

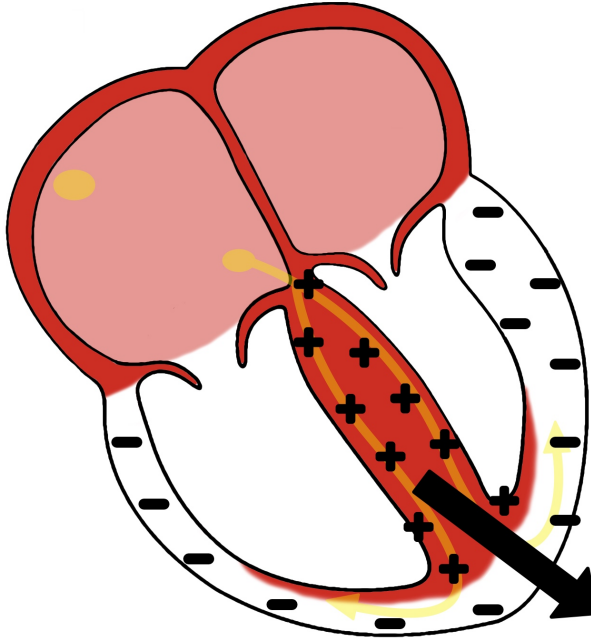


Figure 1.6: As the activation wavefront spreads through the heart the gradient between the depolarized and repolarized cells forms an electrical field which can be summarized with the cardiac vector.

direction. However, during repolarization the myocytes go from a positive membrane potential to a negative, reverse the situation of activation. Thus, the direction of the current flow and the electrical field will be the opposite compared to depolarization. Also, in contrast to depolarization, which transpires during less than 2 ms, repolarization and recovery to a resting membrane potential takes 100 ms or longer. [98]

Electrodes and Leads

An electrode is a conductive pad that is placed on the body surface of the subject. A lead, on the other hand, is a measurement of the difference in potential, in one direction of the cardiac electric field vector, between two electrodes. The direction in which the vector is measured in is the physical direction between the two electrodes on the body. The magnitude of the vector is the difference in potential between the two electrodes and is measured in mV. One electrode is designated positive and the other negative. The negative electrode potential is subtracted from the positive yielding the bipolar potential. [98] The bipolar potential depends on the size of the vector (and, thus, the activation wavefront), on the angle between the direction of the vector and a line drawn from the site of activation to the recording site, and the distance from activation front to the recording site. A vector

pointing directly towards the positive electrode will result in maximal voltage sensed while a vector pointing directly perpendicular to the positive electrode will result in a voltage of zero.

In order to get a “complete” picture of the cardiac vector, we have, 3 limb leads, 3 augmented leads and 6 precordial leads (described in detail below). These, in total, 12 leads measure the vector in 12 different directions. The 12-lead ECG, however, only use 10 electrodes, 4 on the extremities and 6 placed on the chest.[99] A modern ECG machine makes these measurements up to 2000 times per second, which in turn is plotted on paper with mV on the y-axis and ms on the x-axis, making up the well-known ECG waveforms.

Limb Leads

The limb leads consists of lead I, II and III (Figure 1.7). The name comes from the electrode positions on the distal part of the arms and the left leg.

- Lead I is the potential between the (positive) left arm (LA) electrode and right arm (RA) electrode.
- Lead II is the potential between the (positive) left leg (LL) electrode and the right arm (RA) electrode.
- Lead III is the potential between the (positive) left leg (LL) electrode and the left arm (LA) electrode.

The three limb leads form a triangle, called the Einthoven’s triangle, in the frontal plane and will measure the electric field vector in three different directions, 0° , 60° and 120° respectively.

Augmented Leads

In order to gain more leads, and “views”, of the cardiac vector multiple electrodes can be connected together by calculating the mean of the included electrode’s potentials, this value then form the negative member of a bipolar electrode pair. This virtual electrode is called a compound electrode. The resulting lead is the potential difference between the positive (physical) electrode and the negative (virtual) compound electrode.[98] These leads in the frontal plane are called the augmented leads and include:

- Lead augmented vector right (aVR) is the potential between the (positive) right arm (RA) electrode and the (negative) compound electrode of the left arm (LA) and the left leg (LL) electrode.
- Lead augmented vector left (aVL) is the potential between the (positive) left arm (LA) electrode and the (negative) compound electrode of the right arm (RA) and the left leg (LL) electrode.

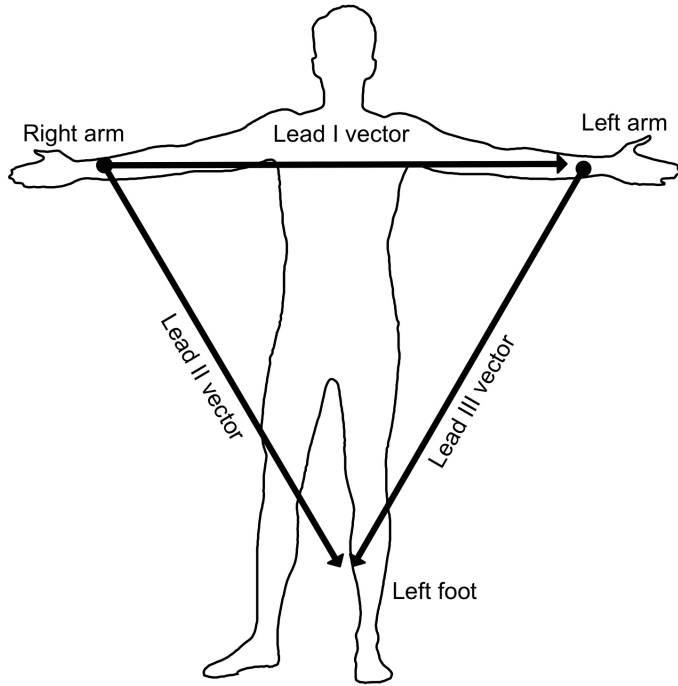


Figure 1.7: Einthoven's triangle.

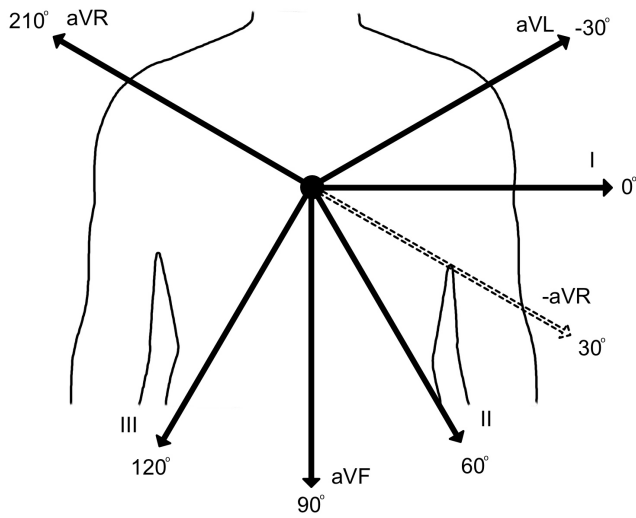


Figure 1.8: The hexaxial reference frame.

- Lead augmented vector foot (aVF) is the potential between the (positive) left leg (LL) electrode and the (negative) compound electrode of the right arm (RA) and the left arm (LA) electrode.

The augmented leads also measure the cardiac vector in three different directions on the frontal plane. Together, the limb and augmented leads vectors can be superimposed to form the hexaxial reference frame (Figure 1.8). If aVR is converted to -aVR it will shift 180° and thereby the 6 leads cover 150° of the frontal plane in 30° slices. Since the cardiac vector usually points between 0° and 90° during depolarization of the ventricles, the limb and augmented leads give the physician a good picture of the heart activity.

Precordial Leads

The precordial leads are derived from 6 chest electrodes that sits on specific predetermined sites on the torso (Figure 1.9) and spans the transverse plane. Each of the 6 electrodes is the positive electrode but they all share the same compound (negative) electrode. In this case the negative electrode is the mean value of all the limb electrode potentials, known as Wilson central terminal (WCT). [95] The WCT resides in the center of the heart or, rather, the “electric center” of the heart (Figure 1.10). [100] The 6 precordial leads are V_1 , V_2 , V_3 , V_4 , V_5 and V_6 .

The ECG Waveforms

To interpret the waveforms of an ECG it is fundamental to understand the theory of the cardiac electric field, electrodes and leads (see above). The four following points sums up our previous knowledge:

- depolarization of the myocardium toward the positive electrode produces a positive deflection
- depolarization of the myocardium away from the positive electrode produces a negative deflection
- repolarization of the myocardium toward the positive electrode produces a negative deflection
- repolarization of the myocardium away from the positive electrode produces a positive deflection

The basic waveforms of the ECG are shown in Figure 1.11 from the “view” of lead II, which is generally used for standard representation of an ECG waveform. The first positive deflection is the P wave, which represents the depolarization of the atria, when the vector generally always points towards lead II and, thus, results in a positive deflection. Figure 1.12

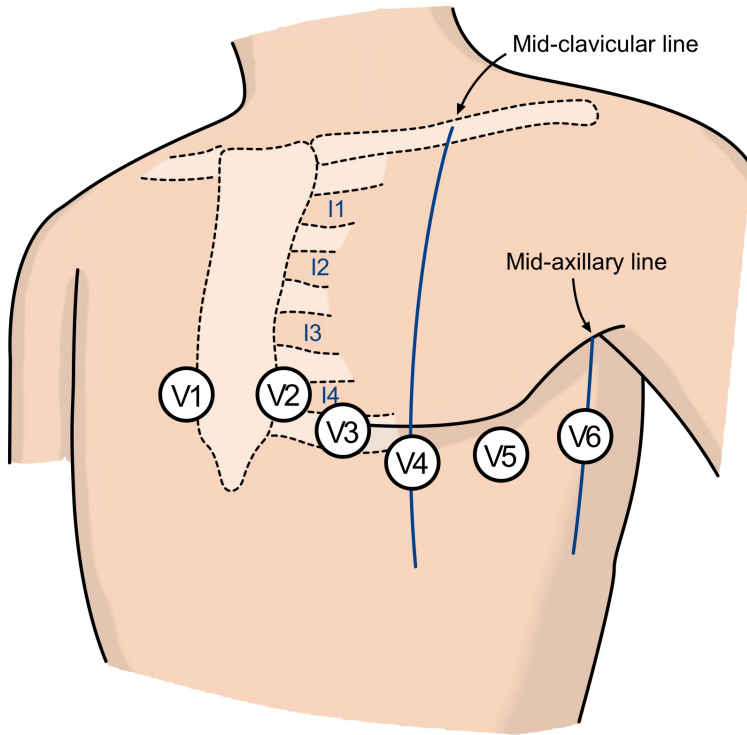


Figure 1.9: Precordial electrode placement. I1-4 = Intercostal space 1-4.

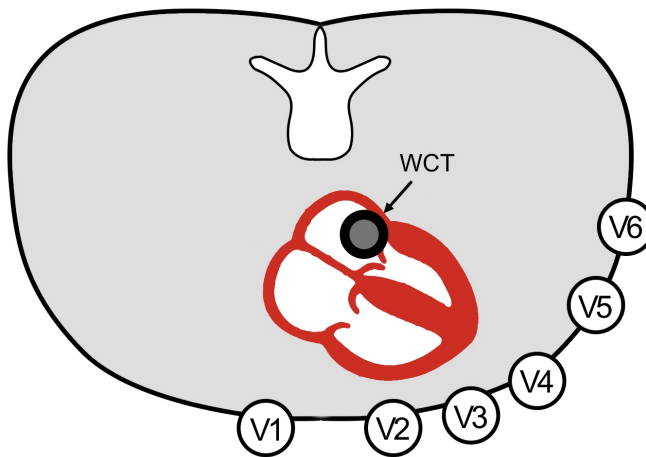


Figure 1.10: Precordial electrodes in the transverse plane with the Wilson central terminal (WCT) marked.

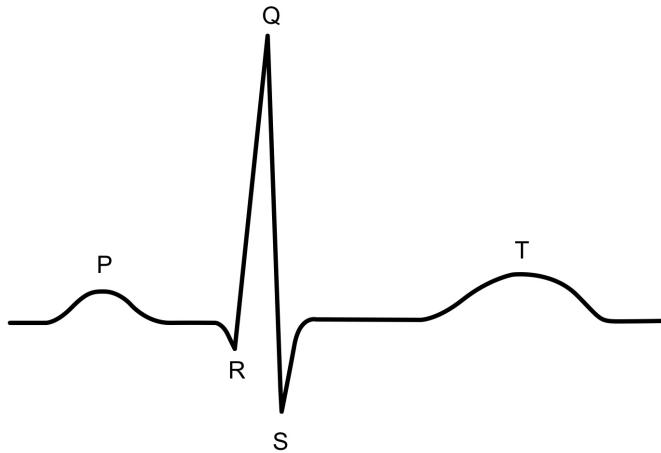


Figure 1.11: Standard ECG waveform from lead II with P, Q, R, S and T wave.

summarizes, in general the cardiac vector throughout the heart cycle and the accompanying ECG waveforms.

The QRS complex represents the depolarization of the ventricles, which begins with His bundle, the right and left bundle branch, the septum, the purkinje fibers and lastly the myocardial cells of the ventricles. Furthermore, the depolarization wavefront spreads generally from the endocardium to the epicardium due to the purkinje fibers lining the endocardium.

The Q wave is defined as the first negative deflection of the QRS complex and represents the depolarization of the septum when the vector points away from lead II (Figure 1.12). As the depolarization spreads through endocardium to epicardium, the vector predominately points toward lead II due to the larger mass of the LV, producing the R wave. The R wave is also defined as the first positive deflection of the QRS complex. The last portion of myocardium to be depolarized is the base of the LV, the vector now again points away from lead II and results in a second negative deflection. As you can imagine, the QRS complex varies significantly in morphology depending on which lead is analyzed, with not all of the waves necessarily present. [90, 101]

The T wave represents the repolarization of the ventricles and is generally a positive deflection in lead II. The repolarization wavefront moves in the same direction of the depolarization but the cells go from a positive membrane potential to a negative, resulting in a positive deflection in lead II.

The ST-segment is the period from the end of the QRS complex to the beginning of the T-wave. If the QRS complex represents the depolarization of the cardiac cells and the T-wave represents the repolarization, then, the ST-segment, in relation to the AP, represents

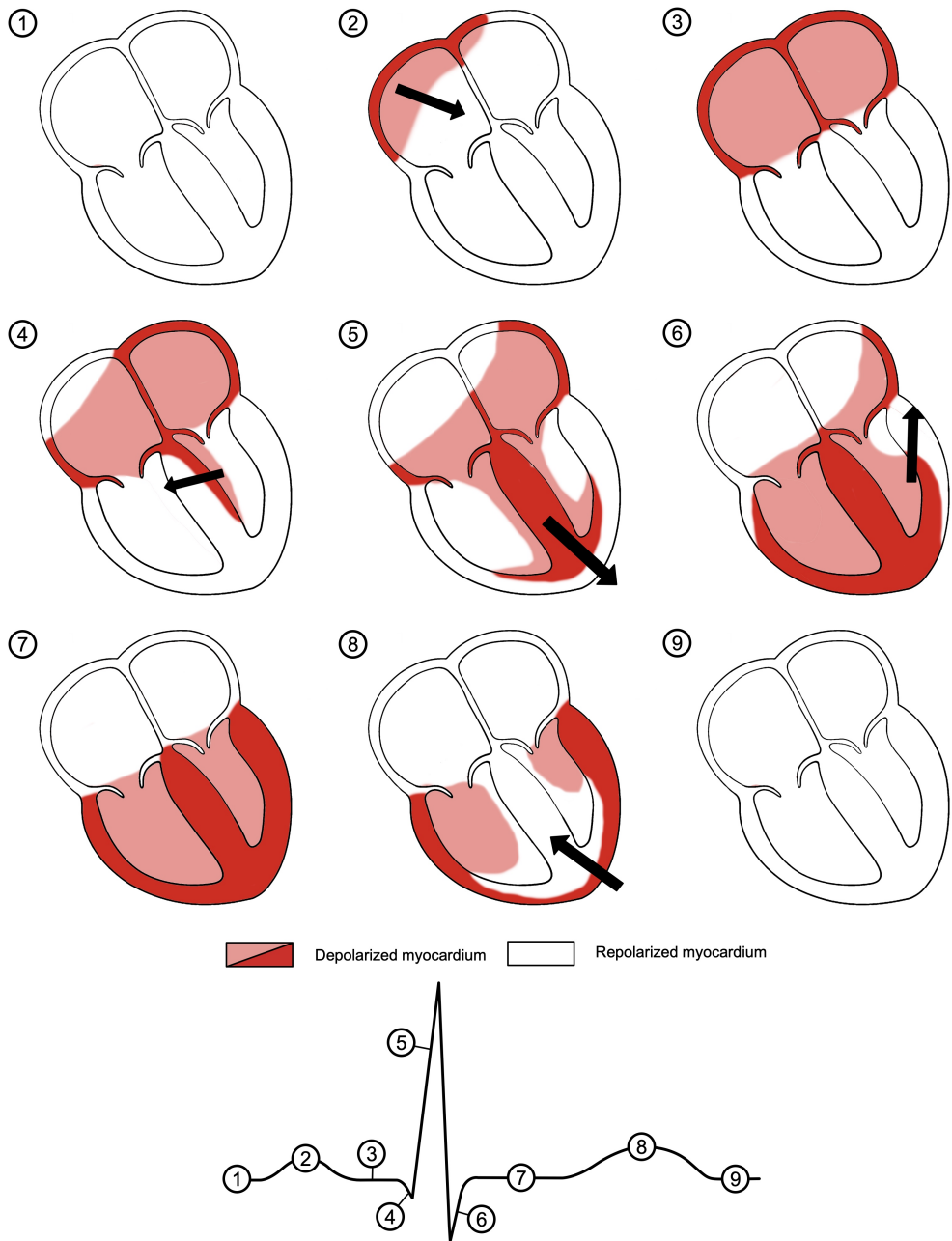


Figure 1.12: The cardiac vector throughout the heart cycle and the accompanying ECG waveforms. The gradient of electric charge between depolarized and repolarized produce the cardiac electric field which is summarized by the heart vector.

the plateau phase (phase 2). During the plateau all cells are activated with a positive, but stationary, membrane potential and there is no electric field generated since there is no difference in charge between the different parts of the heart. Since the ECG records only changes in voltage, the ST-segment remains isoelectric and without deflection. [98]

1.3.3 Ischemia

The effects of ischemia on cell respiration and the ischemic cascade is described in section 1.1.1. To briefly recapture, during acute myocardial ischemia the ATP pool is depleted to a varying degree depending on the severity of ischemia. This causes the ATP driven ion pumps to decrease in productivity and, thus, the membrane potential is affected, becoming more positive. Also, the decreased inward current of Ca^{2+} and increased outward current of K^+ cause impaired relaxation and repolarization. [102, 103] The effects on the AP are, thus, several; decreased resting potential, shortened duration, decreased rate of rise and decreased amplitude (Figure 1.13). [98]

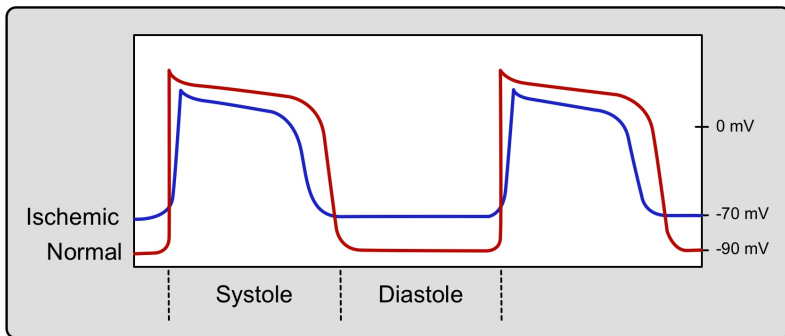


Figure 1.13: Effects on the myocardial action potential during ischemia; decreased resting potential, shortened duration, decreased rate of rise and decreased amplitude.

Figure 1.14 shows an overview of the underlying metabolic changes due to ischemia. Apart from the depletion of ATP and increase in ADP, the cell also becomes acidic due to accumulation of lactic acid and H^+ . These biochemical changes causes leakage of potassium and accumulation of catecholamines and lipid metabolites (amphiphiles) in the extracellular space, in turn affecting the electrical properties of the cell. [104] The acidosis of the intracellular space activates the Na^+/H^+ exchanger which accumulates Na^+ and in turn activates the $\text{Na}^+/\text{Ca}^{2+}$ exchanger, causing accumulation of calcium and cell swelling. [105] The consequences of these metabolic changes are depolarization of the membrane potential, Na^+ channel inactivation and slow conduction. [106]

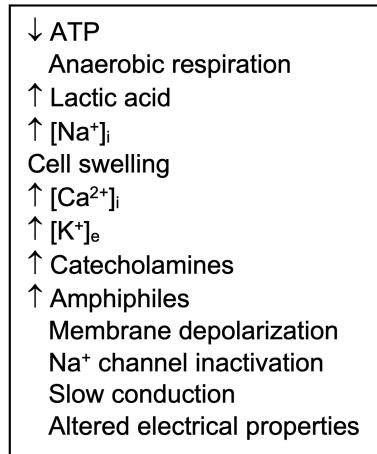


Figure 1.14: Overview of underlying metabolic changes due to ischemia. Subscript i = intracellular, e = extracellular.

ST-segment Elevation

One of the earliest signs of acute myocardial ischemia is ST-segment elevation (STE). Injury currents are thought to cause the STE, however, this is a still active area in research and consensus have not been reached.[\[106\]](#) The two main theories are that of diastolic and systolic injury currents which causes TQ depression and STE respectively. First to provide evidence of both these phenomena was Samson and Scher who recorded local ECGs from electrodes directly on the surface of dog hearts.[\[107\]](#)

Diastolic Injury Current

Rather than a STE, the diastolic injury current theory proposes that it is the TQ segment that is depressed, resulting in a seemingly STE. Due to the reduced resting membrane potential of the ischemic cells during phase 4 of the AP (see above) they are less negatively charged compared to normally repolarized myocardium cells and a voltage gradient is, therefore, generated in border zones between ischemic and non-ischemic cells.[\[108\]](#) This difference causes an altered potential difference in the lead overlaying the ischemic region during phase 4, or diastole (Figure [1.15](#)), resulting in a TQ depression. Since the ECG recorder is not able to compensate for baseline shift the TQ-segment will look normal while the ST-segment is elevated.

Systolic Injury Current

The systolic injury current is practically the reverse of the diastolic injury current. In systole the same phenomenon occurs but instead of TQ it is the ST-segment that is affected and instead of depression the ST-segment is elevated. This is due to three underlying changes in

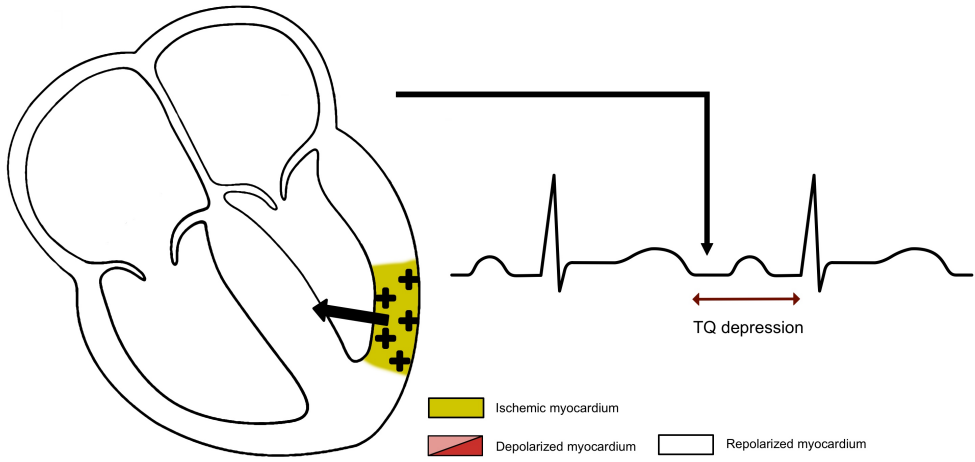


Figure 1.15: Diastolic injury current.

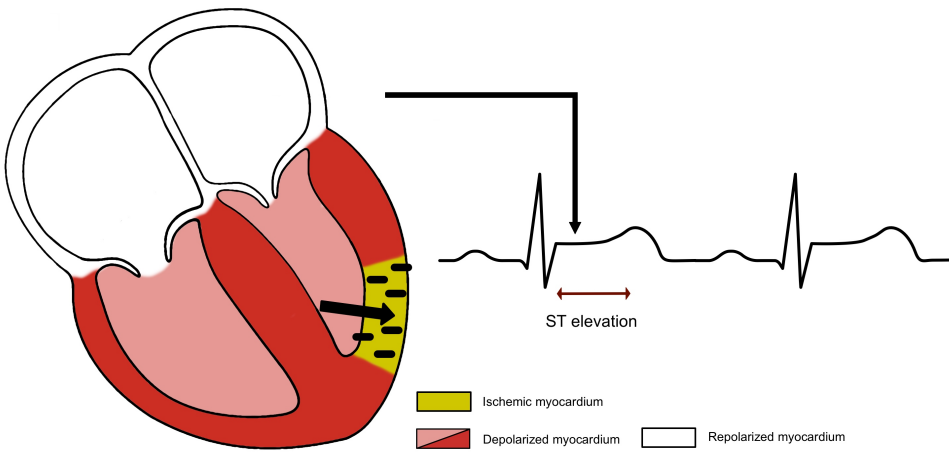


Figure 1.16: Diastolic injury current.

the ischemic AP; 1) shortening of the AP duration, 2) decrease in AP upstroke velocity and 3) decreased amplitude of the AP (Figure 1.13). [98] Because of these changes an potential gradient will form between ischemic and non-ischemic zones during the QT interval and cause a 'true' STE (Figure 1.16).

Reciprocal Changes

Since a lead measures the potential difference of the cardiac vector in one direction, a lead exactly opposite (180°) will show the first lead recording "upside-down" or negative. This is called reciprocal leads. Therefore, sometimes a reciprocal ST depression in lead II is the most apparent change due to acute posterior-medial myocardial ischemia, since there are no leads covering the contralateral surface. Vice versa, sometimes an STE is actually a reciprocal ST-segment depression. This phenomenon is reflected in the STEMI equivalent criteria, where ST-segment depression in V_1 - V_2 is used to detect e.g. a left circumflex artery (LCX) occlusion. [109]

1.3.4 The Severity of Ischemia and Terminal QRS Distortion

The visualization of ischemia and STE on the ECG depends primarily on the severity of ischemia as well as topography and presence of underlying heart disease such as prior AMI or arrhythmias. As discussed above, the metabolic changes in the cell not only affects the ST-segment but also the conductivity of the cell, slowing the speed at which the electrical signal is transferred across the ischemic myocardium. This phenomenon has been attributed primarily to the leakage of potassium into the extracellular space, [110, 111] and high potassium concentration (4.0-9.0 mM) has been shown to slow the myocardial conduction since the high K^+ levels reduce the fast Na^+ inward current. [112, 113]

Already within 30-60 seconds of the onset of a ACO, the electrical conduction begin to slow down in the ischemic myocardium. [114-119] During acute coronary occlusion in canines, giant R waves, due to acute transmural ischemia, has been correlated to increase in transmural conduction time assessed by measuring the activation time between endo- and epicardial electrograms. [110, 120] Slowing of the depolarization and phase 0, thus, seems to result in an altered morphology of the QRS complex, especially broadening. Furthermore, distortion of the QRS complex during angina, although rare, has been known as a harbinger of doom for a long time.

These morphologic changes to the QRS complex has been referred to as "giant R wave", "mono-phasic QRS-ST complex" and "tombstoning", the latter due to the likeness in both appearance and prognosis of these patients (Figure 1.17). [106, 121-124] It has also been termed 'terminal QRS distortion', [114-117, 121, 125, 126] which the author of this thesis finds to be a more neutral term. Prior studies have indicated that the amount of terminal QRS distortion is related to the severity of ischemia and an independent negative prognostic factor in patients presenting with ACO. [39, 127-132] Furthermore, previous studies have shown that terminal QRS distortion is related to poor collateral flow and, thus, the severity



Figure 1.17: Example of tombstone QRS morphology.

of ischemia. [45] Balci *et al.* have shown that ‘tombstoning’ morphology is associated with increased mortality, in-hospital cardiogenic shock, ventricular tachycardia and VF. [133] These results were confirmed by Ayhan *et al.*, [134] showing that ‘tombstoning’ morphology is an independent predictor of 6-month all-cause mortality in anterior STEMI.

More than twenty-five years ago, Sclarovsky *et al.* introduced an ECG method for grading the severity of ischemia following an ACO: Grade I – tall peaked T waves, Grade II – STE, and Grade III – terminal QRS distortion. [135, 136] Grade III of ischemia (G3I) is defined as STE with positive T waves, distortion of the terminal portion of the QRS and disappearance of the S waves below the isoelectric lines in leads with Rs configuration (usually V_1 – V_3) or emergence of the J-point > 50% of the R waves in leads with qR configuration. [128] A G3I pattern on the presenting ECG has been shown to correlate with infarct size, myocardium at risk, impaired myocardial salvage, reperfusion injury and poor clinical outcomes. [128, 137–141] However, this potentially important method failed to achieve clinical acceptance because of; the challenge of its accurate manual application, [142] and because it has still only proven chronic prognostic value (i.e. correlation with larger infarct size and higher mortality). [128, 129] Its diagnostic value regarding triage is yet to be documented. Therefore, currently, there is no clinically used method for determining the severity of ischemia in patients with suspected ACO, and triage of the reperfusion therapy strategy is not considered.

In previous experimental studies that have investigated ischemia-induced QRS changes, QRS duration was measured from QRS onset to an estimated J point. [39, 130, 138] However, terminal QRS distortion consists of an prolongation of the complex along with a significant STE which results in a merging of the R and the T wave (Figure 1.18), making the limits of the QRS complex and T wave undefinable. This is due to the prolonged depolarization phase of the myocardium, still going on as repolarization starts at the origin. G3I and ‘tombstoning’ criteria addresses these issues to some extent but are, however, di-

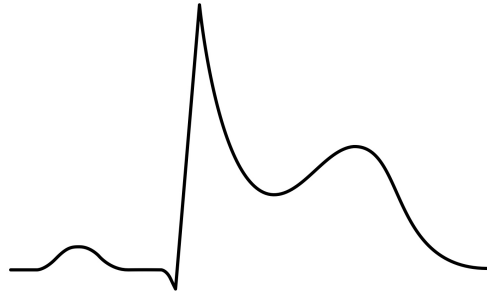


Figure 1.18: R and T wave merging.

chotomous. Furthermore, the criteria do not cover a reciprocal ST-segment depression of a posterior LCX occlusion.

1.3.5 Malignant Arrhythmias and Cardiac Arrest

Ischemia-Induced Arrhythmias

Patients with ACO and severe ischemia may also suffer from malignant arrhythmias during different phases of the ischemic cascade. Within this context, malignant arrhythmias are defined as uncontrolled and pulseless ventricular rhythms, such as ventricular tachycardia (VT) and ventricular fibrillation (VF). Malignant arrhythmias in turn lead to CA, either in-hospital, out-of-hospital (OHCA), [8] or sudden cardiac death (SCD). [143] Transient ischemic QRS widening has been shown to predict impending VF and size of the myocardial injury in an experimental acute ischemia setting in pigs. [144–146] Furthermore, as described above, Balci *et al.* have shown that ‘tombstoning’ morphology is associated with increased mortality, in-hospital cardiogenic shock, VT and VF. [133]

There are many possible causes for these conditions, however, within this thesis acute myocardial ischemia as the underlying pathology will be considered. The biochemical imbalance of ischemia following a total coronary occlusion, causing arrhythmias, develop as a consequence of automatic or nonautomatic ectopic excitation. [105] Automatic excitation is due to abnormal automaticity in the myocardial cells and early or delayed afterdepolarizations. Afterdepolarizations are when myocytes partially depolarize. i.e. move to a more positive membrane potential, during a different phase than phase 0. Early afterdepolarizations occur during phase 2 or 3 (after normal depolarization) and delayed afterdepolarizations during phase 4 (before normal depolarization).

Nonautomatic excitation, however, is due to classical reentry, where the disordered and slow ischemic-induced conduction causes the electrical signal to persist to reexcite the myocardium instead of dying out after complete activation. [147]

In the reversible phase of ischemia, 2-30 minutes after the ACO, there is a distinct difference in etiology depending on early (2-10 minutes) or late (15-30 minutes) occurrence

of arrhythmias. In early arrhythmogenesis classical reentry seems to be predominant, giving rise to bursts of VT but seldom sustained VF. [105] However, late arrhythmogenesis is due to both focal and non-focal sources such as automatic automaticity, reentry, injury currents and phase 2 reentry. Late arrhythmogenesis in the reversible phase more often evolve into sustained VF and SCD, probably due to the higher Ca^{2+} load. [148]

However, ischemia arrhythmogenesis is not straightforward but rather a complex interaction between biochemical and electrophysiological disturbances and it is difficult to indicate one culprit process. Furthermore, genetics play a large and widely unexplored role in arrhythmogenesis.

Reperfusion Arrhythmias

In some cases, arrhythmias do not appear during the ischemic phase but rather during reperfusion therapy when the blood flow is restored to the affected myocardium. Non-lethal reperfusion arrhythmias such as; bradycardia, premature ventricular beats and bursts of VT is common. [149] Thus, reperfusion arrhythmias rarely cause any reperfusion injury. However, in some cases lethal arrhythmias, such as pulseless VT or VF, occurs, usually within seconds of reperfusion. [150] These malignant arrhythmias can be devastating and most often lead to CA. The electrophysiological mechanism behind lethal reperfusion arrhythmias seems to be a washout of various ions, such as lactate and potassium. However, there is no consensus on the exact electrophysiological mechanism. [151]

1.3.6 CMR

Cardiovascular magnetic resonance imaging (CMR) is currently considered the reference standard for assessment of myocardium at risk (MaR), final infarct size (IS) and myocardial salvage index (MSI) in the setting of ACO. [152]

Assessment of MaR is based on the phenomenon that ischemic myocytes becomes edematous and therefore generates a high signal intensity in T-2 weighted images and an increased extracellular volume, which gives rise to increased signal intensity in CE-SSFP images. [153]

Infarct size (IS) is usually quantified with late gadolinium-enhanced CMR. Gadolinium-DOTA is an extracellular contrast agent that effects protons in its surroundings, shortening the T1 relaxation time and thereby enhances contrast when nulling the signal from viable myocardium. When myocardium is infarcted myocytes die and the extracellular compartment becomes increased. These infarcted areas appear bright on late gadolinium-enhanced CMR and can be assessed to calculate IS. [154]

Previous studies in STEMI patients have shown that terminal QRS distortion due to ischemia is associated with larger IS (acute and 4 months post STEMI), larger MaR, lower MSI and more severe microvascular obstruction. [139–141, 155] Furthermore, low collateral flow, and thereby more severe ischemia, has been correlated to lower MSI and more rapid infarct development on CMR. [38]

Chapter 2

Aims

Acute myocardial ischemia and its subsequent ramifications (AMI, OHCA etc.) are a common cause of death. The overall aim of this thesis, therefore, is to evaluate a proposed improvement on the identification of these patients. The aims of the individual papers are stated below.

Paper I

To 1) test a novel method for quantifying terminal QRS distortion termed 'ischemic QRS prolongation' (IQP), 2) establish the relationship between IQP and collateral arterial flow during acute ischemia in an experimental dog model and 3) test if the same pattern of IQP occurs in patients with coronary artery disease (CAD) undergoing prolonged, elective angioplasty balloon inflation.

Paper II

To introduce an ECG method for quantification of IQP that considers all 12 standard leads and does not require comparison with a baseline recording.

Paper III

To test the hypothesis that IQP during the initial 15 minutes of acute coronary occlusion can serve as predictor for occurrence of reperfusion VF in an experimental canine model.

Paper IV

To evaluate the relation between IQP and myocardial injury assessed by CMR in patients presenting with acute STEMI.

Paper V

To explore to what extent IQP is present in STEMI patients suffering from OHCA compared to those who do not.

Chapter 3

Materials and Methods

3.1 Experimental Canine Model

All experiments involving the use of laboratory animals conform to the guidelines of the American Physiological Society and the standards in the Guide for the Care and Use of Laboratory Animals, DHEW Publ. No. NIH 85–23, revised 1985, and was approved by the institutional review board.

3.1.1 Study Population

Paper I

Data from 23 healthy mongrel dogs originally studied in the early 1980's were included. [40] All dogs underwent proximal occlusion of the left circumflex coronary artery (LCX) for 5 minutes. Collateral flow was evaluated using microspheres as described below. [40]

Paper III

Data from 24 healthy mongrel dogs, previously included in studies of reperfusion effects in late ischemic injury originally published in 1985, were included. [26] All dogs underwent proximal occlusion of the LCX for 15 minutes.

3.1.2 Collateral Blood Flow Measurement

As previously described, myocardial collateral blood flow was expressed in ml/min/g wet. [39, 40] In short, the ischemic and non-ischemic myocardium was measured by injecting radioactive microspheres labeled with ^{46}Sc , ^{88}Sr , ^{113}Sn , ^{141}Ce , or ^{153}Gd at 2.5 minutes into the ischemic episode. Beginning just before and continuing 2.5 minutes after microsphere injection, reference blood samples were withdrawn from the aorta via a femoral artery catheter. Microsphere radioactivity was measured with a gamma counter (Model

A5912, Packard Instruments, Downer's Grove, IL, USA). Myocardial blood flow was calculated according to the formula: $tissue\ flow = \frac{(tissue\ counts) * (reference\ blood\ flow)}{(reference\ blood\ counts)}$.

3.2 Human Study Populations

The original studies were approved by the institutional review board (USA) and the regional ethics committee (Sweden) and written consent was obtained from all surviving participating patients. Detailed population description can be found in the individual papers.

Paper I & II

ECGs for the human cohort were obtained from the STAFF-III dataset, originally acquired at the Charleston Area Medical Center, WV, USA. [156, 157] Patients included were referred for prolonged 5 minutes elective balloon PCI due to stable angina pectoris and informed consent was obtained from each patient before enrolment. Digital 12-lead ECGs were recorded continuously pre-occlusion and during the procedure.

Paper IV

Patients included were originally a part of the randomized controlled SOCCER (Supplemental Oxygen in Catheterized Coronary Emergency Reperfusion) trial. This trial was conducted at Skåne University Hospital, Sweden and consisted of 160 normoxic (O_2 -saturation $\geq 94\%$) STEMI patients who underwent primary PCI and randomized to either standard oxygen therapy or no supplemental oxygen in the ambulance. 95 patients underwent CMR 2-6 days after the PCI. Patients with previous AMI or inability to decide whether to participate were excluded. [158]

Paper V

The study cohort consisted of data derived from two different clinical trials; one group of STEMI patients who suffered from an acute OHCA (the targeted temperature management [TTM] trial) and one that did not (the Supplemental Oxygen in Catheterized Coronary Emergency Reperfusion [SOCCER] trial; described above). [158, 159] Data was acquired at Skåne University Hospital in Lund and Malmö (TTM and SOCCER), and the hospital of Helsingborg, Sweden (TTM). [158, 160]

The TTM-trial included adult, unconscious patients resuscitated from an OHCA of a presumed cardiac cause. Within the original study, two different target temperatures for post-return of spontaneous circulation (ROSC) cooling were studied (33°C vs. 36°C). [160] Due to logistic and regulatory reasons Swedish patients were only considered.

3.3 Electrocardiography

3.3.1 ECG Acquisition

Paper I & III (canines)

All dogs were anesthetized with 30-40 mg/kg of sodium pentobarbital intravenously, intubated and ventilated as previously described in detail.[\[26\]](#), [\[40\]](#), [\[44\]](#) In short, a left thoracotomy was performed through the fourth intercostal space and the heart was suspended in a pericardial cradle. The LCX was identified and occluded for 5 (paper I) or 15 (paper III) minutes with a silk snare. Using a Gould model 2400 recorder, ECG lead II was recorded continuously before, during the occlusion and also during reperfusion until the heart was excised. QRS waveform measurements were obtained from ECG lead II at a paper speed of 25mm/s and magnified x2 in a standard photocopier i.e. achieving 50mm/s and 20mm/mV.

Paper I & II

A detailed description of the STAFF-III study was recently presented.[\[156\]](#), [\[157\]](#) In short, all patients included received approximately 5 minutes of balloon occlusion of the right coronary artery (RCA), the left anterior descending artery (LAD) or the LCX. Digital 12-lead ECGs were recorded continuously (Siemens-Elema AB, Solna, Sweden) pre-occlusion and during the procedure until approximately 4 minutes after balloon deflation.

Waveform measurements were obtained from the digital continuous 12-lead ECG recordings. Measurements were made from print-outs of the ECGs at a paper speed of 50mm/s and gain of 10mm/mV. Values were measured from a single lead in order to emulate the method used in the experimental dog cohort. The extremity leads were considered for assessments of RCA occlusions and precordial leads for LAD and LCX occlusions. Since the dog and human cardiac anatomies differ, the lead with the most pronounced ischemic QRS prolongation among the considered leads and within 5 minutes of occlusion was used.

Paper IV & V

Digital, 10 second, 12-lead ECGs were recorded. The first post-ROSC ECG was used for the TTM population. If no ECG was available within 6 hours from OHCA, the patient was excluded. For the SOCCER population, the first ECG prior to PCI was used. If an ambulance ECG was unavailable, the first ECG recorded at hospital admission, before PCI, was used.

Other exclusion criteria were bundle branch block (BBB) or any ventricular or pacemaker rhythm on the ECG. During the recording, all patients were resting in a supine position. Manual measurements were made from print outs of median beats of the ECG at a paper speed of 50mm/s and gain of 10mm/mV.

On the ECG, IQP, maximal ST-deviation, occurrence of pathological Q waves, [161] occurrence of ST changes meeting current STEMI or STEMI equivalent criteria, [109, 162] and the computer generated QRS duration ($QRSd_{cg}$) were recorded.

3.3.2 Ischemic QRS Prolongation

As discussed in the introduction, terminal QRS distortion hinders the normal methodology of measuring QRS duration. The slow and thus delayed depolarization of the ischemic myocardium results in QRS prolongation by which the QRS complex and T wave are merged and the J-point disappears in leads overlying the ischemic myocardium (Figure I.18). In the present thesis we introduce a new method for assessing ischemic QRS prolongation even in the absence of a defined J-point, in an attempt to solve this problem. The method was developed by Dr. Galen Wagner and the author of the current thesis. The concept of defining a line between the R/S wave and the intersect of the PR baseline, as described for the proposed method, is similar to a previously described method of determining the offset of the T wave. [163] The term for this change in the QRS complex has, however, been hard to determine. Since the current method does not use the J-point as offset, the measurement from QRS onset to PR intercept cannot be termed ‘QRS duration’. We have, therefore, decided to refer to the difference between baseline QRS duration and the distance from QRS onset to PR intercept as ischemic QRS prolongation (IQP). It should be noted that the true QRS duration in patients with terminal QRS distortion is problematic to evaluate and is not what this method is aimed at.

Single-Lead Method (paper I & III)

Before occlusion, measurement of a baseline QRS duration, defined as the time between QRS onset and the J-point, were undertaken in all animals and patients. During ischemia when no J-point could be clearly distinguished, due to the merging of the R and T wave, a line was drawn through the peak of the R (or R’ if it was present) wave and along 40% of the downslope between the R peak and the nadir of the ST segment (Figure B.1). The time between onset of the QRS complex and the intersection of this line with the PR baseline was then determined. In dogs where the J-point could be clearly distinguished, even during ischemia, the time between QRS onset and the J-point was determined. The difference between QRS duration during ischemia, either by distinct or indistinct J-point, and the baseline QRS duration was referred to as IQP, expressed in ms (absolute ischemic QRS prolongation [aIQP], measured to nearest 5 ms) and normalized to baseline (relative ischemic QRS prolongation [rIQP]). If there was an S wave associated with a ST-segment depression (basal lateral ischemia in LCX occlusions) a superimposed line from the S wave nadir along the first 40% of the S wave upslope was used and the intersection with the PR baseline marked the offset.

Each value was measured as the average of measurements in 2 contiguous beats. IQP was measured at one-minute intervals during first 5 minutes of occlusion, the maximum

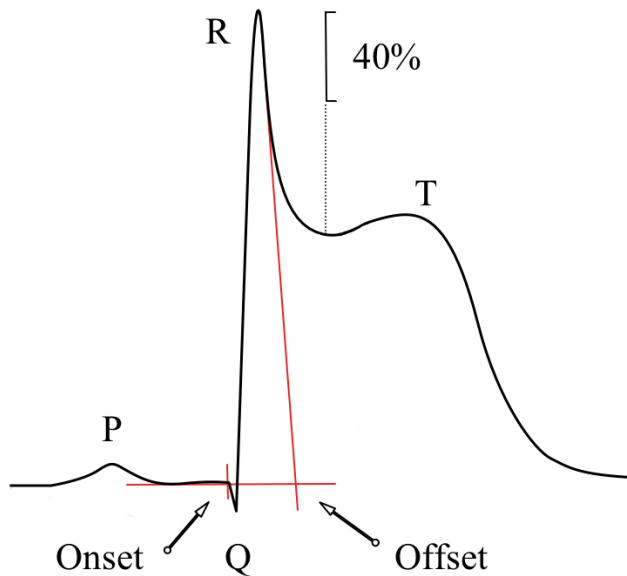


Figure 3.1: Depiction of ischemic QRS prolongation measurement method. During ischemia when no J-point could be clearly distinguished due to ST-elevation a line was drawn through the peak of the R (or R' if it was present) wave and along 40% of the downslope between the R peak and the nadir of the ST segment.

value during this period was used in data analysis. Furthermore, the timing of the maximum IQP was recorded to the nearest minute post occlusion.

In paper III (canines) timing and occurrence of VF was recorded to the nearest second after reperfusion. VF was defined as occurrence of bizarre, irregular, random waveforms, no clearly identifiable QRS complexes or P waves and/or wandering baseline continuing for more than 10 seconds without reverting to sinus rhythm.

12-Lead Method (Paper IV & V)

The single-lead method described above have, however, limitations to consider. It only considers a single ECG-lead, and the quantification of IQP requires a baseline ECG for quantitative comparison. To address these issues the method was improved in paper II.

Severe ischemia causes delayed activation in the ischemic region, which thus depolarizes slower than the rest of the myocardium. This leaves the electrical field moving toward the ischemic region the only remaining vector during late depolarization. Thus, QRS duration will be prolonged globally but this prolongation is only visible in leads facing the ischemic region. Leads that are perpendicular to the ischemic region will show a shorter, incorrect, QRS duration that, however, is theoretically close to the baseline duration (in a non-ischemic situation) as these leads will be unable to detect the delayed activity in the

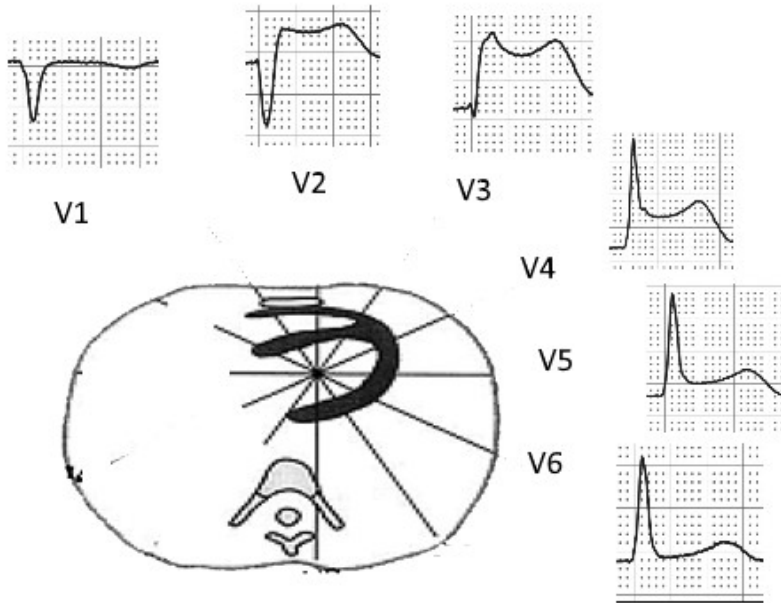


Figure 3.2: Demonstration of the concept of parallel and perpendicular leads. Leads facing the ischemic region (V_2 – V_4) show significant ST deviation and terminal QRS distortion. Leads that are perpendicular to this region show minimal ST deviation and terminal QRS distortion.

ischemic region. This is demonstrated in Figure 3.2 which shows the electrical axis of the heart in the transverse plane. Leads that are relatively parallel to the ischemic region (V_2 – V_4) show significant ST-segment deviation (STD) while leads that are relatively perpendicular to the ischemic region (V_5 and V_6) shows almost no STD. Analogously, terminal QRS distortion is present in the leads that are parallel to the ischemic region as a consequence of the slowed conduction. This regional slowing of conduction results in delayed activation of the severely ischemic area after the non-ischemic myocardium is already completely depolarized. Consequently, the only vector during this delayed depolarization, as displayed in Figure 3.2, will be moving in the approximate direction towards V_3 that also shows the maximum STD. Leads that are perpendicular to this vector will be unable to register this late activity when “viewed from the side”. A theoretical negative V_3 lead, directly opposite of V_3 , would show changes mirroring V_3 , while leads perpendicular to the injury vector will show both minimal STD and minimal terminal QRS distortion. Thus, leads that are perpendicular to an acutely ischemic region could be used to estimate a surrogate baseline QRS duration. As STD is the established method for identifying the ischemic area the lead with maximal STD was used for measurement in contrast to the lead with maximal IQP which was used in paper I and III.

The ECG measurement of IQP was performed according to the method above. In short, patients meeting STEMI or STEMI equivalent criteria were analyzed with regards to IQP. The lead with the maximum STD was determined and the amplitude of the ST segment was recorded. The same method for cutoff determination as in the single-lead method was used in this lead (Figure 3.1). If the changes in the lead with maximum STD were so large as to prevent measurement, the closest adjacent lead is used instead (i.e. the lead with the 2nd largest STD). This measurement will be referred to as $QRSd_{mSTD}$ (QRS duration at max STD) from this point in the thesis. All measurements were made to the nearest 5 ms.

All 12 leads are evaluated for STD and the lead that showed the least deviation was defined as the lead most 'perpendicular' to the ischemic region. If more than one lead showed minimal STD ($<0,05$ mV) a lead in the same plane, as the lead with maximum STD, was preferred. If more than one lead in the same plane showed minimal STD the median was used. The measured QRS duration in this lead was then used as the reference QRS duration ($QRSd_r$). The difference between the $QRSd_{mSTD}$, in the lead parallel to the injury, and the $QRSd_r$ was referred to as absolute IQP (aIQP, in ms). Relative IQP (rIQP) was the aIQP divided by $QRSd_r$.

3.3.3 Sclarovsky-Birnbaum Ischemia Grade (paper IV)

The Sclarovsky-Birnbaum Ischemia Grade was determined from the acute ECG using the algorithm of the refined grading system described by Billgren *et al.* [142]. In short, each ECG was analyzed and assigned an ischemia grade from 1-3 where grade 3 of ischemia (G3I) is associated with terminal QRS distortion. The algorithm has previously been described in detail. [142]

3.3.4 Anderson-Wilkins Acuteness Score (paper IV)

For estimation of the acuteness of the ischemic ECG changes, the ECGs were also analyzed using the Anderson-Wilkins (AW) acuteness score, which has previously been described in detail. [164]. In short, each standard lead (except -aVR) with ≥ 0.1 mV STE in the precordial leads, ≥ 0.05 mV in the limb leads, or abnormally tall T waves, were considered. An acuteness score (1-4) was assigned to each lead based on the presence or absence of a tall T wave or an abnormal Q wave, where 1 is least acute and 4 most acute. The final AW acuteness score was then calculated as the average score of the included leads.

3.4 Magnetic Resonance Imaging

3.4.1 CMR Image Acquisition (paper IV)

The magnetic resonance image acquisition is described earlier in detail by Khoshnood *et al.* [158]. In short, acquisition of imaging data was done with a Philips 1.5T Achieva or a

Siemens 1.5T Avanto scanner.

First, scout images were acquired to locate the heart. For visualization of MaR, short-axis T2-weighted triple inversion recovery (STIR) images, T2-prepared steady state free precession (SSFP) images as well as multi-slice, multi-phase contrast-enhanced (CE)-SSFP images were acquired covering the entire LV. The CE-SSFP images were acquired approximately 5 minutes after intravenous administration of 0.2 mmol/kg of a gadolinium-based extracellular contrast agent (DOTAREM, Gothia Medical, Billdal, Sweden). The slice thickness was 8 mm with no slice gap. In-plane resolution was typically 1.5 x 1.5 mm and the temporal resolution for the CE-SSFP images was 20-30 frames per cardiac cycle. For infarct visualization, late gadolinium enhancement (LGE) images corresponding to the CE-SSFP images were acquired approximately 15 minutes after injection of gadolinium. The LGE-images were acquired using an inversion-recovery gradient-recalled echo sequence with a slice thickness of 8 mm with no slice gap. In-plane resolution was typically 1.5 x 1.5 mm. Inversion time was manually adjusted to null the signal from viable myocardium.

3.4.2 CMR Image Analysis (paper IV)

All quantitative CMR analysis were performed on short-axis images using the software Segment v.1.9 R3084 (<http://segment.heiberg.se>). [165] MaR was calculated using T2-weighted triple inversion recovery imaging, STIR, (Philips Achieva) or T2-prepared steady-state free precession (SSFP) (Siemens Avanto) as well as contrast-enhanced (CE)-SSFP short-axis images. T2-STIR and CE-SSFP have previously been validated both experimentally and in the clinical settings. [166–171] Infarct size was quantified from the LGE images using an automated computer algorithm taking partial volume effects into consideration. [172] MaR and IS were expressed as a percentage of the left ventricular myocardium and the MSI was quantified as $(1 - \frac{IS}{MaR}) * 100\%$. Figure 3.3 shows an example of MaR, IS and MSI in a patient with an infarction in the right coronary artery (RCA) vessel territory.

For assessment of left ventricular ejection fraction (LVEF), endo- and epicardial borders were manually delineated in end-diastole (ED) and end-systole (ES) in all the CE-SSFP short-axis images and in percent $(100 * \frac{ED\ volume - ES\ volume}{ED\ volume})$.

3.5 Statistical Methods

Visual evaluation of distribution, comparisons of mean to median as well as the relation of the SD to the mean was used to evaluate if data were normally distributed. For parameters that was not normally distributed, non-parametric tests were applied for statistical significance. Continuous variables are presented as mean \pm 1SD (normally distributed) or median (range)(not normally distributed). Categorical data are presented as frequency (%). For continuous variables the Student t-test and the Mann-Whitney U test were used for comparison between groups. Chi-square test was used for comparison of proportions. All statistical tests were 2-sided and a p value of <0.05 was considered to indicate statisti-

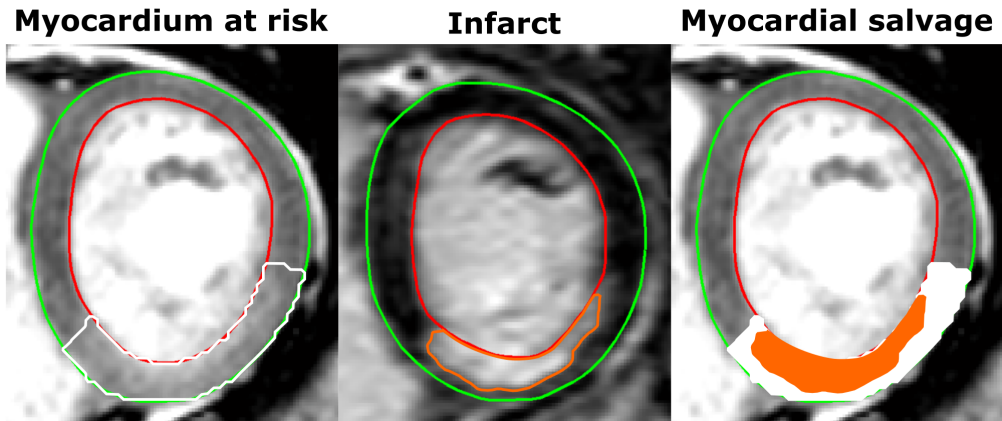


Figure 3.3: Co-localized mid-ventricular left ventricular slices showing myocardium at risk, infarction and myocardial salvage in a patient after myocardial injury caused by occlusion-reperfusion of the right coronary artery. Green lines delineate epicardium, red lines endocardium, white line myocardium at risk, and orange line infarction. In the image to the right the infarct delineation has been superimposed upon the myocardium at risk delineation where salvaged myocardium is indicated in white.

cal significance. SPSS version 19.0 and 23.0 (IBM corporation, Armonk, NY, USA) and MATLAB version R2013a were used for the statistical analyses.

Paper I

The relationship between IQP and collateral flow was modeled using a reciprocal function with non-linear least squares regression. The equation of the model was given by $y(x) = \frac{a}{x}$; where a was constant while y and x were the IQP and collateral flow, respectively. Using a non-linear least squares regression a was calculated from the dog results to the value of 0.8725.

Paper III & V

ROC analyses were performed to evaluate optimum cut-off value of IQP, using the Youden method. Sensitivity, specificity and area under the curve (AUC) was analyzed.

Paper IV

For correlations of IQP to data from CMR Spearman's rank correlation coefficient was calculated. When adjusting for co-morbidities timing variables and AW-score, multivariable logistic regression analysis was used.

Paper V

Odds ratios (OR) was calculated using multivariable logistic regression in order to adjust for co-morbidities. All statistical tests were 2-tailed and a p value of <0.05 was considered statistically significant.

Chapter 4

Results and Discussion

The following is a synopsis of the main points of the results and discussion sections in the respective papers. Population selection and characteristics as well as detailed limitations sections can be found in the full papers in the end.

4.1 IQP and Ischemia Severity

4.1.1 Collateral Flow (canines; paper I)

The mean flow in 23 canines was 0.099 ± 0.086 ml/min/g wet. There was a statistically significant relationship between collateral blood flow and aIQP ($r=0.61$, $p=0.008$; Figure 4.1). Furthermore, there was a significant difference in collateral flow in the dogs above ($n=11$) vs below ($n=12$) 5 ms (median) of aIQP. The dogs with >5 ms of aIQP exhibited significantly lower collateral flow compared to dogs with ≤ 5 ms aIQP (0.04 ± 0.03 vs 0.15 ± 0.09 ml/min/g wet, $p=0.001$; Figure 4.2).

4.1.2 Translation (paper I)

In the STAFF III cohort mean overall aIQP ($n=54$) was 49 ± 57 ms (44 ± 49 , 62 ± 71 and 29 ± 28 ms for RCA, LAD and LCX occlusions, respectively) without significant differences between the groups. Maximum aIQP was reached after 3.4 ± 0.8 minutes of occlusion. Moreover, it was frequently noted that IQP reached a plateau after the maximum was reached, staying at a similar magnitude throughout the rest of the 5-minute occlusion. In all patients with significant aIQP, the QRS duration returned to baseline values within 30 seconds of reperfusion.

As shown in Table 4.1 and Figure 4.3 there was no statistically significant difference between canines and humans regarding rIQP during occlusion. Side by side examples of ECGs from humans and dogs are shown in Figure 4.4.

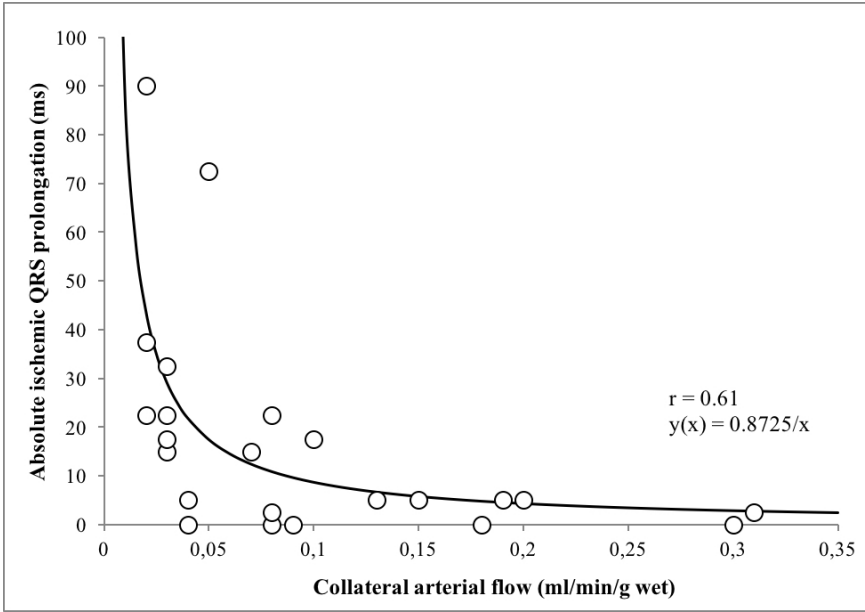


Figure 4.1: Scatter plot of dog data. Collateral blood flow (ml/min/g wet) was plotted against aIQP. The relationship between aIQP and collateral flow was modeled using a reciprocal function calculated with a non-linear least squares regression $y(x) = \frac{0.8725}{x}$; $r=0.61$ and $p=0.008$.

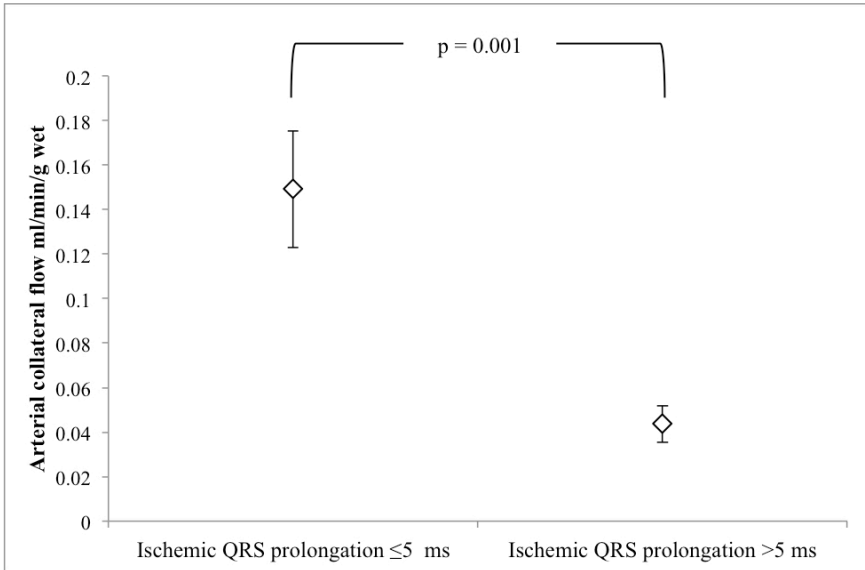


Figure 4.2: Relation between groups with aIQP of ≤ 5 ms or > 5 ms. Whisker plot with mean \pm standard error of the mean (SEM).

Relative ischemic QRS prolongation	Humans, Mean \pm 1SD (range)	Dogs, Mean \pm 1SD (range)	p-value
RCA in human (n=21)	60% \pm 69% (0-243%)		0.345*
LAD in human (n=22)	79% \pm 85% (0-294%)		0.092*
LCX in human (n=11)	40% \pm 43% (0-154%)		0.993*
All arteries in humans (n=54)	64% \pm 74% (0-294%)		0.202*
LCX in dogs (n=23)		42% \pm 59% (0-225%)	
Time to max ischemic QRS prolongation (min)	3.4 \pm 0.9 (2.0-5.0)	3.4 \pm 0.7 (2.0-4.0)	0.911**

Table 4.1: RCA = Right coronary artery, LAD = Left anterior descending artery, LCX = Left circumflex artery.
* Two-tailed p value calculated with an unpaired t-test where the p-value indicates the statistical difference between the mean rIQP in dogs (LCX) and the human data. ** Two-tailed p value calculated with an unpaired t-test.

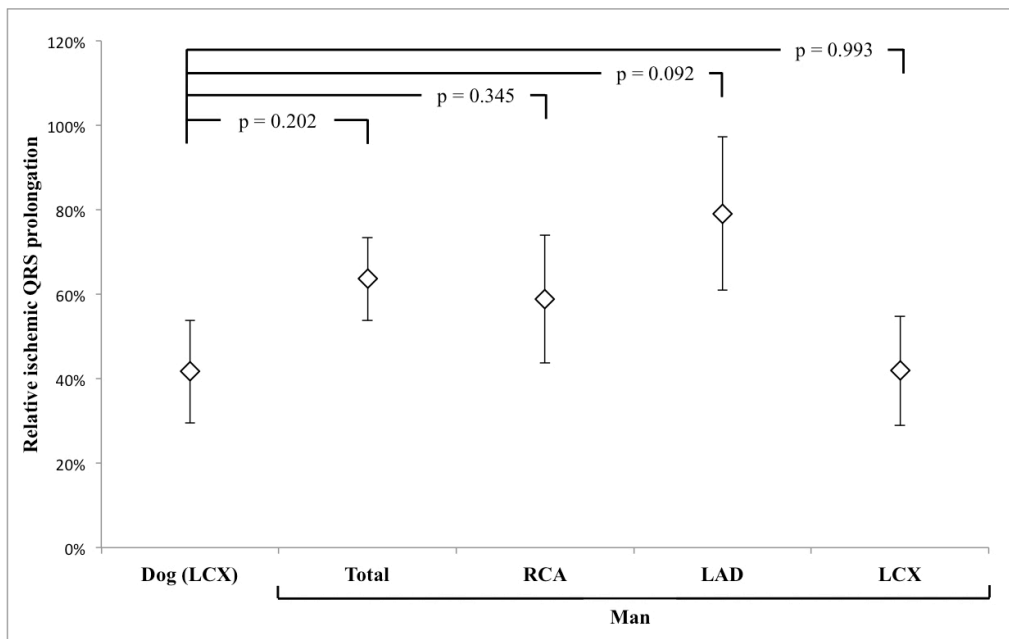


Figure 4.3: Relation between humans (divided into total, RCA, LAD and LCX) and dogs as regards relative ischemic QRS prolongation. Whisker plot with mean \pm standard error of the mean (SEM). No statistical significant difference between the dogs and any of the human subgroups were found.

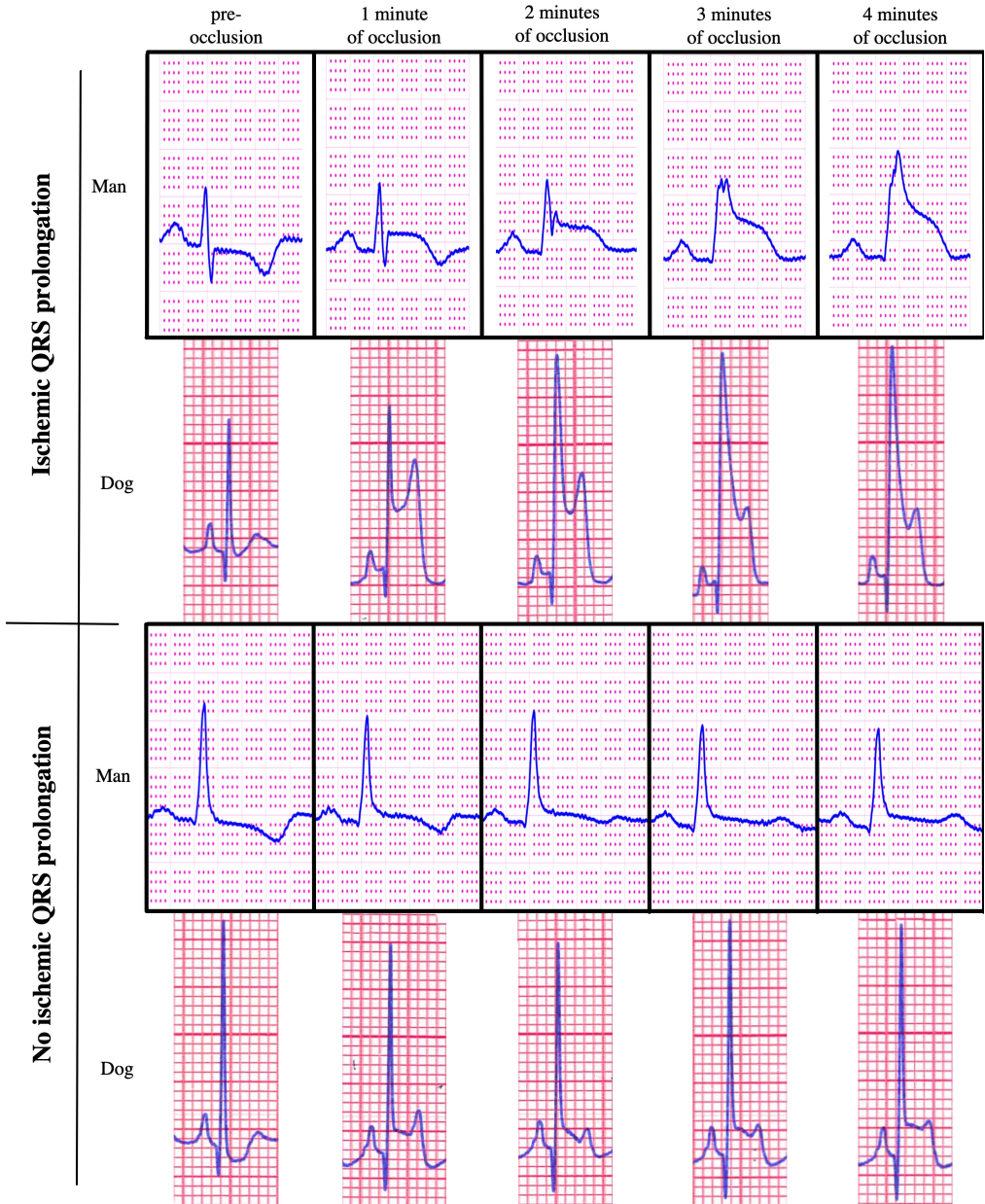


Figure 4.4: Example of ECG lead II at 0, 1, 2, 3 and 4 minutes of occlusion in two dogs (LCX) and two humans (RCA), with one example of significant ischemic QRS prolongation and one with no ischemic QRS prolongation within each species. The grid systems have been transformed to be comparable.

4.1.3 Myocardial Injury (CMR; paper IV)

In 77 included patients median aIQP was 10 (0 - 115) ms. No significant linear correlations between $QRSd_{cg}$, $QRSd_{mSTD}$ and aIQP to any of the CMR markers for myocardial injury were found (Table 4.2). Anderson-Wilkins score did not correlate to any IQP measure or CMR measure of myocardial injury or LVEF. Adjusting for the acuteness of the ischemia according to the AW score did not affect the results. Adjusting for time from pain onset to ECG or time from ECG to PCI did not affect the results either. Figure 4.5 shows example ECGs of patient without (A) and with (B) significant IQP.

Sixty-seven patients (87%) had a Sclarovsky-Birnbaum ischemia grade 2 (G2I) and nine patients (12%) had G3I. One patient had only ST-depressions could therefore not be assigned any ischemia grade.[142] There was no significant difference between the G2I and G3I groups regarding any measure of IQP or any of the CMR variables for myocardial injury.

4.1.4 Discussion

Arterial Collateral Blood Flow

The findings in paper I, with lower collateral blood flow in dogs with more pronounced IQP, is in accordance with earlier studies.[39, 45, 130] Dogs with an aIQP of >5 ms all had low collateral flow whereas those with ≤ 5 ms showed a variable amount of collateral flow (Figure 4.1). This indicates that presence of a significant IQP during coronary occlusion might have high positive predictive value for low collateral flow.

Translation

The findings in paper I indicate similarities between coronary occlusion in dogs and in humans (Figure 4.3). The magnitude and range of IQP during coronary occlusion were similar between the species, especially as regards to patients with LCX occlusions. Furthermore, the timing of maximum IQP was similar between the two species.

Although, given the results in paper I, no correlations were found between IQP and CMR variables of myocardial injury in patients experiencing first time STEMI. Furthermore, patients with G3I did not differ from G2I with regard to CMR markers of myocardial injury or IQP.

Several measures of the severity of ischemia in ACO have previously been suggested, such as the Sclarovsky-Birnbaum Ischemia Severity Grading System,[128] and the morphology criteria of 'tombstoning', presented by Guo *et al.*[173] QRS 'tombstoning' morphology have been reported to correlate to mortality, in-hospital cardiogenic shock, ventricular tachycardia and ventricular fibrillation, in patients with anterior AMI.[121] Furthermore, Sclarovsky-Birnbaum G3I has been correlated to IS (acute and at 4 months post STEMI), impaired myocardial salvage and reperfusion injury.[128, 139, 140] Thus, although markers of terminal QRS distortion have been shown to be related to myocardial

	Correlation coefficient	p-value
MaR/LV mass (%)	-0,02	0,89
IS (%)	0,03	0,80
MSI (%)	-0,05	0,68
LVEF (%)	-0,16	0,34

Table 4.2: aIQP = absolute ischemic QRS prolongation, IS = infarct size, LV = left ventricular, LVEF = left ventricular ejection fraction, MaR = myocardium at risk, MSI = myocardial salvage index



Figure 4.5: ECG examples from a patient with a LAD occlusion (A) and a patient with an RCA occlusion (B). A) 12-lead ECG with maximum ST-deviation in lead V₂ (1) of 0.525 mV. Since there is a distinguished J-point, it is used as offset, resulting in a QRS duration at maximum ST deviation of 90 ms. Lead V₆ (2) was used as a reference, showing a QRS duration of 85 ms, resulting in an absolute ischemic QRS prolongation of 5 ms. B) 12-lead ECG with maximum ST-deviation in lead III (3) of 0.425 mV. Since no clear j point can be determined, the intersect method for QRS duration was applied, resulting in a QRS duration at maximum ST deviation of 150 ms. Lead I (4) was used as a reference, showing a QRS duration of 82 ms, resulting in an absolute ischemic QRS prolongation of 65 ms.

injury, IQP or G3I show no such correlation paper IV. Paper I show a mean aIQP of 49 ± 57 ms (mean \pm SD), in patients with a controlled experimental total coronary occlusion, compared to the median of 10 ms in paper IV. This could potentially be explained by less severe ischemia in the latter study population.

The findings so far suggest that IQP is of limited use in the clinical context of ACO (Paper IV). It would, however, be of clinical importance to investigate if IQP could be used as an indicator of severe ischemia in the pre-hospital setting, when the patient is earlier in the ischemic injury process, which more resembles the experimental situation where IQP has been shown to be useful (Paper I).

4.2 IQP and Malignant Arrhythmias

4.2.1 Reperfusion VF (canines; paper III)

Twelve dogs (57%) developed VF at 20 ± 11 s post-reperfusion. Mean aIQP was 47 ± 29 ms and differed significantly ($p=0.001$) from the 9 dogs that did not develop VF, 12 ± 10 ms (Figure 4.6).

An ROC analysis produced an optimum cut-off value of 21 ms with sensitivity of 92% and specificity of 89%. The AUC was 0.94 (95% CI 0,83 – 1,00)(Figure 4.7).

4.2.2 Out-of-Hospital Cardiac Arrest (paper V)

All of the IQP measures and aSTD were significantly higher in the OHCA group ($n=28$) compared to the non-OHCA group ($n=79$, Table 4.3, Figure 4.8-4.11), with the largest difference for $QRSd_{mSTD}$ (140 ± 54 ms vs 99 ± 25 ms; $p < 0.001$).

A ROC analysis was performed of the main variables. AUCs are presented in Table 4.4. $QRSd_{mSTD}$ had the largest AUC, 0.79 (CI; 0.68-0.90). The optimum cutoff was 99 ms and at this cutoff sensitivity was 79% and specificity 68%. OR for OHCA at $QRSd_{mSTD} > 99$ ms was 7.9 and when adjusted for co-morbidities it decreased to 6.5 (95% CI; 2.0 – 21.2). OR for 30-day mortality, adjusted for OHCA and co-morbidities was 32.0 (95% CI; 1.2 – 825.5). Figure 4.12 show example ECGs of large IQP (OHCA) and small IQP (non-OHCA), respectively.

For OHCA patients in the TTM study subpopulation not meeting STEMI or BBB criteria post-ROSC ($n=24$), the mean $QRSd_{cg}$ (101 ± 12 ms) was not different from the non-OHCA STEMI patients (98 ± 14 ms; $p=0.5$), but significantly shorter than the OHCA STEMI patients (112 ± 24 ms; $p=0.004$).

4.2.3 Discussion

According to the results of paper III an early QRS prolongation due to acute myocardial ischemia may have the potential to predict impending reperfusion VF, which is in accordance with the findings of Demidova *et al.* in an experimental pig model of myocardial

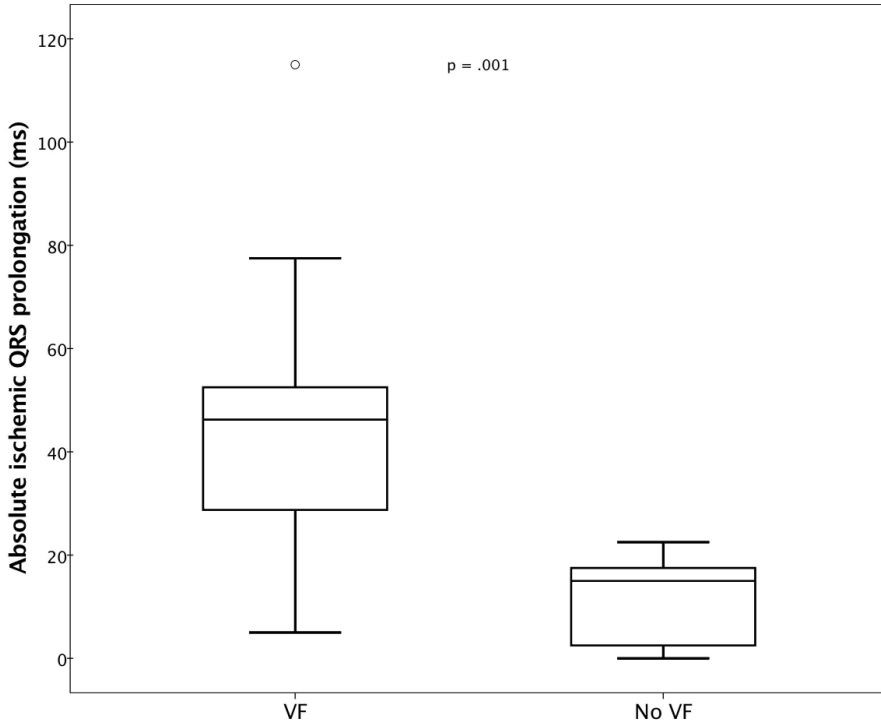


Figure 4.6: Box plot of reperfusion VF and no VF groups.

	STEMI		Non-STEMI
	Non-OHCA (n=79) Mean \pm SD (range)	OHCA (n=28) Mean \pm SD (range)	OHCA (n=24) Mean \pm SD (range)
QRSd _{cg} (ms)	98 \pm 14 (76-152)***	112 \pm 24 (76-178)	101 \pm 12 (80-130)**
QRSd _{mSTD} (ms)	99 \pm 25 (75-200)***	140 \pm 54 (67-300)	
Absolute IQP (ms)	17 \pm 23 (-10-115)***	40 \pm 43 (0-160)	
Relative IQP	0.22 \pm 0.27 (-0.12-1.53)*	0.38 \pm 0.38 (0-1.15)	
Absolute ST-segment deviation (mV)	0.33 \pm 0.19 (0.13-1.40)*	0.44 \pm 0.36 (0.15-2.00)	
Pathological Q-wave	23/79 (29%)**	16/27 (59%)	

Table 4.3: OHCA = Out-of-Hospital Cardiac Arrest; PCI = Percutaneous Coronary Intervention; LAD = Left anterior descending artery; RCA = Right coronary artery; LCX = Left circumflex artery.

Statistical significance indication is vs the STEMI OHCA group. * = $P \leq 0.05$; ** = $P \leq 0.01$; *** = $P \leq 0.001$

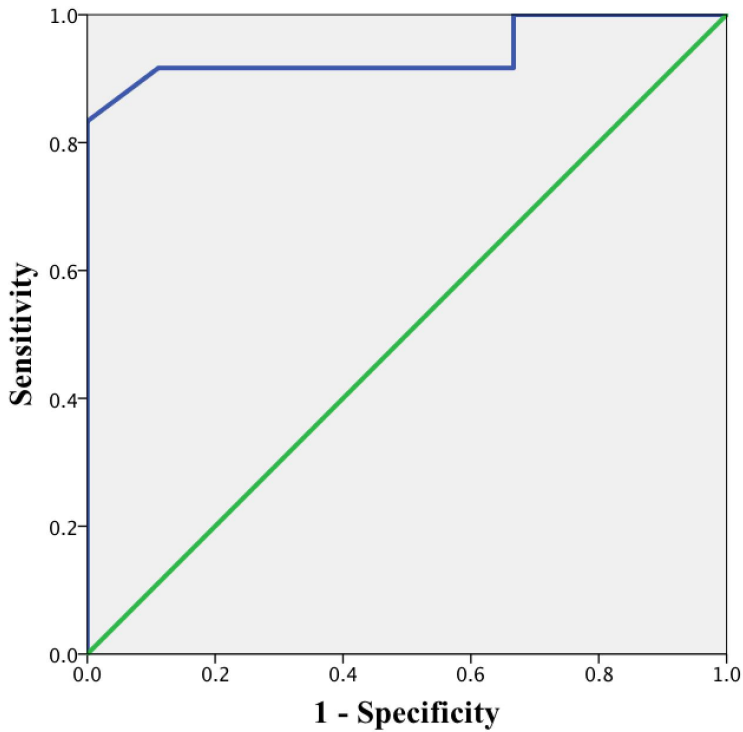


Figure 4.7: Blue line: ROC curve of aIQP indicating VF or not. Green line: reference line indicating an AUC of 0.5

	AUC (95% CI)
Computer generated QRS duration	0.68 (0.55 – 0.81)
QRS duration at max ST-deviation	0.79 (0.68 – 0.90)
Absolute IQP	0.63 (0.48 – 0.77)
Relative IQP	0.60 (0.46 – 0.74)
Absolute ST-segment deviation	0.60 (0.47 – 0.73)

Table 4.4: IQP = Ischemic QRS prolongation

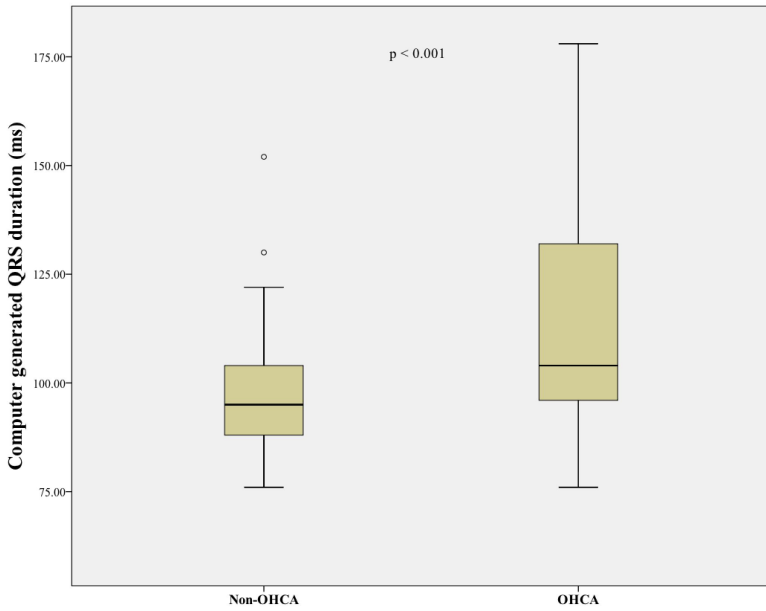


Figure 4.8: Box plots comparing OHCA or non-OHCA groups with regards to the computer generated QRS duration on the y-axis.

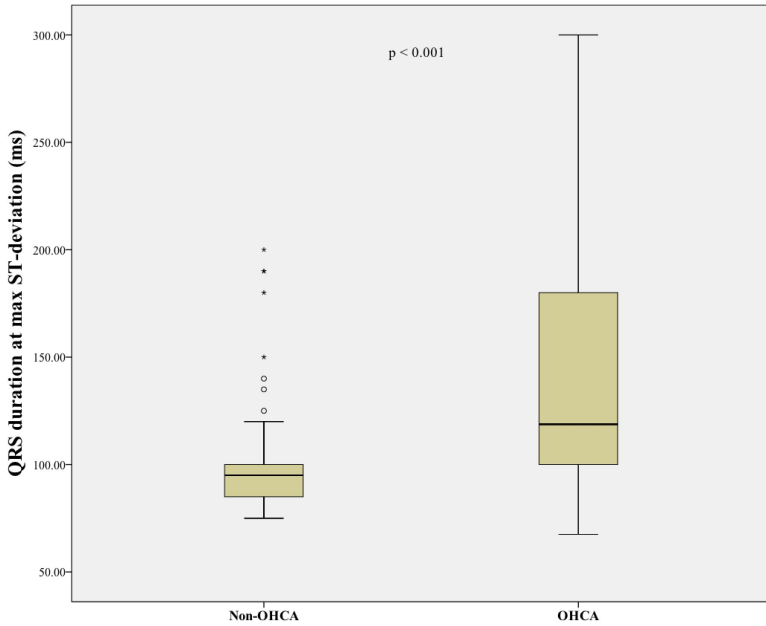


Figure 4.9: Box plots comparing OHCA or non-OHCA groups with regards to the QRS duration at max ST-deviation on the y-axis.

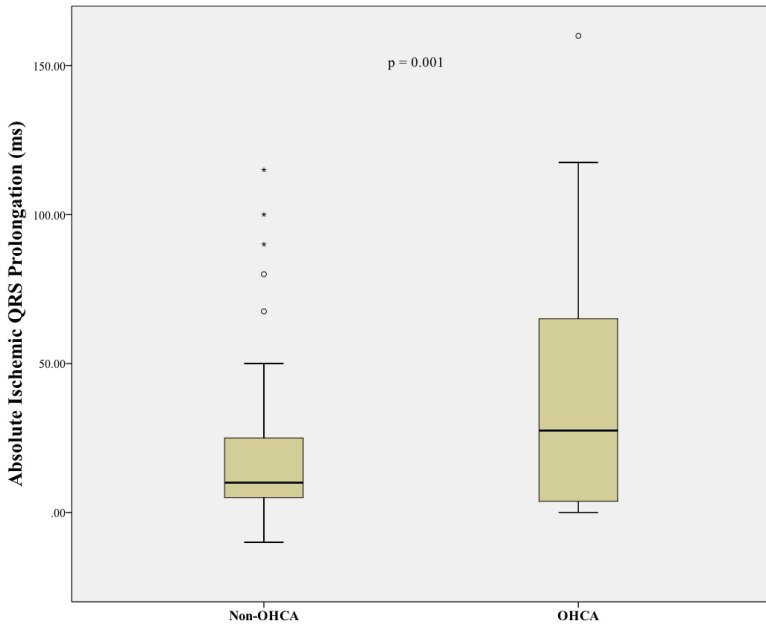


Figure 4.10: Box plots comparing OHCA or non-OHCA groups with regards to the absolute IQP on the y-axis.

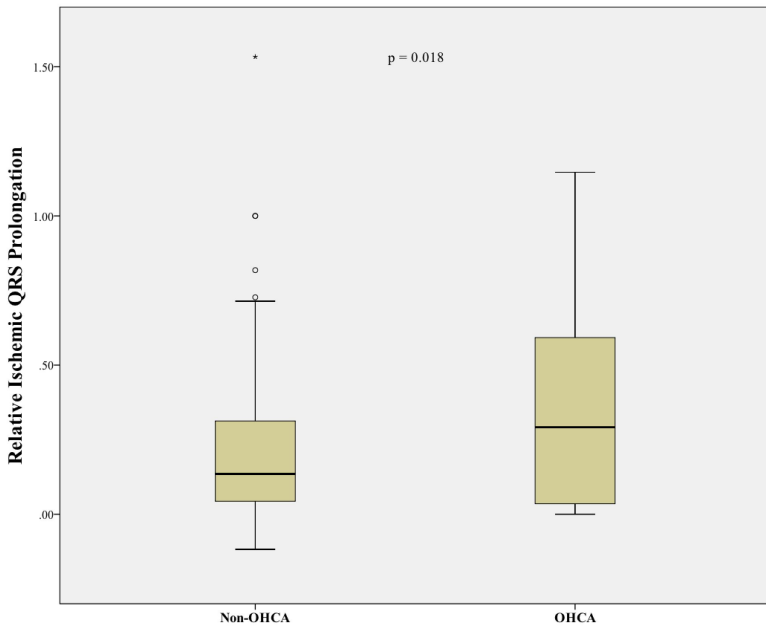


Figure 4.11: Box plots comparing OHCA or non-OHCA groups with regards to the relative IQP on the y-axis.

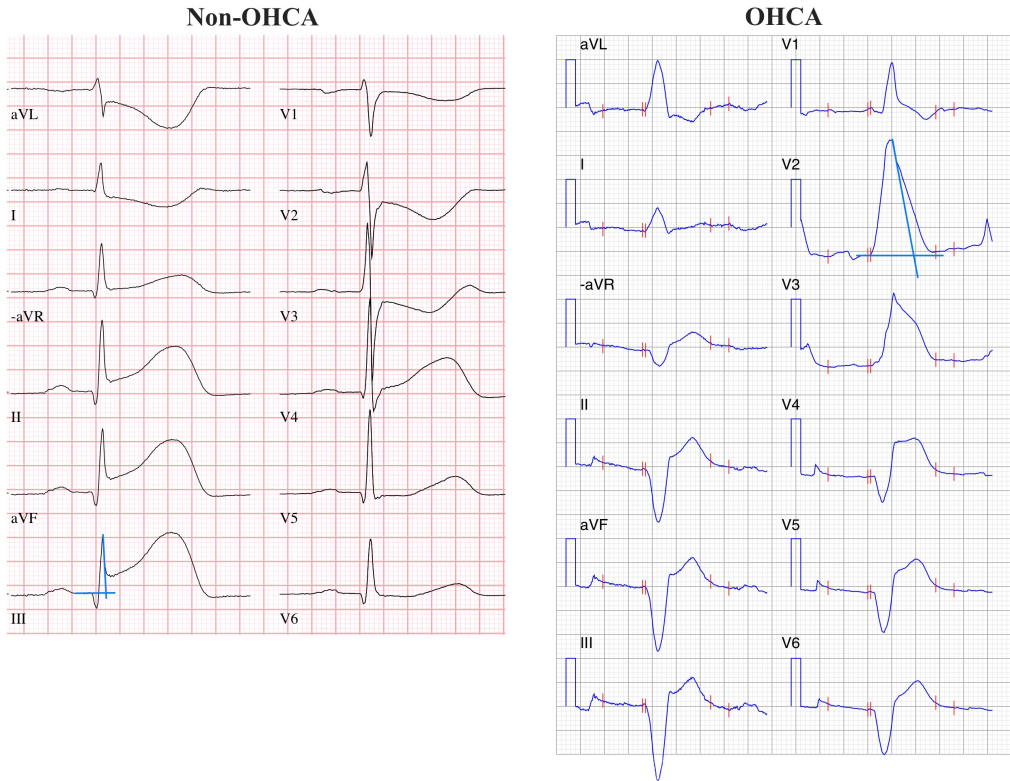


Figure 4.12: Non-OHCA. 12-lead ECG using the Cabrera format. Maximum ST-deviation in lead III was 0.35 mV. Here the ‘Almer method’ is being used, producing a $QRSd_{mSTD}$ of 80 ms. Lead V_5 was used as a reference. $QRSd_r$ was 80 ms. Thus, aIQP was 0 ms. **OHCA.** 12-lead ECG using the Cabrera format. Maximum ST-deviation in lead V_2 was 2.0 mV. Here the ‘Almer method’ is being used, producing a $QRSd_{mSTD}$ of 170 ms. The least amount of ST-deviation was found in lead I which was used as a reference. $QRSd_r$ was 105 ms. Thus, aIQP was 65 ms.

infarction. [144, 146, 174] Earlier studies have also found that similar patterns to the ones found in our population positively predict VF in humans, although not appreciated as QRS prolongation. [175] Furthermore, in paper I dogs with >5 ms of aIQP exhibited significantly lower collateral flow compared to dogs with ≤ 5 ms aIQP. Hence, the increased risk of developing VF in acute ischemic heart disease might be related to more severe myocardial ischemia due to lower coronary collateral flow.

Translating the results to a human population is, however, not necessarily straightforward. Within the study there were controlled experiments with total occlusion of the LCX in the dog. In a clinical setting this may differ widely where the initial thrombus may occlude the entire lumen of a vessel but also dissolve and/or add thrombus material continuously causing spontaneous reperfusion and/or reocclusion. While a spontaneous reperfusion in the acute phase of an AMI could be similar to the experimental setup, many

more factors affect a clinical situation such as vessel spasms, previous heart disease etc.. Furthermore, Hedström *et al.* describes the difference in infarct evolution, using MRI, between dog and human, where the time to reach 50% of myocardium at risk is about 59% longer in humans than dogs. [38] Therefore, 15 minutes of occlusion probably corresponds to a longer time period in a human clinical setting. Although the results from paper III have little implication in a clinical situation the results of paper V is in line with paper III where IQP is associated with a malignant arrhythmia (OHCA).

The results of paper V correlates to previous studies with regards to poor clinical outcome and the association of terminal QRS distortion to mortality. Within the paper, a cutoff of 99 ms using $QRSd_{mSTD}$ yielded a sensitivity of 79% with a specificity of 68% for OHCA. Adjusted OR was 6.5 for OHCA and 32.0 for 30-day mortality. Previous animal studies have shown similar results, where in a porcine model, IQP or 'QRS widening' was predictive of reperfusion VF. [144, 146] Mart *et al.* showed in pigs, using a threshold of 28 ms, that 8 out of 10 VF episodes could be predicted (sensitivity 80%, specificity 91%). [146] In a study by Demidova *et al.* a QRS widening of 28 ms during a 3-minute time window was observed in 14 pigs and also predicted impending VF (sensitivity 80%, specificity 73%). [144] Thus, together paper III and V showcase IQP as a potential ECG marker of malignant arrhythmias.

ROC analysis of paper V showed that the variable with greatest AUC was $QRSd_{mSTD}$ and not aIQP, which has been the focus of previous papers. Thus, there might be less need to measure the $QRSd_r$ at the lead with minimum STD in order to calculate aIQP. This simplifies the method and makes it more clinically applicable. A plausible explanation for the significance of $QRSd_{mSTD}$ and not aIQP could be same as to why QT dispersion was shown to have limited diagnostic value in the early 00's. [176] Even though some leads will be almost perpendicular to the main vector and show none or little IQP, the depolarization is a global event. Since there is a set number of leads in a set number of directions in space, there will often be cases when no lead is perfectly perpendicular to the main depolarization vector, resulting in a somewhat prolonged QRS duration in the so-called baseline lead, which affects the assessment of aIQP as an independent variable.

STD was considered in paper V and showed significant difference in the OHCA vs non-OHCA groups. In alignment with these results Weston *et al.* reported in a dog model that for a given magnitude of STE, the presence of concurrent QRS prolongation was associated with less myocardial salvage. [130] We performed a ROC analysis on STD showing, however, a significantly lower AUC compared to $QRSd_{mSTD}$.

Post-ROSC ECGs were used for the OHCA group. Pre-arrest ECG recordings would have been preferable, however, this is difficult to achieve. The post-ROSC ECG waveforms might be affected in many ways other than by regional ischemia caused by the coronary occlusion. The global myocardial ischemia during cardiac arrest could potentially cause IQP. However, QRS duration on the post-ROSC ECG was significantly shorter in the patients with OHCA with no sign of STEMI compared to those with STEMI, indicating that the global ischemia during cardiac arrest cannot explain the IQP seen in the OHCA

STEMI patients.

4.3 Clinical Significance

Current guidelines for treatment of STEMI recommend primary PCI if a PCI center is available within 120 min from first medical contact.[55–58] Stable patients with STEMI have better outcomes compared to those in whom the ischemia develops into a malignant arrhythmia and OHCA.[8] If patients at risk of OHCA could be identified, a potential treatment strategy would be to offer pre-hospital administration of fibrinolytic therapy before PCI in order to minimize the risk of developing malignant arrhythmia and OHCA, especially if there is a need for long transport. Renard *et al.* have shown that OHCA patients treated with fibrinolysis in ambulance have a higher chance of arriving at hospital alive.[72] In light of the results in the current thesis, IQP might serve as a novel pre-hospital biomarker for identification of these patients at risk of cardiac arrest.

To bring this concept further, to be used in a clinical situation with ongoing ischemia and threatening infarction, the method needs to be robust, reproducible and shown to add clinical value in terms of outcome. Larger studies performed on QRS prolongation as well as evaluation of the Sclarovsky-Birnbaum (SB) ischemia grading system have shown that QRS changes in STEMI patients could potentially be used as a means of risk stratification.[128, 129, 131] Furthermore, the SB grading system has shown a relationship between terminal QRS distortion and infarct size as well as outcomes.[128, 129] However, the present method adds the value of being independent of a distinct J point, and it also provides a continuous scale of QRS distortion, in contrast to the dichotomized SB grading scale. It, therefore, enables definition of cutoffs based on the desired sensitivity and specificity of the demanded application, i.e. risk stratification in STEMI patients. Furthermore, the criteria do not cover a reciprocal ST-segment depression of a posterior LCX occlusion, which IQP does.

Chapter 5

Conclusions

Paper I

IQP correlates to collateral arterial flow during acute ischemia in an experimental canine model and the same pattern of ischemic QRS prolongation occurs in patients with CAD undergoing prolonged, elective angioplasty balloon inflation.

Paper II

This paper presents a 12-lead ECG method for estimating IQP. Using the proposed method, we are able to identify and quantify IQP independent of a distinct J point and without a prior baseline ECG.

Paper III

There was a significant difference in IQP between dogs developing VF after reperfusion of an ACO and those who did not. Thus, an early QRS prolongation due to acute myocardial ischemia may have the potential to predict impending reperfusion VF.

Paper IV

Unlike paper I, IQP was limited in patients presenting at the emergency room with first-time STEMI and no correlation was found between IQP and CMR variables of myocardial injury. Therefore, IQP does not seem to be a suitable biomarker for triaging patients in this clinical context.

Paper V

IQP in the situation of an acute coronary occlusion may be associated with a risk of OHCA and might therefore have a potential role as a biomarker for risk assessment in patients with acute STEMI.

5.1 Compiled Conclusion and Future Directions

In summary, the current thesis takes a new look at the concept of terminal QRS distortion during acute myocardial ischemia. IQP quantifies terminal QRS distortion, collateral flow and probably the severity of the ischemia. Bringing this concept from canine studies to human data further elucidates the applicability. Stable STEMI patients does not seem to have significant IQP, especially compared to OHCA patients, and in this patient group the novel method does not seem to add much value. However, a significant IQP seems to be associated with malignant arrhythmias, both reperfusion VF in canines and OHCA in patients. The underlying pathophysiologic mechanisms are, however, different for these two conditions, one being reperfusion-induced and the other ischemia-induced. The presence of significant IQP seems, however, to be able to identify these patients. It is, therefore, of outmost importance to promote further research of IQP as a biomarker of severe ischemia since it has potential to serve as an identifier of STEMI patients in risk of malignant arrhythmias and very poor prognosis.

There are several future directions to consider. First, an investigation into presence of IQP in patients with chest pain, who have recorded an ECG, by ambulance personnel, before they suffer from a CA. We believe that IQP is strongly associated with OHCA but do not know if it is able to predict it. Second, the applicability of IQP in the clinic must be investigated. Are cardiologists able to learn how to measure IQP? Is it cumbersome and will it distract them from giving the patient the best care available? Third, a prospective study of STEMI patients admitted to the PCI lab and cardiac ICU with and without significant IQP, investigating several outcomes but especially presence of malignant arrhythmias, would be preferable. Fourth, the end goal for IQP as an identification method of at risk STEMI patients is, given further positive studies, a clinical trial comparing traditional PCI treatment to in-ambulance fibrinolytics and rescue PCI in STEMI patients with significant IQP. Theoretically, early fibrinolytic therapy with later rescue PCI might minimize risk and prevent the development of malignant arrhythmias and OHCA.

References

- [1] A. D. Lopez, C. D. Mathers, M. Ezzati, D. T. Jamison, and C. J. Murray. Global and regional burden of disease and risk factors, 2001: systematic analysis of population health data. *Lancet*, 367(9524):1747–1757, 6 2006.
- [2] Sveriges officiella statistik. Statistik om hjärtinfarkter 2016. Technical report, Socialstyrelsen, 2017.
- [3] M. J. Juntila, E. Hookana, K. S. Kaikkonen, M. L. Kortelainen, R. J. Myerburg, and H. V. Huikuri. Temporal Trends in the Clinical and Pathological Characteristics of Victims of Sudden Cardiac Death in the Absence of Previously Identified Heart Disease. *Circulation: Arrhythmia and Electrophysiology*, 9(6), 2016.
- [4] A. Farb, A. L. Tang, A. P. Burke, L. Sessums, Y. Liang, and R. Virmani. Sudden coronary death: Frequency of active coronary lesions, inactive coronary lesions, and myocardial infarction. *Circulation*, 92(7):1701–1709, 1995.
- [5] C. Sasson, M. A. M. Rogers, J. Dahl, and A. L. Kellermann. Predictors of survival from out-of-hospital cardiac arrest: a systematic review and meta-analysis. *Circulation. Cardiovascular quality and outcomes*, 3(1):63–81, 2010.
- [6] J. Berdowski, R. A. Berg, J. G. P. Tijssen, and R. W. Koster. Global incidences of out-of-hospital cardiac arrest and survival rates: Systematic review of 67 prospective studies. *Resuscitation*, 81(11):1479–1487, 2010.
- [7] C. Atwood, M. S. Eisenberg, J. Herlitz, and T. D. Rea. Incidence of EMS-treated out-of-hospital cardiac arrest in Europe. *Resuscitation*, 67(1):75–80, 2005.
- [8] A. Myat, K. J. Song, and T. Rea. Out-of-hospital cardiac arrest: current concepts. *The Lancet*, 391(10124):970–979, 2018.
- [9] J. Engdahl, M. Holmberg, B. W. Karlson, R. Luepker, and J. Herlitz. The epidemiology of out-of-hospital 'sudden' cardiac arrest. *Resuscitation*, 52(3):235–245, 2002.

- [10] C. Hawkes, S. Booth, C. Ji, S. J. Brace-McDonnell, A. Whittington, J. Mapstone, M. W. Cooke, C. D. Deakin, C. P. Gale, R. Fothergill, J. P. Nolan, N. Rees, J. Soar, A. N. Siriwardena, T. P. Brown, and G. D. Perkins. Epidemiology and outcomes from out-of-hospital cardiac arrests in England. *Resuscitation*, 110(1): 133–140, 2017.
- [11] C. M. Spaulding, L.-M. Joly, A. Rosenberg, M. Monchi, S. N. Weber, J.-F. A. Dhainaut, and P. Carli. Immediate Coronary Angiography in Survivors of Out-of-Hospital Cardiac Arrest. *New England Journal of Medicine*, 336(23):1629–1633, 1997.
- [12] F. Crea and G. Liuzzo. Pathogenesis of acute coronary syndromes. *Journal of the American College of Cardiology*, 61(1):1–11, 2013.
- [13] K. J. Woollard and F. Geissmann. Monocytes in atherosclerosis: subsets and functions. *Nature Reviews Cardiology*, 7(2):77–86, 2 2010.
- [14] P. Ridker, P. Libby, and J. Buring. Chapter 45. Risk Markers and the Primary Prevention of Cardiovascular Disease. In D. P. Zipes, P. Libby, R. Bonow, D. Mann, and G. Tomaselli, editors, *Braunwald's Heart Disease 11th Edition*, chapter 45, pages 876–910. Elsevier Inc., Philadelphia, 11 edition, 2018.
- [15] P. Libby. Molecular bases of the acute coronary syndromes. *Circulation*, 91(11): 2844–2850, 1995.
- [16] P. Libby. Mechanisms of Acute Coronary Syndromes and Their Implications for Therapy. *New England Journal of Medicine*, 368(21):2004–2013, 2013.
- [17] R. W. Nesto and G. J. Kowalchuk. The ischemic cascade: Temporal sequence of hemodynamic, electrocardiographic and symptomatic expressions of ischemia. *The American Journal of Cardiology*, 59(7), 1987.
- [18] G. Embden, H. J. Deuticke, and G. Kraft. Über die Intermediären Vorgänge bei der Glykolyse in der Muskulatur. *Klinische Wochenschrift*, 12(6):213–215, 1933.
- [19] E. Annau, I. Banga, A. Blazsó, V. Bruekner, K. Laki, F. B. Straub, and A. Szent-Györgyi. Über die Bedeutung der Fumarsäure für die tierische Gewebsatmung: III. Mitteilung. *Hoppe-Seyler's Zeitschrift für Physiologische Chemie*, 244(3-4):105–116, 1936.
- [20] H. A. Krebs and W. A. Johnson. Metabolism of ketonic acids in animal tissues. *The Biochemical journal*, 31(4):645–60, 1937.
- [21] A. L. Lehninger. Fatty acid oxidation and the Krebs trocarboxylic acid cycle. *The Journal of biological chemistry*, 161:413, 1945.

- [22] A. L. Lehninger. The oxidation of higher fatty acids in heart muscle suspensions. *The Journal of biological chemistry*, 165(1):131–145, 1946.
- [23] R. B. Jennings and C. E. Ganote. Mitochondrial structure and function in acute myocardial ischemic injury. *Circ Res*, 38:80–91, 1976.
- [24] D. J. Duncker and J. M. Canty. Chapter 57. Coronary Blood Flow and Myocardial Ischemia. In D. P. Zipes, P. Libby, R. Bonow, D. Mann, and G. Tomaselli, editors, *Braunwald's Heart Disease 11th Edition*, chapter 57, pages 1069–1094. Elsevier Inc., Philadelphia, 11 edition, 2018.
- [25] R. B. Jennings and C. E. Ganote. Structural Changes in Myocardium During Acute Ischemia. *Circulation Research*, 35(III):156–172, 1974.
- [26] R. B. Jennings, J. Schaper, M. L. Hill, C. Steenbergen, and K. a. Reimer. Effect of reperfusion late in the phase of reversible ischemic injury. Changes in cell volume, electrolytes, metabolites, and ultrastructure. *Circulation research*, 56(2):262–278, 2 1985.
- [27] P. L. Vághy. Role of mitochondrial oxidative phosphorylation in the maintenance of intracellular pH. *Journal of Molecular and Cellular Cardiology*, 11(10):933–940, 1979.
- [28] R. A. Robergs, F. Ghiasvand, and D. Parker. Biochemistry of exercise-induced metabolic acidosis. *AJP: Regulatory, Integrative and Comparative Physiology*, 287 (3):R502–R516, 2004.
- [29] S. E. Anderson, E. Murphy, C. Steenbergen, R. E. London, and P. M. Cala. Na-H exchange in myocardium: effects of hypoxia and acidification on Na and Ca. *The American journal of physiology*, 259(6 Pt 1):C940–C948, 1990.
- [30] A. Meissner and J. P. Morgan. Contractile dysfunction and abnormal Ca²⁺ modulation during postischemic reperfusion in rat heart. *Am J Physiol*, 268(1 Pt 2): 100–11, 1995.
- [31] S. A. Camacho, V. M. Figueredo, R. Brandes, and M. W. Weiner. Ca(2+)-dependent fluorescence transients and phosphate metabolism during low-flow ischemia in rat hearts. *The American journal of physiology*, 265(1 Pt 2):114–22, 1993.
- [32] C. Sylvén. Mechanisms of pain in angina pectoris-A critical review of the adenosine hypothesis. *Cardiovascular Drugs and Therapy*, 7(5):745–759, 1993.
- [33] K. A. Reimer and R. B. Jennings. The "wavefront phenomenon" of myocardial ischemic cell death. II. Transmural progression of necrosis within the framework of ischemic bed size (myocardium at risk) and collateral flow. *Laboratory investigation; a journal of technical methods and pathology*, 40(6):633–44, 1979.

- [34] B. Ibanez, S. James, S. Agewall, M. J. Antunes, C. Bucciarelli-Ducci, H. Bueno, A. L. Caforio, F. Crea, J. A. Goudevenos, S. Halvorsen, G. Hindricks, A. Kasrati, M. J. Lenzen, E. Prescott, M. Roffi, M. Valgimigli, C. Varenhorst, P. Vranckx, P. Widimský, A. Baumbach, R. Bugiardini, I. M. Coman, V. Delgado, D. Fitzsimons, O. Gaemperli, A. H. Gershlick, S. Gielen, V. P. Harjola, H. A. Katus, J. Knuuti, P. Kolh, C. Leclercq, G. Y. Lip, J. Morais, A. N. Neskovic, F. J. Neumann, A. Niessner, M. F. Piepoli, D. J. Richter, E. Shlyakhto, I. A. Simpson, P. G. Steg, C. J. Terkelsen, K. Thygesen, S. Windecker, J. L. Zamorano, and U. Zeymer. 2017 ESC Guidelines for the management of acute myocardial infarction in patients presenting with ST-segment elevation. *European Heart Journal*, 39(2), 2018.
- [35] M. Roffi, C. Patrono, J.-P. Collet, C. Mueller, M. Valgimigli, F. Andreotti, J. J. Bax, M. A. Borger, C. Brotons, D. P. Chew, B. Gencer, G. Hasenfuss, K. Kjeldsen, P. Lancellotti, U. Landmesser, J. Mehilli, D. Mukherjee, R. F. Storey, and S. Windecker. 2015 ESC Guidelines for the management of acute coronary syndromes in patients presenting without persistent ST-segment elevation. *European Heart Journal*, 37(3):213–215, 2015.
- [36] R. B. Jennings and G. S. Wagner. Roles of collateral arterial flow and ischemic preconditioning in protection of acutely ischemic myocardium. *Journal of Electrocardiology*, 47(4):491–499, 7 2014.
- [37] B. M. Scirica, P. Libby, and D. Morrow. Chapter 58: ST-elevation Myocardial Infarction, Pathophysiology and Clinical Evolution. In D. P. Zipes, P. Libby, R. Bonow, D. Mann, and G. Tomaselli, editors, *Braunwald's Heart Disease 11th Edition*, chapter 58, pages 1095–1123. Elsevier Inc., Philadelphia, 11 edition, 2018.
- [38] E. Hedström, H. Engblom, F. Frogner, K. Aström-Olsson, H. Ohlin, S. Jovinge, and H. Arheden. Infarct evolution in man studied in patients with first-time coronary occlusion in comparison to different species - implications for assessment of myocardial salvage. *Journal of cardiovascular magnetic resonance : official journal of the Society for Cardiovascular Magnetic Resonance*, 11(1):38, 2009.
- [39] J. S. Floyd, C. Maynard, P. Weston, P. Johanson, R. B. Jennings, and G. S. Wagner. Effects of ischemic preconditioning and arterial collateral flow on ST-segment elevation and QRS complex prolongation in a canine model of acute coronary occlusion. *Journal of Electrocardiology*, 42(1):19–26, 1 2009.
- [40] C. E. Murry, R. B. Jennings, and K. a. Reimer. Preconditioning with ischemia: a delay of lethal cell injury in ischemic myocardium. *Circulation*, 74(5):1124–1136, 11 1986.

- [41] K. Thygesen, J. S. Alpert, A. S. Jaffe, M. L. Simoons, B. R. Chaitman, and H. D. White. Third universal definition of myocardial infarction. *Journal of the American College of Cardiology*, 60(16):1581–1598, 2012.
- [42] G. W. Reed, J. E. Rossi, and C. P. Cannon. Acute myocardial infarction. *The Lancet*, 389(10065):197–210, 2017.
- [43] P. Meier, S. Gloekler, R. Zbinden, S. Beckh, S. F. De Marchi, S. Zbinden, K. Wustmann, M. Billinger, R. Vogel, S. Cook, P. Wenaweser, M. Togni, S. Windecker, B. Meier, and C. Seiler. Beneficial effect of recruitable collaterals: A 10-year follow-up study in patients with stable coronary artery disease undergoing quantitative collateral measurements. *Circulation*, 116(9):975–983, 2007.
- [44] C. E. Murry, V. J. Richard, K. A. Reimer, and R. B. Jennings. Ischemic preconditioning slows energy metabolism and delays ultrastructural damage during a sustained ischemic episode. *Circulation research*, 66(4):913–931, 4 1990.
- [45] J. C. Garcia-Rubira, I. Nuñez-Gil, R. Garcia-Borbolla, M. C. Manzano, A. Fernandez-Ortiz, M. A. Cobos, L. P. De Isla, R. Hernández, and C. Macaya. Distortion of the terminal portion of the QRS is associated with poor collateral flow before and poor myocardial perfusion after percutaneous revascularization for myocardial infarction. *Coronary Artery Disease*, 19(6):389–393, 2008.
- [46] P. J. Sabia, E. R. Powers, M. Ragosta, I. J. Sarembock, L. R. Burwell, and S. Kaul. An association between collateral blood flow and myocardial viability in patients with recent myocardial infarction. *The New England journal of medicine*, 327(26):1825–31, 1992.
- [47] R. Charney and M. Cohen. The role of the coronary collateral circulation in limiting myocardial ischemia and infarct size. *American Heart Journal*, 126(4):937–945, 1993.
- [48] W. Schaper and W. D. Ito. Molecular mechanisms of coronary collateral vessel growth. *Circulation Research*, 79(5):911–919, 1996.
- [49] W. Schaper. Collateral circulation. Past and present. *Basic Research in Cardiology*, 104(1):5–21, 2009.
- [50] J. M. Canty and G. Suzuki. Myocardial perfusion and contraction in acute ischemia and chronic ischemic heart disease. *Journal of Molecular and Cellular Cardiology*, 52(4):822–831, 2012.
- [51] P. T. O’Gara, F. G. Kushner, D. D. Ascheim, D. E. Casey, M. K. Chung, J. A. de Lemos, S. M. Ettinger, J. C. Fang, F. M. Fesmire, B. A. Franklin, C. B. Granger,

- H. M. Krumholz, J. A. Linderbaum, D. A. Morrow, L. K. Newby, J. P. Ornato, N. Ou, M. J. Radford, J. E. Tamis-Holland, C. L. Tommaso, C. M. Tracy, Y. J. Woo, and D. X. Zhao. 2013 ACCF/AHA Guideline for the Management of ST-Elevation Myocardial Infarction: A Report of the American College of Cardiology Foundation/American Heart Association Task Force on Practice Guidelines. *Circulation*, 127(4):e362–e425, 2013.
- [52] S. Windecker, P. Kolh, F. Alfonso, J.-P. Collet, J. Cremer, V. Falk, G. Filippatos, C. Hamm, S. J. Head, P. Jüni, A. P. Kappetein, A. Kastrati, J. Knuuti, U. Landmesser, G. Laufer, F.-J. Neumann, D. J. Richter, P. Schauerte, M. Sousa Uva, G. G. Stefanini, D. P. Taggart, L. Torracca, M. Valgimigli, W. Wijns, and A. Witkowski. 2014 ESC/EACTS Guidelines on myocardial revascularization. *European Heart Journal*, 35(37):2541–2619, 10 2014.
- [53] P. G. Steg, S. K. James, D. Atar, L. P. Badano, C. B. Lundqvist, M. A. Borger, C. Di Mario, K. Dickstein, G. Ducrocq, F. Fernandez-Aviles, A. H. Gershlick, P. Gianniuzzi, S. Halvorsen, K. Huber, P. Juni, A. Kastrati, J. Knuuti, M. J. Lenzen, K. W. Mahaffey, M. Valgimigli, A. Van’T Hof, P. Widimsky, D. Zahger, J. J. Bax, H. Baumgartner, C. Ceconi, V. Dean, C. Deaton, R. Fagard, C. Funck-Brentano, D. Hasdai, A. Hoes, P. Kirchhof, P. Kolh, T. McDonagh, C. Moulin, B. A. Popescu, Ø. Reiner, U. Sechtem, P. A. Sirnes, M. Tendera, A. Torbicki, A. Vahanian, S. Windecker, F. Astin, K. Åström-Olsson, A. Budaj, P. Clemmensen, J. P. Collet, K. A. Fox, A. Fuat, O. Gustiene, C. W. Hamm, P. Kala, P. Lancellotti, A. P. Maggioni, B. Merkely, F. J. Neumann, M. F. Piepoli, F. Van De Werf, F. Verheugt, and L. Wallentin. ESC Guidelines for the management of acute myocardial infarction in patients presenting with ST-segment elevation. *European Heart Journal*, 33(20):2569–2619, 2012.
- [54] C. P. Cannon. Relationship of Symptom-Onset-to-Balloon Time and Door-to-Balloon Time With Mortality in Patients Undergoing Angioplasty for Acute Myocardial Infarction. *JAMA*, 283(22):2941, 2000.
- [55] E. R. Joy, J. Kurian, and C. P. Gale. Comparative effectiveness of primary PCI versus fibrinolytic therapy for ST elevation myocardial infarction: a review of the literature. *Journal of comparative effectiveness research*, 5(2):217–26, 3 2016.
- [56] F. Liu, Q. Guo, G. Xie, H. Zhang, Y. Wu, and L. Yang. Percutaneous Coronary Intervention after Fibrinolysis for ST-Segment Elevation Myocardial Infarction Patients: An Updated Systematic Review and Meta-Analysis. *PLOS ONE*, 10(11): e0141855, 11 2015.
- [57] X. Carrillo, E. Fernandez-Nofrerias, O. Rodriguez-Leor, T. Oliveras, J. Serra, J. Mauri, A. Curos, F. Rueda, C. García-García, R. Tresserras, A. Rosas, M. T.

- Faixedas, A. Bayes-Genis, and Codi IAM Investigators. Early ST elevation myocardial infarction in non-capable percutaneous coronary intervention centres: in situ fibrinolysis vs. percutaneous coronary intervention transfer. *European Heart Journal*, 37(13):1034–1040, 4 2016.
- [58] A. Solhpour and S. W. Yusuf. Fibrinolytic therapy in patients with ST-elevation myocardial infarction. *Expert Review of Cardiovascular Therapy*, 12(2):201–215, 2 2014.
- [59] M. Busk, M. Maeng, K. Rasmussen, H. Kelbaek, P. Thayssen, U. Abildgaard, E. Vigholt, L. S. Mortensen, L. Thuesen, S. D. Kristensen, T. T. Nielsen, and H. R. Andersen. The Danish multicentre randomized study of fibrinolytic therapy vs. primary angioplasty in acute myocardial infarction (the DANAMI-2 trial): Outcome after 3 years follow-up. *European Heart Journal*, 29(10):1259–1266, 2008.
- [60] P. Widimský, T. Budesinsky, D. Voráč, L. Groch, M. Želízko, M. Aschermann, M. Branny, J. Štřásek, and P. Formánek. Long distance transport for primary angioplasty vs immediate thrombolysis in acute myocardial infarction: Final results of the randomized national multicentre trial-PRAGUE-2. *European Heart Journal*, 24(1):94–104, 2003.
- [61] M. M. Zhu, A. Feit, H. Chadow, M. Alam, T. Kwan, and L. T. Clark. Primary Stent Implantation Compared With Primary Balloon Angioplasty for Acute Myocardial Infarction: A Meta-Analysis of Randomized Clinical Trials. *Am J Cardiol*, 88:297–301, 2001.
- [62] A. J. Nordmann, P. Hengstler, T. Harr, J. Young, and H. C. Bucher. Clinical outcomes of primary stenting versus balloon angioplasty in patients with myocardial infarction: a meta-analysis of randomized controlled trials. *The American Journal of Medicine*, 116(4):253–262, 2004.
- [63] J. F. Lassen, H. E. Bøtker, and C. J. Terkelsen. Timely and optimal treatment of patients with STEMI. *Nature Reviews Cardiology*, 10(1):41–48, 2013.
- [64] E. A. Amsterdam, N. K. Wenger, R. G. Brindis, D. E. Casey, T. G. Ganiats, D. R. Holmes, A. S. Jaffe, H. Jneid, R. F. Kelly, M. C. Kontos, G. N. Levine, P. R. Liebson, D. Mukherjee, E. D. Peterson, M. S. Sabatine, R. W. Smalling, and S. J. Ziemman. 2014 AHA/ACC Guideline for the Management of Patients With Non-ST-Elevation Acute Coronary Syndromes. *Journal of the American College of Cardiology*, 64(24):e139–e228, 12 2014.
- [65] F. W. Mohr, M.-C. Morice, A. P. Kappetein, T. E. Feldman, E. Stähle, A. Colombo, M. J. Mack, D. R. Holmes, M.-a. Morel, N. V. Dyck, V. M. Houle, K. D. Dawkins,

- and P. W. Serruys. Coronary artery bypass graft surgery versus percutaneous coronary intervention in patients with three-vessel disease and left main coronary disease: 5-year follow-up of the randomised, clinical SYNTAX trial. *The Lancet*, 381(9867): 629–638, 2 2013.
- [66] GUSTO Trial. An International Randomized Trial Comparing Four Thrombolytic Strategies for Acute Myocardial Infarction. *New England Journal of Medicine*, 329(10):673–682, 1993.
- [67] R. G. Wilcox. Randomised, double-blind comparison of reteplase double-bolus administration with streptokinase in acute myocardial infarction (INJECT): trial to investigate equivalence. International Joint Efficacy Comparison of Thrombolytics. *The Lancet*, 346(8971):329–336, 1995.
- [68] J. K. French, T. A. Hyde, H. Patel, D. J. Amos, S. C. McLaughlin, B. J. Webber, and H. D. White. Survival 12 years after randomization to streptokinase: The influence of thrombolysis in myocardial infarction flow at three to four weeks. *Journal of the American College of Cardiology*, 34(1):62–69, 1999.
- [69] Fibrinolytic Therapy Trialists’ (FTT) Collaborative Group. Indications for fibrinolytic therapy in suspected acute myocardial infarction: collaborative overview of early mortality and major morbidity results from all randomised trials of more than 1000 patients. *The Lancet*, 343(8893):311–322, 1994.
- [70] H. R. Andersen, T. T. Nielsen, K. Rasmussen, L. Thuesen, H. Kelbaek, P. Thayssen, U. Abildgaard, F. Pedersen, J. K. Madsen, P. Grande, A. B. Villadsen, L. R. Krusell, T. Haghfelt, P. Lomholt, S. E. Husted, E. Vigholt, H. K. Kjaergard, L. S. Mortensen, and DANAMI-2 Investigators. A comparison of coronary angioplasty with fibrinolytic therapy in acute myocardial infarction. *The New England journal of medicine*, 349(8):733–42, 2003.
- [71] E. C. Keeley, J. A. Boura, and C. L. Grines. Primary angioplasty versus intravenous thrombolytic therapy for acute myocardial infarction: A quantitative review of 23 randomised trials. *Lancet*, 361(9351):13–20, 2003.
- [72] A. Renard, C. Verret, D. Jost, J.-B. Meynard, J. Tricehreau, O. Hersan, D. Fontaine, F. Briche, P. Benner, O. de Stabenrath, C. Bartou, N. Segal, and L. Domanski. Impact of fibrinolysis on immediate prognosis of patients with out-of-hospital cardiac arrest. *Journal of Thrombosis and Thrombolysis*, 32(4):405–409, 11 2011.
- [73] Y. Rudy. Molecular basis of cardiac action potential repolarization. *Annals of the New York Academy of Sciences*, 1123:113–118, 2008.

- [74] L. F. Santana, E. P. Cheng, and W. J. Lederer. How does the shape of the cardiac action potential control calcium signaling and contraction in the heart? *Journal of Molecular and Cellular Cardiology*, 49(6):901–903, 12 2010.
- [75] M. Morad and L. Tung. Ionic events responsible for the cardiac resting and action potential. *The American Journal of Cardiology*, 49(3):584–594, 1982.
- [76] M. Grunnet. Repolarization of the cardiac action potential. Does an increase in repolarization capacity constitute a new anti-arrhythmic principle? *Acta Physiologica*, 198(SUPPL. 676):1–48, 2010.
- [77] S. Kurtenbach, S. Kurtenbach, and G. Zoidl. Gap junction modulation and its implications for heart function. *Frontiers in Physiology*, 5:82, 2014.
- [78] G. Tomaselli, M. Rubart, and D. P. Zipes. Chapter 34: Mechanisms of Cardiac Arrhythmias. In D. P. Zipes, P. Libby, R. Bonow, D. Mann, and G. Tomaselli, editors, *Braunwald's Heart Disease 11th Edition*, chapter 34, pages 619–647. Elsevier Inc., Philadelphia, 11 edition, 2018.
- [79] H. T. Shih. Anatomy of the action potential in the heart. *Texas Heart Institute journal / from the Texas Heart Institute of St. Luke's Episcopal Hospital, Texas Children's Hospital*, 21(1):30–41, 1994.
- [80] J. T. Koivumäki, T. Korhonen, and P. Tavi. Impact of Sarcoplasmic Reticulum Calcium Release on Calcium Dynamics and Action Potential Morphology in Human Atrial Myocytes: A Computational Study. *PLoS Computational Biology*, 7(1): e1001067, 1 2011.
- [81] A. O. Verkerk, A. C. van Ginneken, and R. Wilders. Pacemaker activity of the human sinoatrial node: Role of the hyperpolarization-activated current, *I_f*. *International Journal of Cardiology*, 132(3):318–336, 3 2009.
- [82] D. DiFrancesco. The Role of the Funny Current in Pacemaker Activity. *Circulation Research*, 106(3):434–446, 2 2010.
- [83] B. Joung, P.-S. Chen, and S.-F. Lin. The Role of the Calcium and the Voltage Clocks in Sinoatrial Node Dysfunction. *Yonsei Medical Journal*, 52(2):211, 3 2011.
- [84] R. B. Clark, M. E. Mangoni, A. Lueger, B. Couette, J. Nargeot, and W. R. Giles. A rapidly activating delayed rectifier K⁺ current regulates pacemaker activity in adult mouse sinoatrial node cells. *Am J Physiol Heart Circ Physiol*, 286(5):H1757–H1766, 2004.
- [85] P. Kligfield. The centennial of the Einthoven electrocardiogram. *Journal of Electrocardiology*, 35:123–129, 2002.

- [86] M. Rivera-Ruiz, C. Cajavilca, and J. Varon. Einthoven's string galvanometer: the first electrocardiograph. *Texas Heart Institute journal*, 35(2):174–8, 2008.
- [87] T. N. Raju. The Nobel chronicles. 1924: Willem Einthoven (1860-1927). *Lancet (London, England)*, 352(9139):1560, 11 1998.
- [88] J. B. Sanderson and F. J. M. Page. Experimental Results Relating to the Rhythmical and Excitatory Motions of the Ventricle of the Heart of the Frog, and of the Electrical Phenomena Which Accompany Them. *Proceedings of the Royal Society of London*, 27 (185-189):410–414, 1 1878.
- [89] A. D. Waller. A Demonstration on Man of Electromotive Changes accompanying the Heart's Beat. *The Journal of physiology*, 8(5):229–34, 10 1887.
- [90] J. W. Hurst. Naming of the waves in the ECG, with a brief account of their genesis. *Circulation*, 98(18):1937–42, 11 1998.
- [91] Einthoven W. Ueber die Form des menschlichen Electrocardiogramms. *Arch f d Ges Physiol*, 60:101–123, 1895.
- [92] W. Einthoven. Le telecardiogramme. *Arch Int de Physiol*, 4:132–164, 1906.
- [93] J. K. Cooper. Electrocardiography 100 years ago. Origins, pioneers, and contributors. *New England Journal of Medicine*, 315(7):461–464, 8 1986.
- [94] H. E. B. Pardee. An electrocardiographic sign of coronary artery obstruction. *Archives of Internal Medicine*, 26:244–257, 1920.
- [95] F. N. Wilson, F. D. Johnston, A. G. Macleod, and P. S. Barker. Electrocardiograms that represent the potential variations of a single electrode. *American Heart Journal*, 9(4):447–458, 1934.
- [96] A. Barnes, H. E. B. Pardee, P. White, F. N. Wilson, and C. Wolfarth. Standardization of Precordial Leads. *Am Heart J*, 15:235–239, 1938.
- [97] E. Goldberger. A simple, indifferent, electrocardiographic electrode of zero potential and a technique of obtaining augmented, unipolar, extremity leads. *American Heart Journal*, 23:483–492, 1942.
- [98] D. M. Mirvis and A. L. Goldberger. Chapter 12: Electrocardiography. In D. P. Zipes, P. Libby, R. Bonow, D. Mann, and G. Tomaselli, editors, *Braunwald's Heart Disease 11th Edition*, chapter 12, pages 117–153. Elsevier Inc., Philadelphia, 11 edition, 2018.

- [99] P. Kligfield, L. S. Gettes, J. J. Bailey, R. Childers, B. J. Deal, E. W. Hancock, G. Van Herpen, J. A. Kors, P. Macfarlane, D. M. Mirvis, O. Pahlm, P. Rautaharju, and G. S. Wagner. Recommendations for the standardization and interpretation of the electrocardiogram: Part I: The electrocardiogram and its technology. *Circulation*, 115(10):1306–1324, 2007.
- [100] L. Bacharova, R. H. Selvester, H. Engblom, and G. S. Wagner. Where is the central terminal located? In search of understanding the use of the Wilson central terminal for production of 9 of the standard 12 electrocardiogram leads. *Journal of electrocardiology*, 38(2):119–27, 4 2005.
- [101] D. Durrer. Electrical aspects of human cardiac activity: A clinical-physiological approach to excitation and stimulation. *Cardiovascular Research*, 2(1):1–18, 1968.
- [102] A. Vleugels, J. Vereecke, and E. Carmeliet. Ionic currents during hypoxia in voltage-clamped cat ventricular muscle. *Circulation research*, 47(4):501–8, 10 1980.
- [103] G. Isenberg, J. Vereecke, G. van der Heyden, and E. Carmeliet. The shortening of the action potential by DNP in guinea-pig ventricular myocytes is mediated by an increase of a time-independent K conductance. *Pflugers Archiv : European journal of physiology*, 397(4):251–9, 6 1983.
- [104] K. E. Baker and M. J. Curtis. Left regional cardiac perfusion in vitro with platelet-activating factor, norepinephrine and K⁺ reveals that ischaemic arrhythmias are caused by independent effects of endogenous 'mediators' facilitated by interactions, and moderated by paradoxical antag. *British Journal of Pharmacology*, 142:352–66, 2004.
- [105] J. M. Di Diego and C. Antzelevitch. Ischemic ventricular arrhythmias: Experimental models and their clinical relevance. *Heart Rhythm*, 8(12):1963–1968, 2011.
- [106] J. M. Di Diego and C. Antzelevitch. Acute myocardial ischemia: Cellular mechanisms underlying ST segment elevation. *Journal of Electrocardiology*, 47(4):486–490, 2014.
- [107] W. E. Samson and a. M. Scher. Mechanism of S-T segment alteration during acute myocardial injury. *Circulation research*, 8:780–7, 1960.
- [108] G. T. Smith, G. Geary, W. Ruf, T. H. Roelofs, and J. J. McNamara. Epicardial mapping and electrocardiographic models of myocardial ischemic injury. *Circulation*, 60(4):930–8, 1979.
- [109] T. N. Martin, B. A. Groenning, H. M. Murray, T. Steedman, J. E. Foster, A. T. Elliot, H. J. Dargie, R. H. Selvester, O. Pahlm, and G. S. Wagner. ST-segment

- deviation analysis of the admission 12-lead electrocardiogram as an aid to early diagnosis of acute myocardial infarction with a cardiac magnetic resonance imaging gold standard. *Journal of the American College of Cardiology*, 50(11):1021–8, 9 2007.
- [110] D. David, M. Naito, E. Michelson, Y. Watanabe, C. C. Chen, J. Morganroth, M. Shaffenburg, and T. Blenko. Intramyocardial conduction: a major determinant of R-wave amplitude during acute myocardial ischemia. *Circulation*, 65(1): 161–7, 1 1982.
- [111] R. P. Holland, H. Brooks, R. P. Houiam, and H. Brooks. The QRS complex during myocardial ischemia. An experimental analysis in the porcine heart. *J Clin Invest*, 57(3):541–50, 1976.
- [112] J. L. Hill and L. S. Gettes. Effect of acute coronary artery occlusion on local myocardial extracellular K⁺ activity in swine. *Circulation*, 61:768, 1980.
- [113] G. Dominguez and H. A. Fozzard. Influence of extracellular K⁺ concentration on cable properties and excitability of sheep cardiac Purkinje fibers. *Circulation research*, 26:565, 1970.
- [114] N. B. Wagner, D. C. Sevilla, M. W. Krucoff, K. S. Pieper, K. L. Lee, R. D. White, K. M. Kent, R. Renzi, R. H. Selvester, and G. S. Wagner. Transient alterations of the QRS complex and ST segment during percutaneous transluminal balloon angioplasty of the right and left circumflex coronary arteries. *The American journal of cardiology*, 63(17):1208–13, 1989.
- [115] B. Surawicz. Reversible QRS changes during acute myocardial ischemia. *Journal of electrocardiology*, 31(3):209–220, 7 1998.
- [116] B. Surawicz, C. M. Orr, J. B. Hermiller, K. D. Bell, and R. P. Pinto. QRS changes during percutaneous transluminal coronary angioplasty and their possible mechanisms. *Journal of the American College of Cardiology*, 30(2):452–458, 8 1997.
- [117] L. Bacharova, V. Szathmary, and A. Mateasik. QRS complex and ST segment manifestations of ventricular ischemia: the effect of regional slowing of ventricular activation. *Journal of electrocardiology*, 46(6):497–504, 11 2013.
- [118] L. L. Conrad, T. E. Cuddy, and R. H. Bayley. Activation of the ischemic ventricle and acute peri-infarction block in experimental coronary occlusion. *Circulation research*, 7(4):555–564, 1959.
- [119] M. J. Janse, A. G. Kleber, A. Capucci, R. Coronel, and F. Wilms-Schopman. Electrophysiological basis for arrhythmias caused by acute ischemia. Role of the subendocardium. *Journal of molecular and cellular cardiology*, 18(4):339–355, 4 1986.

- [120] A. Arenal, C. Villemaire, and S. Nattel. Mechanism of selective epicardial activation delay during acute myocardial ischemia in dogs. *Circulation*, 88:2381–8, 1993.
- [121] B. Balci. Tombstoning ST-Elevation Myocardial Infarction. *Current cardiology reviews*, 5(4):273–278, 2009.
- [122] H. S. K. Wimalaratna. "Tombstoning" of ST segment in acute myocardial infarction. *The Lancet*, 342(8869):496, 1993.
- [123] R. Childers. R wave amplitude in ischemia, injury, and infarction: Plenary address. *Journal of Electrocardiology*, 29:171–8, 1996.
- [124] J. E. Madias. The "giant R waves" ECG pattern of hyperacute phase of myocardial infarction. A case report. *Journal of Electrocardiology*, 26:77–82, 1993.
- [125] J. M. Di Diego and C. Antzelevitch. Cellular basis for ST-segment changes observed during ischemia. *Journal of Electrocardiology*, 36:1–5, 2003.
- [126] A. A. Cantor, B. Goldfarb, and R. Ilia. QRS prolongation: A sensitive marker of ischemia during percutaneous transluminal coronary angioplasty. *Catheterization and Cardiovascular Interventions*, 50:177–183, 2000.
- [127] R. Bigi, A. Mafriaci, P. Colombo, D. Gregori, E. Corrada, A. Alberti, A. De Biase, P. S. Orrego, C. Fiorentini, and S. Klugmann. Relation of terminal QRS distortion to left ventricular functional recovery and remodeling in acute myocardial infarction treated with primary angioplasty. *The American journal of cardiology*, 96(9):1233–6, 2005.
- [128] G. D. Birnbaum, I. Birnbaum, and Y. Birnbaum. Twenty years of ECG grading of the severity of ischemia. *Journal of Electrocardiology*, 47(4):546–555, 7 2014.
- [129] Y. Birnbaum, D. a. Criger, G. S. Wagner, B. Strasberg, A. Mager, K. Gates, C. B. Granger, A. M. Ross, and G. I. Barbash. Prediction of the extent and severity of left ventricular dysfunction in anterior acute myocardial infarction by the admission electrocardiogram. *American Heart Journal*, 141(6):915–924, 6 2001.
- [130] P. Weston, P. Johanson, L. M. Schwartz, C. Maynard, R. B. Jennings, and G. S. Wagner. The value of both ST-segment and QRS complex changes during acute coronary occlusion for prediction of reperfusion-induced myocardial salvage in a canine model. *Journal of Electrocardiology*, 40(1):18–25, 1 2007.
- [131] C.-K. Wong, W. Gao, R. A. H. Stewart, J. K. French, P. E. G. Aylward, and H. D. White. Relationship of QRS duration at baseline and changes over 60 min after fibrinolysis to 30-day mortality with different locations of ST elevation myocardial infarction: results from the Hirulog and Early Reperfusion or Occlusion-2 trial. *Heart (British Cardiac Society)*, 95(4):276–282, 2 2009.

- [132] D. Romero, M. Ringborn, P. Laguna, and E. Pueyo. Detection and quantification of acute myocardial ischemia by morphologic evaluation of QRS changes by an angle-based method. *Journal of Electrocardiology*, 46(3):204–214, 2013.
- [133] B. Balci and O. Yesildag. Correlation between clinical findings and the ”tombstoning” electrocardiographic pattern in patients with anterior wall acute myocardial infarction. *Am J Cardiol*, 92(11):1316–1318, 2003.
- [134] E. Ayhan, T. Isäk, H. Uyarel, M. Ergelen, G. Cicek, S. Altay, M. Eren, and C. Michael Gibson. Patients with tombstoning pattern on the admission electrocardiography who have undergone primary percutaneous coronary intervention for anterior wall ST-elevation myocardial infarction: In-hospital and midterm clinical outcomes. *Annals of Noninvasive Electrocardiology*, 17(4):315–322, 2012.
- [135] S. Sclarovsky, A. Mager, J. Kusniec, E. Rechavia, A. Sagie, R. Bassevich, and B. Strasberg. Electrocardiographic classification of acute myocardial ischemia. *Israeli Journal of Medical Science*, 26(525), 1990.
- [136] Y. Birnbaum, S. Sclarovsky, A. Blum, A. Mager, and U. Gabbay. Prognostic significance of the initial electrocardiographic pattern in a first acute anterior wall myocardial infarction. *Chest*, 103(6):1681–1687, 1993.
- [137] D. V. Mulay and S. M. Mukhedkar. Prognostic significance of the distortion of terminal portion of QRS complex on admission electrocardiogram in ST segment elevation myocardial infarction. *Indian Heart Journal*, 65(6):671–677, 2013.
- [138] M. Ringborn, Y. Birnbaum, S. S. Nielsen, A. K. Kalsoft, H. E. Bøtker, O. Pahlm, G. S. Wagner, P. G. Platonov, and C. J. Terkelsen. Pre-hospital evaluation of electrocardiographic grade 3 ischemia predicts infarct progression and final infarct size in ST elevation myocardial infarction patients treated with primary percutaneous coronary intervention. *Journal of Electrocardiology*, 47(4):556–565, 7 2014.
- [139] K.-P. Rommel, H. Badarnih, S. Desch, M. Gutberlet, G. Schuler, H. Thiele, and I. Eitel. QRS complex distortion (Grade 3 ischaemia) as a predictor of myocardial damage assessed by cardiac magnetic resonance imaging and clinical prognosis in patients with ST-elevation myocardial infarction. *European Heart Journal – Cardiovascular Imaging*, 17(2):194–202, 2 2016.
- [140] M. E. Hassell, R. Delewi, C. P. Lexis, M. W. Smulders, A. Hirsch, G. Wagner, S. C. Bekkers, I. C. Van Der Horst, F. Zijlstra, A. C. Van Rossum, J. J. Piek, P. Van Der Harst, and R. Nijveldt. The relationship between terminal QRS distortion on initial ECG and final infarct size at 4 months in conventional ST- segment elevation myocardial infarct patients. *Journal of Electrocardiology*, 49(3):292–299, 2016.

- [141] M. J. Valle-Caballero, R. Fernández-Jiménez, R. Díaz-Munoz, A. Mateos, M. Rodríguez-Álvarez, J. A. Iglesias-Vázquez, C. Saborido, C. Navarro, M. L. Dominguez, L. Gorjón, J. C. Fontoira, V. Fuster, J. C. García-Rubira, and B. Ibanez. QRS distortion in pre-reperfusion electrocardiogram is a bedside predictor of large myocardium at risk and infarct size (a METOCARD-CNIC trial substudy). *International Journal of Cardiology*, 202:666–673, 1 2016.
- [142] T. Billgren, Y. Birnbaum, E. B. Sgarbossa, M. Sejersten, N. E. Hill, H. Engblom, C. Maynard, O. Pahlm, and G. S. Wagner. Refinement and interobserver agreement for the electrocardiographic Sclarovsky-Birnbaum Ischemia Grading System. *Journal of Electrocardiology*, 37(3):149–156, 7 2004.
- [143] A. B. de Luna, P. Coumel, and J. F. Leclercq. Ambulatory sudden cardiac death: Mechanisms of production of fatal arrhythmia on the basis of data from 157 cases. *American Heart Journal*, 117(1):151–9, 1989.
- [144] M. M. Demidova, A. Martín-Yebra, J. van der Pals, S. Koul, D. Erlinge, P. Laguna, J. P. Martínez, and P. G. Platonov. Transient and rapid QRS-widening associated with a J-wave pattern predicts impending ventricular fibrillation in experimental myocardial infarction. *Heart rhythm : the official journal of the Heart Rhythm Society*, 11(7):1195–201, 7 2014.
- [145] M. M. Demidova, A. Martín-Yebra, S. Koul, H. Engblom, J. P. Martínez, D. Erlinge, and P. G. Platonov. QRS broadening due to terminal distortion is associated with the size of myocardial injury in experimental myocardial infarction. *Journal of Electrocardiology*, 49(3):300–306, 2016.
- [146] A. Mart, M. M. Demidova, P. Platonov, P. Laguna, J. P. Mart, and B. N. Ciberbbn. Increase of QRS Duration as a Predictor of Impending Ventricular Fibrillation during Coronary Artery Occlusion. *Computing in Cardiology*, (40):133–136, 2013.
- [147] B. Gorenek, C. B. Lundqvist, J. B. Terradellas, A. J. Camm, G. Hindricks, K. Huber, P. Kirchhof, K. H. Kuck, G. Kudaiberdieva, T. Lin, A. Raviele, M. Santini, R. R. Tilz, M. Valgimigli, M. A. Vos, C. Vrints, and U. Zeymer. Cardiac arrhythmias in acute coronary syndromes: Position paper from the joint EHRA, ACCA, and EAPCI task force. *European Heart Journal: Acute Cardiovascular Care*, 4(4):386, 2015.
- [148] E. Carmeliet. Cardiac Ionic Currents and Acute Ischemia: From Channels to Arrhythmias. *Physiological Reviews*, 79(3):917–1017, 7 1999.
- [149] E. Bohula and D. Morrow. Chapter 59: ST-elevation Myocardial Infarction, Management. In D. P. Zipes, P. Libby, R. Bonow, D. Mann, and G. Tomaselli, editors,

- Braunwald's Heart Disease 11th Edition*, chapter 59, pages 1123–1180. Elsevier Inc., Philadelphia, 11 edition, 2018.
- [150] D. J. Hausenloy and D. M. Yellon. Ischaemic conditioning and reperfusion injury. *Nature Reviews Cardiology*, 13(4):193–209, 2016.
- [151] A. S. Manning and D. J. Hearse. Reperfusion-induced arrhythmias: mechanisms and prevention. *Journal of molecular and cellular cardiology*, 16(6):497–518, 6 1984.
- [152] D. Corcoran, C. Berry, M. Sciences, G. Jubilee, N. Hospital, and M. Sciences. How to measure myocardial infarct size by cardiac magnetic resonance imaging. *Heart and Metabolism*, (70):14–18, 2016.
- [153] D. García-Dorado, J. Oliveras, J. Gili, E. Sanz, F. Pérez-Villa, J. Barrabés, M. J. Carreras, J. Solares, and J. Soler-Soler. Analysis of myocardial oedema by magnetic resonance imaging early after coronary artery occlusion with or without reperfusion. *Cardiovascular Research*, 27(8):1462–1469, 1993.
- [154] G. Liney. *MRI in clinical practice*. Springer-Verlag, London, 2006.
- [155] J. C. Weaver, D. Rees, A. M. Prasan, D. D. Ramsay, M. F. Binnekamp, and J. A. McCrohon. Grade 3 ischemia on the admission electrocardiogram is associated with severe microvascular injury on cardiac magnetic resonance imaging after ST elevation myocardial infarction. *Journal of Electrocardiology*, 44(1):49–57, 2011.
- [156] S. G. Warren and G. S. Wagner. The STAFF studies of the first 5 minutes of percutaneous coronary angioplasty balloon occlusion in man. *Journal of electrocardiology*, 47(4):402–407, 7 2014.
- [157] P. Laguna and L. Sörnmo. The STAFF III ECG database and its significance for methodological development and evaluation. *Journal of Electrocardiology*, 47(4): 408–417, 2014.
- [158] A. Khoshnood, M. Carlsson, M. Akbarzadeh, P. Bhiladvala, A. Roijer, D. Nordlund, P. Höglund, D. Zughaft, L. Todorova, A. Mokhtari, H. Arheden, D. Erlinge, and U. Ekelund. Effect of oxygen therapy on myocardial salvage in ST elevation myocardial infarction: the randomised SOCCER trial. *European Journal of Emergency Medicine*, 25(2):78–84, 4 2018.
- [159] T. N. England. Mild therapeutic hypothermia to improve the neurologic outcome after cardiac arrest. *The New England journal of medicine*, 346(8):549–56, 2002.
- [160] N. Nielsen, J. Wetterslev, T. Cronberg, D. Erlinge, Y. Gasche, C. Hassager, J. Horn, J. Hovdenes, J. Kjaergaard, M. Kuiper, T. Pellis, P. Stammer, M. Wanscher, M. P. Wise, A. Aneman, N. Al-Subaie, S. Boesgaard, J. Bro-Jeppesen, I. Brunetti, J. F.

- Bugge, C. D. Hingston, N. P. Juffermans, M. Koopmans, L. Kober, J. Langorgen, G. Lilja, J. E. Moller, M. Rundgren, C. Rylander, O. Smid, C. Werer, P. Winkel, H. Friberg, and T. T. M. T. Investigators. Targeted temperature management at 33C versus 36C after cardiac arrest. *N Engl J Med*, 369(23):2197–2206, 2013.
- [161] K. Thygesen, J. S. Alpert, H. D. White, A. S. Jaffe, F. S. Apple, M. Galvani, H. A. Katus, L. K. Newby, J. Ravkilde, B. Chaitman, P. Clemmensen, M. Dellborg, H. Hod, P. Porela, R. Underwood, J. J. Bax, G. A. Beller, R. Bonow, E. E. Van der Wall, J.-P. Bassand, W. Wijns, T. B. Ferguson, P. G. Steg, B. F. Uretsky, D. O. Williams, P. W. Armstrong, E. M. Antman, K. A. Fox, C. W. Hamm, E. M. Ohman, M. L. Simoons, P. A. Poole-Wilson, E. P. Gurfinkel, J.-L. Lopez-Sendon, P. Pais, S. Mendis, J.-R. Zhu, L. C. Wallentin, F. Fernández-Avilés, K. M. Fox, A. N. Parkhomenko, S. G. Priori, M. Tendera, L.-M. Voipio-Pulkki, A. Vahanian, A. J. Camm, R. De Caterina, V. Dean, K. Dickstein, G. Filippatos, C. Funck-Brentano, I. Hellemans, S. D. Kristensen, K. McGregor, U. Sechtem, S. Silber, P. Widimsky, J. L. Zamorano, J. Morais, S. Brener, R. Harrington, D. Morrow, M. Lim, M. A. Martinez-Rios, S. Steinhubl, G. N. Levine, W. B. Gibler, D. Goff, M. Tubaro, D. Dudek, and N. Al-Attar. Universal definition of myocardial infarction. *Circulation*, 116(22):2634–53, 11 2007.
- [162] G. S. Wagner, P. Macfarlane, H. Wellens, M. Josephson, A. Gorgels, D. M. Mirvis, O. Pahlm, B. Surawicz, P. Kligfield, R. Childers, L. S. Gettes, J. J. Bailey, B. J. Deal, E. W. Hancock, J. A. Kors, J. W. Mason, P. Okin, P. M. Rautaharju, and G. van Herpen. AHA/ACCF/HRS Recommendations for the Standardization and Interpretation of the Electrocardiogram. Part VI: Acute Ischemia/Infarction A Scientific Statement From the American Heart Association Electrocardiography and Arrhythmias Committee, Council on Clinical. *Circulation*, 119(10):262–70, 3 2009.
- [163] E. Lepschkin and B. Surawicz. The measurement of the Q-T interval of the electrocardiogram. *Circulation*, 6(3):378–388, 9 1952.
- [164] B. Heden, R. Ripa, E. Persson, Q. Song, C. Maynard, P. Leibrandt, T. Wall, T. F. Christian, S. C. Hammill, S. S. Bell, O. Pahlm, and G. S. Wagner. A modified Anderson-Wilkins electrocardiographic acuteness score for anterior or inferior myocardial infarction. *Am Heart J*, 146(5):797–803, 2003.
- [165] E. Heiberg, J. Sjögren, M. Ugander, M. Carlsson, H. Engblom, and H. Arheden. Design and validation of Segment—freely available software for cardiovascular image analysis. *BMC medical imaging*, 10:1, 1 2010.
- [166] M. Carlsson, J. F. A. Ubachs, E. Hedström, E. Heiberg, S. Jovinge, and H. Arheden. Myocardium at risk after acute infarction in humans on cardiac magnetic resonance: quantitative assessment during follow-up and validation with single-photon emission computed tomography. *JACC. Cardiovascular imaging*, 2(5):569–76, 5 2009.

- [167] D. Nordlund, G. Klug, E. Heiberg, S. Koul, T. H. Larsen, P. Hoffmann, B. Metzler, D. Erlinge, D. Atar, A. H. Aletras, M. Carlsson, H. Engblom, and H. Arheden. Multi-vendor, multicentre comparison of contrast-enhanced SSFP and T2-STIR CMR for determining myocardium at risk in ST-elevation myocardial infarction. *European heart journal cardiovascular Imaging*, 17(7):744–53, 7 2016.
- [168] P. Sörensson, E. Heiberg, N. Saleh, F. Bouvier, K. Caidahl, P. Tornvall, L. Rydén, J. Pernow, and H. Arheden. Assessment of myocardium at risk with contrast enhanced steady-state free precession cine cardiovascular magnetic resonance compared to single-photon emission computed tomography. *Journal of cardiovascular magnetic resonance : official journal of the Society for Cardiovascular Magnetic Resonance*, 12(1):25, 1 2010.
- [169] J. F. A. Ubachs, P. Sörensson, H. Engblom, M. Carlsson, S. Jovinge, J. Pernow, and H. Arheden. Myocardium at risk by magnetic resonance imaging: head-to-head comparison of T2-weighted imaging and contrast-enhanced steady-state free precession. *European heart journal cardiovascular Imaging*, 13(12):1008–15, 12 2012.
- [170] J. F. A. Ubachs, H. Engblom, S. Koul, M. Kanski, P. Andersson, J. van der Pals, M. Carlsson, D. Erlinge, and H. Arheden. Myocardium at risk can be determined by ex vivo T2-weighted magnetic resonance imaging even in the presence of gadolinium: comparison to myocardial perfusion single photon emission computed tomography. *European heart journal cardiovascular Imaging*, 14(3):261–8, 3 2013.
- [171] D. Nordlund, M. Kanski, R. Jablonowski, S. Koul, D. Erlinge, M. Carlsson, H. Engblom, A. H. Aletras, and H. Arheden. Experimental validation of contrast-enhanced SSFP cine CMR for quantification of myocardium at risk in acute myocardial infarction. *Journal of cardiovascular magnetic resonance : official journal of the Society for Cardiovascular Magnetic Resonance*, 19(1):12, 1 2017.
- [172] E. Heiberg, M. Ugander, H. Engblom, M. Götberg, G. K. Olivecrona, D. Erlinge, and H. Arheden. Automated quantification of myocardial infarction from MR images by accounting for partial volume effects: animal, phantom, and human study. *Radiology*, 246(2):581–8, 2 2008.
- [173] X. H. Guo, Y. G. Yap, L. J. Chen, J. Huang, and A. J. Camm. Correlation of coronary angiography with ”tombstoning” electrocardiographic pattern in patients after acute myocardial infarction. *Clin Cardiol*, 23(5):347–352, 2000.
- [174] M. M. Demidova, J. Carlson, D. Erlinge, and P. G. Platonov. Predictors of ventricular fibrillation at reperfusion in patients with acute ST-elevation myocardial infarction treated by primary percutaneous coronary intervention. *The American journal of cardiology*, 115(4):417–22, 2 2015.

REFERENCES

- [175] Y. Aizawa, M. Jastrzebski, T. Ozawa, K. Kawecka-Jaszcz, P. Kukla, W. Mitsuma, M. Chinushi, T. Ida, Y. Aizawa, K. Ojima, M. Tagawa, S. Fujita, M. Okabe, K. Tsuchida, Y. Miyakita, H. Shimizu, S. Ito, T. Imaizumi, and K. Toba. Characteristics of electrocardiographic repolarization in acute myocardial infarction complicated by ventricular fibrillation. *Journal of Electrocardiology*, 45(3):252–259, 2012.
- [176] G. van Herpen, H. J. Ritsema van Eck, and J. A. Kors. The Evidence Against QT Dispersion. *IJBEM*, 5(1):231–233, 2003.

Part II

Research Papers

Author contributions

Paper I

As first author I was instrumental in study design, derivation of the 'almer' one-lead method, data collection, data analysis, statistical methods, figures, interpretation of the results, drafting of the manuscript, revision of the manuscript and responding to peer review.

Paper II

As second author I was involved in the study design, development of the 'almer' 12-lead method, data analysis, figures, interpretation of the results and revision of the manuscript.

Paper III

As first author I was instrumental in study design, data collection, data analysis, statistical methods, figures, interpretation of the results, drafting of the manuscript, revision of the manuscript and responding to peer review.

Paper IV

As first author I was instrumental in study design, data analysis, statistical methods, figures, interpretation of the results, drafting of the manuscript, revision of the manuscript and responding to peer review.

Paper V

As first author I was instrumental in study design, data analysis, statistical methods, figures, interpretation of the results, drafting of the manuscript, revision of the manuscript and responding to peer review.





Ischemic QRS prolongation as a biomarker of severe myocardial ischemia^{☆,☆☆}

Jakob Almer, MD,^a Robert B. Jennings, MD,^b Arie C. Maan, PhD,^c
Michael Ringborn, MD PhD,^d Charles Maynard, PhD,^c Olle Pahlm, MD, PhD,^a
Håkan Arheden, MD, PhD,^a Galen S. Wagner, MD,^b Henrik Engblom, MD, PhD^{a,*}

^a Department of Clinical physiology and Nuclear medicine, Skåne University Hospital and Lund University, Lund, Sweden

^b Duke University Medical Center, Durham, NC, USA

^c Department of Cardiology, Leiden University Medical Center, Leiden, The Netherlands

^d Thoracic Center, Blekingesjukhuset, Karlskrona, Sweden

^e Department of Health Services, University of Washington, Seattle, WA, USA

Abstract

Background: Previous studies have shown that QRS prolongation is a sign of depressed collateral flow and increased rate of myocardial cell death during coronary occlusion. The aims of this study were to evaluate ischemic QRS prolongation as a biomarker of severe ischemia by establishing the relationship between prolongation and collateral flow experimentally in a dog model, and test if the same pattern of ischemic QRS prolongation occurs in man.

Methods: Degree of ischemic QRS prolongation was measured using a novel method in dogs ($n = 23$) and patients ($n = 52$) during coronary occlusion for 5 min. Collateral arterial flow was assessed in the dogs.

Results: There was a significant correlation between QRS prolongation and collateral flow in dogs ($r = 0.61$, $p = 0.008$). Magnitude and temporal evolution of prolongation during ischemia were similar for dogs and humans ($p = 0.202$ and $p = 0.911$).

Conclusion: Quantification of ischemic QRS prolongation could potentially be used as a biomarker for severe myocardial ischemia.

© 2016 Elsevier Inc. All rights reserved.

Keywords: Electrocardiography; Electrophysiology; Ischemia; Collateral circulation

Introduction

Acute myocardial infarction (AMI), due to acute coronary occlusion (ACO), is one of the leading causes of death in the western world [1]. The rate at which the ischemic myocardium develops into infarction varies among individuals, and depends on the severity of ischemia which is related to the amount of coronary arterial collateral flow [2,3]. The aim of acute ACO treatment is to accomplish reperfusion as soon as possible, either by percutaneous

coronary intervention (PCI) or by intravenous thrombolytic therapy, in order to maximize myocardial salvage.

Patients with ACO are usually diagnosed based on the presence of ischemia-induced ST-segment elevation (STE) or its equivalent ST depression, on the presenting ECG [4,5]. The ischemia-induced changes in the myocardium are, however, manifested not only as acute ST changes, but also as changes to the QRS complex [4,6,7]. Previous experimental studies have shown that increased QRS duration during ischemia is a sign of depressed arterial collateral flow and a rapid rate of myocardial cell death [2,8,9]. Furthermore, Weston et al. reported that for a given magnitude of STE, the presence of concurrent QRS prolongation was associated with less myocardial salvage [8]. Thus, QRS prolongation in the situation of ACO might serve as a biomarker for severe ischemia caused by poor cardiac protection. Human studies of ischemia-induced QRS prolongation are, however, scarce. The short-term prognostic significance of a prolonged QRS duration on the admission ECG has been shown in patients with ST elevation

[☆] Funding sources: All parts of the study have been supported by the Swedish Research Council, Swedish Heart and Lung Foundation, Region of Scania, the Medical Faculty of Lund University and the American Heart Association, Durham, North Carolina, USA (account 5-21628). The canine experimental work i.e. data collection, was supported in part by grants HL 23138 and HL 27416 from the National Heart, Lung and Blood Institute of the National Institutes of Health. There are no relationships with industry.

^{☆☆} Conflicts of interest: None.

* Corresponding author at: Department of Clinical Physiology and Nuclear Medicine, Skåne University Hospital, Lund, 221 85, Lund, Sweden.

E-mail address: henrik.engblom@med.lu.se

myocardial infarction (STEMI) [5,10,11]. Studies considering QRS prolongation in the setting of percutaneous coronary intervention (PCI) have been performed [4,6,7,10,12,13], but have not related the findings to severity of ischemia. Since ischemic QRS prolongation and ST elevation commonly distorts the end of the QRS complex during acute ischemia it is difficult to determine the prolongation of the QRS duration correctly. Thus, development of a robust assessment of ischemic QRS prolongation as a potential biomarker of severe ischemia caused by poor cardiac protection in humans is of great importance.

The aim of this study was to evaluate ischemic QRS prolongation as a potential biomarker of severe ischemia, pursued by 1) testing a novel method for quantifying ischemic QRS prolongation, 2) establishing the relationship between ischemic QRS prolongation and collateral arterial flow during acute ischemia in an experimental dog model and 3) testing if the same pattern of ischemic QRS prolongation occurs in patients with ACO undergoing prolonged, elective angioplasty balloon inflation.

Methods

Study population

The study population consisted of one dog cohort and one human cohort.

Dog cohort

All experiments involving the use of laboratory animals conformed to the guidelines of the American Physiological Society and the standards in the Guide for the Care and Use of Laboratory Animals, DHEW Publ. No. NIH 85-23, revised 1985, and was approved by the institutional review board.

Data from 23 healthy mongrel dogs originally studied in the early 1980's and later by Floyd et al, [9] were included [14]. All dogs underwent proximal occlusion of the left circumflex coronary artery (LCX) for 5 min. Collateral flow was evaluated using microspheres as described below [9,14].

Surgical setup and ECG acquisition

All dogs were anesthetized with 30–40 mg/kg of sodium pentobarbital intravenously, intubated and ventilated as previously described in detail [9,14,15]. In short, a left thoracotomy was performed through the fourth intercostal space and the heart was suspended in a pericardial cradle. The LCX artery was identified and occluded for 5 min with a silk snare. Using a Gould model 2400 recorder, ECG lead II was recorded continuously before, during the occlusion and during reperfusion until the heart was excised.

ECG measurements

QRS waveform measurements were obtained from ECG lead II at a paper speed of 25 mm/s and magnified 200% in a standard photocopier i.e. achieving 50 mm/s and 20 mm/mV. Before occlusion a baseline measurement of QRS duration, defined as the time between QRS onset to the J-point, was performed in all animals. During ischemia when no J-point could be clearly distinguished due to ST elevation,

a line was drawn through the peak of the R (or R' if it was present) wave and along 40% of the downslope between the R peak and the nadir of the ST segment (Fig. 1A). The time between onset of the QRS complex and the intersection of this line with the PR baseline was then determined. The rationale for using the first 40% of the R-wave downslope was empirical. It was derived from observation and measurement of a pilot-subset of dogs and patients, where most often the R-wave downslope began to deviate from a straight line after 40%. In dogs where the J point could be clearly distinguished even during ischemia, the time between QRS onset and the J point was determined. The difference between either of these measurements and the baseline QRS duration was referred to as ischemic QRS prolongation, expressed in ms (absolute ischemic QRS prolongation, measured to nearest 5 ms) and normalized to baseline (relative ischemic QRS prolongation) (Fig. 1A–B). If there was an S wave associated with an ST-segment depression (basal lateral ischemia in LCX occlusions) a superimposed line from the S wave nadir along the first 40% of the S wave

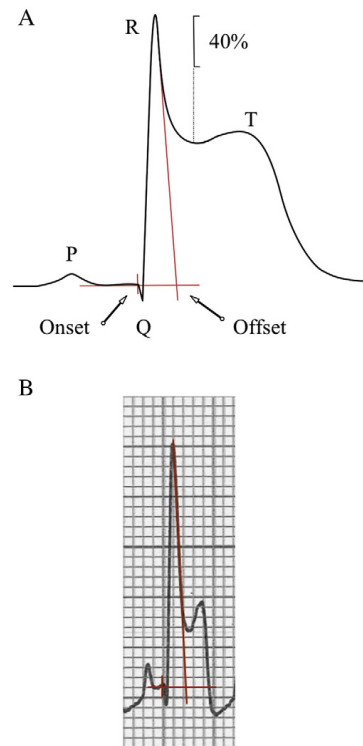


Fig. 1. Depiction of ischemic QRS prolongation measurement method. A. A line was drawn through the peak of the R (or R' if it was present) wave and along 40% of the downslope between the R peak and the nadir of the ST segment. The intersection of this prolonged line with the PR baseline marked the offset of the measurement. B. Example of measurement method in a dog at 3 min of occlusion.

upslope was used and the intersection with the PR baseline marked the offset. Each value was measured as the average of measurements in 2 contiguous beats. Furthermore, the timing of the maximum QRS prolongation during the 5-min occlusion was defined to the nearest minute.

All waveform measurements were manually performed by one observer (JA). Results were adjudicated with an experienced ECG observer (GW) if uncertainties arose.

Collateral blood flow measurement

As previously described, myocardial collateral blood flow was expressed in ml/min/g wet [9,14]. In short, the ischemic and non-ischemic myocardium was measured by injecting radioactive microspheres labeled with ^{46}Sc , ^{85}Sr , ^{113}Sn , ^{141}Ce , or ^{153}Gd at 2.5 min into the ischemic episode. Beginning just before and continuing 2.5 min after microsphere injection, reference blood samples were withdrawn from the aorta via a femoral artery catheter. Microsphere radioactivity was measured with a gamma counter (Model A5912, Packard Instruments, Downer's Grove, IL, USA). Myocardial blood flow was calculated according to the formula: tissue flow = (tissue counts) x (reference blood flow)/(reference blood counts). Collateral blood flow was compared to ischemic QRS prolongation.

Human cohort

ECGs for the human cohort were obtained from the STAFF-III dataset, originally acquired at the Charleston Area Medical Center, WV, USA and approved by the institutional review board in 1995 and 1996 [16,17]. Patients included were referred for prolonged elective balloon PCI due to stable angina pectoris and informed consent was obtained from each patient before enrolment [16,17]. The exclusion criteria were: evidence of an acute or recent myocardial infarction, intraventricular conduction delay with a QRS duration of 120 ms or longer (including right bundle-branch block and left bundle-branch block), any ventricular rhythm at inclusion or during the PCI procedure, absence of ST changes meeting STEMI or STEMI-equivalent criteria following balloon occlusion [18,19], less than 170 s of occlusion and poor signal quality. Baseline variables recorded were gender, age, pre-occlusion heart rate and occlusion time. The previous medical history of the patients was not known. In the situation when more than one of the main coronary arteries was subject to balloon inflation, both inflations were considered for inclusion.

A detailed description of the STAFF-III study was recently published [17]. In short, all patients included received approximately 5 min of balloon occlusion of the right coronary artery (RCA), the left anterior descending artery (LAD) or the LCX. Digital 12-lead ECGs were recorded continuously (Siemens-Elema AB, Solna, Sweden) pre-occlusion and during the procedure until approximately 4 min after balloon deflation. During the recording all patients were resting in a supine position. The signals were digitized at a sampling rate of 1 kHz, with an amplitude resolution of 0.6 μV .

ECG measurements

Waveform measurements were obtained from the digital continuous 12-lead ECG recordings. Measurements were made from print-outs of the ECGs at a paper speed of 50 mm/s and gain of 10 mm/mV. Values were measured from a single lead in order to duplicate the method used in the experimental dog cohort. The extremity leads were considered for assessments of RCA occlusions and precordial leads for LAD and LCX occlusions. Since the dog and human cardiac anatomies differ, the lead with the most pronounced ischemic QRS prolongation among the considered leads and within 5 min of occlusion was used (Fig. 2). The same method for assessing the amount of ischemic QRS prolongation described above for the dog cohort was used for assessment in the patients.

In addition, we investigated the influence of R-wave amplitudes on ischemic QRS prolongation in a subset of the population by measuring R-wave amplitudes in patients with

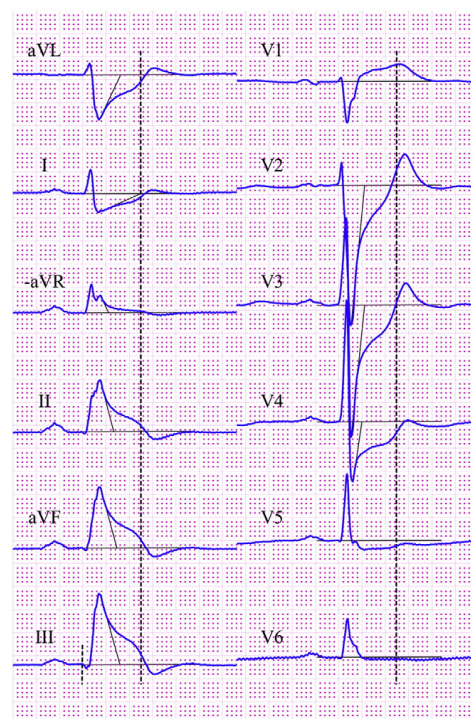


Fig. 2. Example ECG of a patient (subject 108) with occlusion in RCA, taken about 4 min into occlusion at maximum ischemic QRS prolongation. The figure illustrates the novel measuring technique and how leads were compared to find the one with the largest distortion. The dotted line represents the latest QRS offset observed (lead I) with our measure. Furthermore, within certain leads ($-a\text{VR}$, V1 , V5 and V6) the distortion forces are perpendicular to the leads showing the greatest ischemic QRS prolongation and therefore do not show the same amount or any ischemic QRS prolongation. The Cabrera lead system is used in the Figure.

maximum (n = 5) and minimum (n = 5) ischemic QRS prolongation, and compared the two groups.

Statistical analysis

Continuous variables are presented as mean \pm 1 SD. Categorical data are presented as numbers. For continuous variables the Student t-test was used for comparison between groups. The relationship between ischemic QRS prolongation and collateral flow was modeled using a reciprocal function with non-linear least squares regression. The equation of the model was given by $y(x) = \frac{a}{x}$; where a was constant y and x were the ischemic QRS prolongation and collateral flow, respectively. Using a non-linear least squares regression, a was calculated from the dog results to the value of 0.8725. All statistical tests were 2-sided and a p value of <0.05 was considered to indicate statistical significance. SPSS version 19.0 and MATLAB version R2013a were used for the statistical analyses.

Results

Relationship between ischemic QRS prolongation and coronary collateral flow

The characteristics of the 23 dogs included in the study are shown in Table 1. Baseline QRS duration, time from QRS onset to J-point/intercept and absolute ischemic QRS prolongation were 43 ± 5 , 60 ± 23 and 17 ± 23 ms, respectively. The maximum ischemic QRS prolongation was reached after 3.4 ± 0.7 min of occlusion.

The mean flow was 0.099 ± 0.086 ml/min/g wet. There was a statistically significant relationship between collateral blood flow and ischemic QRS prolongation ($r = 0.61$, $p = 0.008$; Fig. 3A). Furthermore, there was a significant difference in collateral flow in the dogs above (n = 11) vs below (n = 12) 5 ms (median) of ischemic QRS prolongation. The dogs with >5 ms of ischemic QRS prolongation exhibited significantly lower collateral flow compared to dogs with ≤ 5 ms ischemic QRS prolongation (0.04 ± 0.03 vs 0.15 ± 0.09 ml/min/g wet, $p = 0.001$; Table 2, Fig. 3B).

Ischemic QRS prolongation in humans

The human cohort included 52 patients (18 [35%] females, mean age 61 ± 10.6 years) with a total of 54

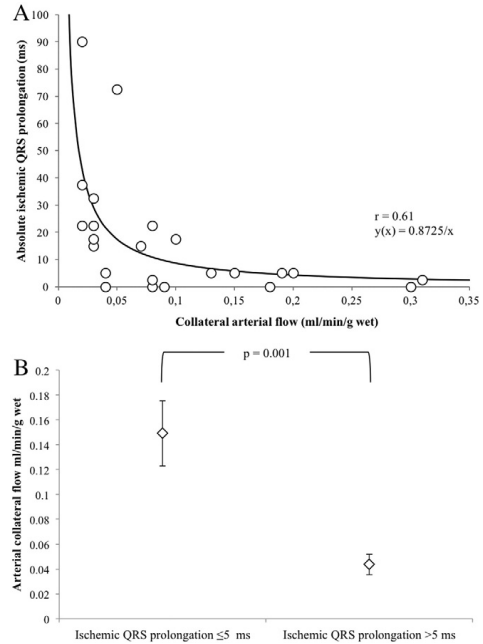


Fig. 3. Relation between ischemic QRS prolongation and collateral blood flow in the dog. A. Collateral blood flow (ml/min/g wet) was plotted against ischemic QRS prolongation in a scatter plot. The relationship between ischemic QRS prolongation and collateral flow was modeled using a reciprocal function calculated with a non-linear least squares regression ($y(x) = \frac{0.8725}{x}$); $r = 0.61$ and $p = 0.008$. B. Relation between groups with ischemic QRS prolongation of ≤ 5 ms or >5 ms. Whisker plot with mean \pm standard error of the mean (SEM).

coronary stenoses subjected to prolonged occlusions, RCA (n = 21), LAD (n = 22) or LCX (n = 11), for a mean of 270 ± 56 s. Thus, two patients had two balloon occlusions in two different coronary arteries. Baseline characteristics are reported in Table 3A.

Mean pre-occlusion QRS duration and maximum time from QRS onset to J-point/intercept were 81 ± 12 ms and

Table 1
Baseline characteristics of dog population.

	All dogs (n = 23), Mean \pm 1SD (range)
Pre-occlusion heart rate (bpm)	161 \pm 20.8 (128–197)
Pre-occlusion blood pressure (systolic mmHg/diastolic mmHg)	163 \pm 26.0 (135–230)/118 \pm 19.5 (95–155)
Pre-occlusion QRS duration (ms)	43 \pm 5 (35–55)
Max time from QRS onset to J-point/intercept during occlusion (ms)	60 \pm 23 (35–130)
Absolute ischemic QRS prolongation (ms)	17 \pm 23 (0–90)
Relative ischemic QRS prolongation (%)	42% \pm 59% (0–225%)
Time to max ischemic QRS prolongation (min)	3.4 \pm 0.7 (2.0–4.0)
Collateral flow (ml/min/g wet)	0.099 \pm 0.086 (0.02–0.31)

Table 2
Comparison between dogs with long or short ischemic QRS prolongation.

	iQRS _p ^b ≤ 5 ms (n = 12), Mean \pm 1SD (range)	iQRS _p ^b > 5 ms (n = 11), Mean \pm 1SD (range)	p-value
Absolute ischemic QRS prolongation (ms)	2.5 \pm 3 (0–5)	33.2 \pm 26 (15–90)	0.0004 ^a
Collateral flow (ml/min/g wet)	0.15 \pm 0.09 (0.04–0.31)	0.04 \pm 0.03 (0.02–0.1)	0.001 ^a
Pre-occlusion QRS duration (ms)	43 \pm 6 (35–50)	44 \pm 6 (35–55)	N.S.

^a Two-tailed p-value calculated with an unpaired t-test.

^b Ischemic QRS prolongation.

Table 3A
Baseline characteristics of human population.

	All patients (n = 52)
Patients	52
Gender (females)	18 (35%) ^a
Age (years)	61 ± 10.6 (39–79) ^b
Number of occlusions	54
Mean time of occlusion (n = 54; s)	270 ± 56.0 (170–420) ^b
Occluded artery (RCA ^c /LAD ^d /LCX ^e)	21 (39%)/22 (41%)/11 (20%)
Mean pre-occlusion heart rate (n = 54; bpm)	76 ± 13.9 (50–102) ^b

^a Difference in ischemic QRS prolongation was N.S. between genders.
^b Mean ± 1SD (range).
^c Right coronary artery.
^d Left anterior descending artery.
^e Left circumflex artery.

129 ± 55 ms, respectively (Table 3B). Mean overall ischemic QRS prolongation was 49 ± 57 ms (44 ± 49, 62 ± 71 and 29 ± 28 ms for RCA, LAD and LCX occlusions, respectively), without significant differences between the groups. Maximum ischemic QRS prolongation was reached after 3.4 ± 0.8 min of occlusion. Moreover, it was frequently noted that ischemic QRS prolongation reached a plateau after the maximum was reached, staying at a similar magnitude throughout the rest of the 5-min occlusion. In all patients with significant ischemic QRS prolongation, the QRS duration returned to baseline values within 30 s of reperfusion.

As shown in Fig. 4 and Table 4 there was no statistically significant difference between dogs and humans regarding the characteristics of ischemic QRS prolongation during occlusion. Side by side examples of ECGs from humans and dogs are shown in Fig. 5. In Fig. 6 examples of significant ischemic QRS prolongation in all three of the major vessels in patients are shown.

There was no significant difference in R-wave amplitude between patients with minimum (0.73 ± 0.48 mV) and maximum (1.06 ± 0.77 mV) ischemic QRS prolongation (p = 0.437).

Table 3B
Human ischemic QRS prolongation measurements.

	All occlusions (n = 54), Mean ± 1SD (range)
Pre-occlusion QRS duration (ms)	81 ± 12 (56–113)
Max time from QRS onset to J-point/intersect during occlusion (ms)	129 ± 55 (60–355)
Absolute ischemic QRS prolongation (ms)	49 ± 57 (0–265)
RCA ^a ischemic QRS prolongation (n = 21; ms)	44 ± 49 (0–170)
LAD ^b ischemic QRS prolongation (n = 22; ms)	62 ± 71 (0–265)
LCX ^c ischemic QRS prolongation (n = 11; ms)	29 ± 28 (0–100)
Relative ischemic QRS prolongation (%)	64% ± 74% (0–294%)
Time to max ischemic QRS prolongation (minutes)	3.4 ± 0.9 (2.0–5.0)

^a Right coronary artery.
^b Left anterior descending artery.
^c Left circumflex artery.

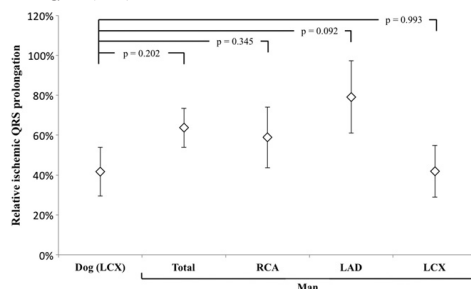


Fig. 4. Relation between humans (divided into total, RCA, LAD and LCX) and dogs as regards relative ischemic QRS prolongation. Whisker plot with mean ± standard error of the mean (SEM). No statistically significant difference between the dogs and any of the human subgroups was found.

Discussion

The main findings of this study were that there was a significant correlation between ischemic QRS prolongation and the amount of collateral flow in dogs with ACO, and that the magnitude and temporal evolution of ischemic QRS prolongation in dogs were similar to those in humans with stable coronary artery disease subjected to prolonged, elective coronary artery balloon occlusion.

Ischemic QRS prolongation as a marker of decreased collateral flow

The findings in the present study, with lower collateral blood flow in dogs with more pronounced ischemic QRS prolongation, are in accordance with results by Floyd et al. [9] and Weston et al. [8] showing a relationship between QRS prolongation and the amount of collateral flow. Dogs with an ischemic QRS prolongation of >5 ms all had low collateral flow, whereas those with ≤5 ms ischemic QRS prolongation showed a variable amount of collateral flow (Fig. 4). This indicates that presence of a significant ischemic QRS prolongation during coronary occlusion might have high positive predictive value for low collateral flow. There are, however, other mechanisms that protect the myocardium from developing severe ischemia including ischemic preconditioning and partial or complete spontaneous dissolution of the obstructing thrombus via fragmentation secondary to the action of endothelial fibrinolysis [2,4].

The present findings indicate similarities between coronary occlusion in dogs and in humans (Fig. 5). The magnitude and range of ischemic QRS prolongation during coronary occlusion were similar between the species, especially as regards to patients with LCX occlusions. Furthermore, the timing of maximum ischemic QRS prolongation was similar between the two species. To what extent ischemic QRS prolongation in humans with coronary occlusion relates to poor cardioprotection and poor collateral blood remains to be determined. There are, however, findings indicating that ischemic QRS

Table 4
Comparison between dog and human cohort.

Relative ischemic QRS prolongation	Humans, Mean ± 1SD (range)	Dogs, Mean ± 1SD (range)	p-value
RCA ^c in human (n = 21)	60% ± 69% (0–243%)		0.345 ^a
LAD ^d in human (n = 22)	79% ± 85% (0–294%)		0.092 ^a
LCX ^e in human (n = 11)	40% ± 43% (0–154%)		0.993 ^a
All arteries in humans (n = 54)	64% ± 74% (0–294%)		0.202 ^a
LCX ^e in dogs (n = 23)		42% ± 59% (0–225%)	
Time to max ischemic QRS prolongation (min)	3.4 ± 0.9 (2.0–5.0)	3.4 ± 0.7 (2.0–4.0)	0.911 ^b

^a Two-tailed p value calculated with an unpaired t-test. The p-value indicates the statistical difference between the mean ischemic QRS prolongation in dogs (LCX) and the human data.

^b Two-tailed p value calculated with an unpaired t-test.

^c Right coronary artery.

^d Left anterior descending artery.

^e Left circumflex artery.

prolongation may be of prognostic importance. Wong et al. [11] have previously shown that increased QRS duration is an independent predictor of 30-day mortality in patients with

anterior AMI. Thus, ischemic QRS prolongation could potentially serve as a biomarker for poor myocardial protection in patients presenting with acute coronary occlusion.

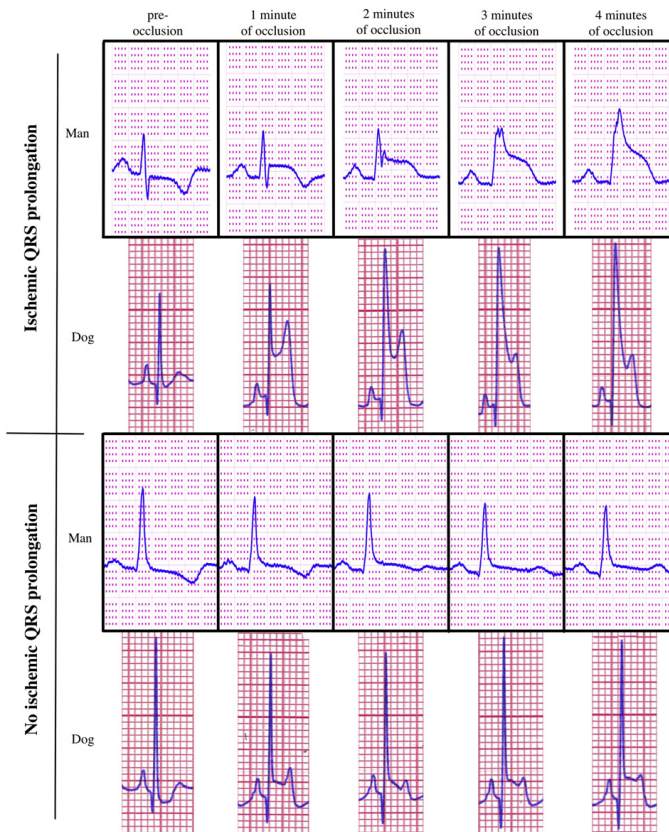


Fig. 5. Example of ECG lead II at 0, 1, 2, 3 and 4 min of occlusion in two dogs (LCX) and two humans (RCA), with one example of significant ischemic QRS prolongation and one with no ischemic QRS prolongation within each species. The grid systems have been transformed to be comparable.

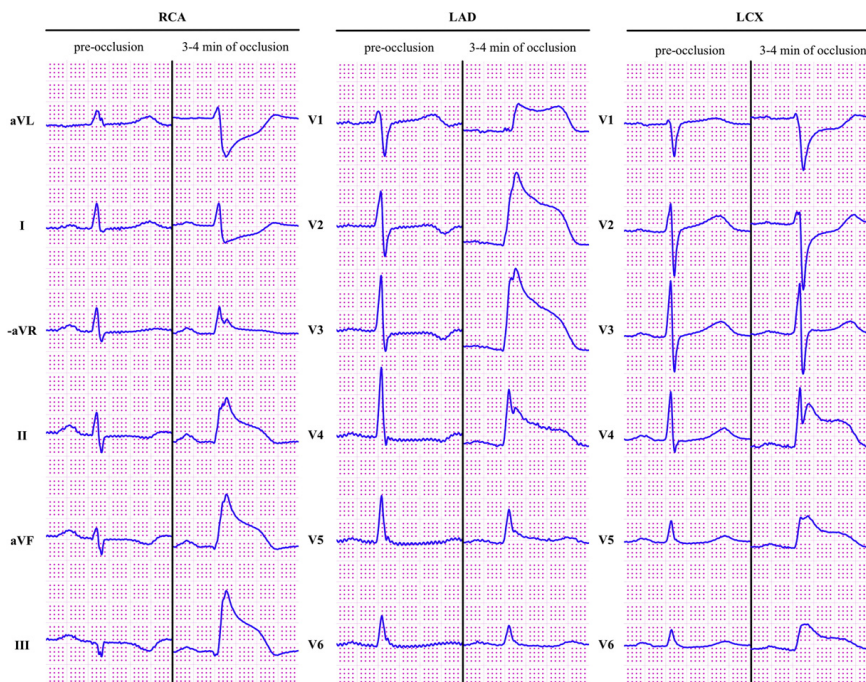


Fig. 6. Example of ECGs in humans. Pre-occlusion and 3–4 min into occlusion for one patient with RCA occlusion (extremity leads), one with LAD occlusion (precordial leads) and one with LCX occlusion (precordial leads). All patients had significant ischemic QRS prolongation.

Within the present study, the magnitude of ST-segment elevation was not considered. However, Weston et al. reported in a dog model, that for a given magnitude of STE, the presence of concurrent QRS prolongation was associated with less myocardial salvage [8]. Thus, evaluating ST-segment elevation together with ischemic QRS prolongation in patients with ACO might provide additional diagnostic value.

Novel method to quantify ischemic QRS prolongation

In previous experimental studies that have investigated ischemia-induced QRS changes, QRS duration was measured from QRS onset to an estimated J point [8,9,12]. However, within 30–60 s of the onset of ACO, the electrical conduction begin to down in the ischemic myocardium [4,7,20–22]. The slow, and thus delayed, depolarization of the ischemic myocardium results in QRS prolongation by which the QRS complex and T wave are merged and the J-point disappears in leads parallel to the ischemic myocardium. In the present study we introduce a new method for assessing ischemic QRS prolongation even in the absence of a defined J-point. The concept of defining a line between the R/S wave and the intersect of the PR baseline as described for the proposed method is similar to the previously described way of determining the offset of the T wave [23]. The term for this change in the QRS complex has, however, been difficult to

determine. Since the current method does not use the J-point as offset, the measurement from QRS onset to PR intercept cannot be termed QRS duration. Within this paper we have, therefore, decided to refer to the difference between baseline QRS duration and the distance from QRS onset to PR intercept as “ischemic QRS prolongation”.

Clinical significance of ischemic QRS prolongation

The preferred treatment for patients with ACO is PCI, to reperfuse the ischemic region. However, this requires the time of transport to a continuously available interventional catheterization laboratory. Intravenous thrombolytic therapy is an alternative means of acute reperfusion therapy, which could be administered immediately by emergency medical staff when transportation to a PCI facility is considerably prolonged [24]. Since severely ischemic myocytes infarct early during the ischemic process, the patients with the most severe ischemia are those likely to benefit the most from early reperfusion. The findings in the present study indicate that the presence of ischemic QRS prolongation is a potential biomarker for severe ischemia, and would thereby possibly aid in risk stratification and clinical decision-making regarding the method of acute reperfusion to be employed in a patient with evolving AMI. Thus, the basis of the decision would be the estimated degree of cardioprotection in individual patients. This, however, remains to be studied.

Limitations

The current study should be viewed in the light of some limitations. First, only a single lead ECG was available in the dog model, whereas in the human model a single coronary specific lead was used to duplicate the experimental situation. In future studies in patients where the culprit vessel is unknown, evaluation of ischemic QRS prolongation in all 12 leads is needed. Second, QRS measurements were made manually. In order to make the proposed method clinically feasible, it needs to be automated and implemented into computerized ECG analysis algorithms. Third, in the human cohort no measure of the severity of ischemia, direct or indirect, was compared to the ischemic QRS prolongation. Fourth, ischemic QRS prolongation in this study was calculated based on the knowledge of pre-occlusion QRS duration in each individual. Although a baseline ECG commonly exists for many ACO patients it is not always easily accessible in the emergency situation. It would, therefore, be optimal not to be dependent on access to prior ECGs, but rather use the patient as his/her own control, which could possibly be accomplished by considering the ischemic QRS prolongation in all 12 leads. Fifth, the patients all had a history of stable angina pectoris and therefore probably have higher collateral arterial flow compared to a general STEMI population for which the proposed method is intended. Sixth, only the first 5 min of coronary occlusion was evaluated. Studies concerning the temporal evolution of ischemic QRS prolongation during the first hours after onset of ACO are therefore warranted. Last, the number of patients included was limited. However, the clinical data on prolonged balloon inflation constitute a unique database, because this procedure is no longer used clinically.

Conclusion

Ischemic QRS prolongation could potentially be used as a biomarker for severe myocardial ischemia. Although arterial collateral flow cannot be measured with precision in the human heart, it seems probable that severe ischemia and its correlate, scant or absent arterial collateral flow, are present when there is a substantial ischemia-induced QRS prolongation.

Acknowledgments

We wish to acknowledge the technical and statistical expertise provided by Sebastian Bidhult (engineer, Department of Clinical Physiology and Nuclear medicine, Skane University Hospital and Lund University, Lund, Sweden).

References

- [1] Lopez AD, Mathers CD, Ezzati M, Jamison DT, Murray CJ. Global and regional burden of disease and risk factors, 2001: systematic analysis of population health data. *Lancet* 2006;367:1747–57, [http://dx.doi.org/10.1016/S0140-6736\(06\)68770-9](http://dx.doi.org/10.1016/S0140-6736(06)68770-9).
- [2] Jennings RB, Wagner GS. Roles of collateral arterial flow and ischemic preconditioning in protection of acutely ischemic myocardium. *J Electrocardiol* 2014;47:491–9, <http://dx.doi.org/10.1016/j.jelectrocard.2014.04.015>.
- [3] Jennings RB, Sommers H, Smyth G, Flack H, Linn H. Myocardial necrosis induced by temporary occlusion of a coronary artery in the dog. *Arch Pathol* 1960;70:68–78.
- [4] Wagner NB, Sevilla DC, Krucoff MW, Lee KL, Pieper KS, Kent KK, et al. Transient alterations of the QRS complex and ST segment during percutaneous transluminal balloon angioplasty of the left anterior descending coronary artery. *Am J Cardiol* 1988;62:1038–42.
- [5] Hathaway WR, Peterson ED, Wagner GS, Granger CB, Zabel KM, Pieper KS, et al. Prognostic significance of the initial electrocardiogram in patients with acute myocardial infarction. GUSTO-I Investigators. Global Utilization of Streptokinase and t-PA for Occluded Coronary Arteries. *JAMA* 1998;279:387–91, <http://dx.doi.org/10.1001/jama.279.5.387>.
- [6] Surawicz B, Orr CM, Hermiller JB, Bell KD, Pinto RP. QRS changes during percutaneous transluminal coronary angioplasty and their possible mechanisms. *J Am Coll Cardiol* 1997;30:452–8.
- [7] Surawicz B. Reversible QRS, changes during acute myocardial ischemia. *J Electrocardiol* 1998;31:209–20.
- [8] Weston P, Johanson P, Schwartz LM, Maynard C, Jennings RB, Wagner GS. The value of both ST-segment and QRS complex changes during acute coronary occlusion for prediction of reperfusion-induced myocardial salvage in a canine model. *J Electrocardiol* 2007;40:18–25, <http://dx.doi.org/10.1016/j.jelectrocard.2008.09.001>.
- [9] Floyd JS, Maynard C, Weston P, Johanson P, Jennings RB, Wagner GS. Effects of ischemic preconditioning and arterial collateral flow on ST-segment elevation and QRS complex prolongation in a canine model of acute coronary occlusion. *J Electrocardiol* 2009;42:19–26, <http://dx.doi.org/10.1016/j.jelectrocard.2008.09.006>.
- [10] Wong C, Gao W, Stewart RAH, Van Pelt N, French JK, Aylward PEG, et al. Risk stratification of patients with acute anterior myocardial infarction and right bundle-branch block. *Heart* 2006;114:783–9, <http://dx.doi.org/10.1161/CIRCULATIONAHA.106.639039>.
- [11] Wong C-K, Gao W, Stewart RAH, French JK, Aylward PEG, White HD. Relationship of QRS duration at baseline and changes over 60 min after fibrinolysis to 30-day mortality with different locations of ST elevation myocardial infarction: results from the Hirulog and Early Reperfusion or Occlusion-2 trial. *Heart* 2009;95:276–82, <http://dx.doi.org/10.1136/hrt.2008.146365>.
- [12] Ringborn M, Romero D, Pueyo E, Pahlm O, Wagner GS, Laguna P, et al. Evaluation of depolarization changes during acute myocardial ischemia by analysis of QRS slopes. *J Electrocardiol* 2011;44:416–24, <http://dx.doi.org/10.1016/j.jelectrocard.2011.03.005>.
- [13] Cantor AA, Goldfarb B, Iliia R. QRS prolongation: a sensitive marker of ischemia during percutaneous transluminal coronary angioplasty. *Catheter Cardiovasc Interv* 2000;50:177–83, [http://dx.doi.org/10.1002/\(SICI\)1522-726X\(200006\)50:2<177::AID-CCD6>3.0.CO;2-H](http://dx.doi.org/10.1002/(SICI)1522-726X(200006)50:2<177::AID-CCD6>3.0.CO;2-H).
- [14] Murry CE, Richard VJ, Reimer KA, Jennings RB. Ischemic preconditioning slows energy metabolism and delays ultrastructural damage during a sustained ischemic episode. *Circ Res* 1990;66:913–31, <http://dx.doi.org/10.1161/01.RES.66.4.913>.
- [15] Murry CE, Jennings RB, Reimer KA. Preconditioning with ischemia: a delay of lethal cell injury in ischemic myocardium. *Circulation* 1986;74:1124–36, <http://dx.doi.org/10.1161/01.CIR.74.5.1124>.
- [16] Warren SG, Wagner GS. The STAFF studies of the first 5 minutes of percutaneous coronary angioplasty balloon occlusion in man. *J Electrocardiol* 2014;47:402–7, <http://dx.doi.org/10.1016/j.jelectrocard.2014.04.011>.
- [17] Laguna P, Sörnmo L. The STAFF III ECG database and its significance for methodological development and evaluation. *J Electrocardiol* 2014;47:408–17.
- [18] Wagner GS, Macfarlane P, Wellens H, Josephson M, Gorgels A, Mirvis DM, et al. AHA/ACCF/HRS recommendations for the standardization and interpretation of the electrocardiogram. *J Am Coll Cardiol* 2009;53:1003–11, <http://dx.doi.org/10.1016/j.jacc.2008.12.016>.
- [19] Martin TN, Groenning BA, Murray HM, Steedman T, Foster JE, Elliot AT, et al. ST-segment deviation analysis of the admission 12-lead electrocardiogram as an aid to early diagnosis of acute myocardial infarction with a cardiac magnetic resonance imaging gold standard. *J Am Coll Cardiol* 2007;50:1021–8, <http://dx.doi.org/10.1016/j.jacc.2007.04.090>.

- [20] Bacharova L, Szathmary V, Mateasik A. QRS complex and ST segment manifestations of ventricular ischemia: the effect of regional slowing of ventricular activation. *J Electrocardiol* 2013;46:497–504, <http://dx.doi.org/10.1016/j.jelectrocard.2013.08.016>.
- [21] Conrad LL, Cuddy TE, Bayley RH. Activation of the ischemic ventricle and acute peri-infarction block in experimental coronary occlusion. *Circ Res* 1959;7:555–64, <http://dx.doi.org/10.1161/01.RES.7.4.555>.
- [22] Janse MJ, Kleber AG, Capucci A, Coronel R, Wilms-Schopman F. Electrophysiological basis for arrhythmias caused by acute ischemia. Role of the subendocardium. *J Mol Cell Cardiol* 1986;18:339–55, [http://dx.doi.org/10.1016/S0022-2828\(86\)80898-7](http://dx.doi.org/10.1016/S0022-2828(86)80898-7).
- [23] Lepeschkin E, Surawicz B. The measurement of the Q-T interval of the electrocardiogram. *Circulation* 1952;6:378–88, <http://dx.doi.org/10.1161/01.CIR.6.3.378>.
- [24] Dianati Maleki N, Ehteshami Afshar A, Armstrong PW. Use of electrocardiogram indices of myocardial ischemia for risk stratification and decision making of reperfusion strategies. *J Electrocardiol* 2014;47:520–4, <http://dx.doi.org/10.1016/j.jelectrocard.2014.04.006>.

Paper II





A 12-lead ECG-method for quantifying ischemia-induced QRS prolongation to estimate the severity of the acute myocardial event[☆]

Viktor ElMBERG, MD,^a Jakob Almer, MD,^b Olle Pahlm, MD, PhD,^b Galen S. Wagner, MD,^c Henrik Engblom, MD, PhD,^b Michael Ringborn, MD, PhD^{d,*}

^a Department of Clinical Physiology, Blekingesjukhuset, Karlskrona, Sweden

^b Department of Clinical Physiology and Nuclear Medicine, Skåne University Hospital and Lund University, Lund, Sweden

^c Duke University Medical Center, Durham, NC, USA

^d Thoracic Center, Blekingesjukhuset, Karlskrona, Sweden

Abstract

Introduction: Studies have shown terminal QRS distortion and resultant QRS prolongation during ischemia to be a sign of low cardiac protection and thus a faster rate of myocardial cell death. A recent study introduced a single lead method to quantify the severity of ischemia by estimating QRS prolongation. This paper introduces a 12-lead method that, in contrast to the previous method, does not require access to a prior ECG.

Methods: QRS duration was estimated in the lead that showed the maximal ST deviation according to a novel method. The degree of prolongation was determined by subtracting the measured QRS duration in the lead that showed the least ST deviation.

Results: The method is demonstrated in examples of acute occlusion in two of the major coronary arteries.

Conclusion: This paper presents a 12-lead method to quantify the severity of ischemia, by measuring QRS prolongation, without requiring comparison with a previous ECG.

© 2016 Elsevier Inc. All rights reserved.

Keywords:

Electrocardiography; Ischemia; ECG; Acute myocardial infarction; Severity of ischemia

Introduction

In acute coronary occlusion (ACO), rapid reperfusion is essential to salvage the ischemic myocardium at risk of infarction. This may be accomplished by primary percutaneous coronary intervention (pPCI) or by intravenous thrombolysis [1]. The rate of myocardial cell death during ACO depends to a large extent on the severity of ischemia within the myocardium at risk [2]. Ischemia severity has been shown to depend on the level of “protection” provided by both metabolic preconditioning and collateral blood flow [3]. Thus, it would be clinically important to enable accurate identification of patients with severe ischemia, so that they can receive the most rapidly available reperfusion strategy.

The most widely used diagnostic method in patients with suspected ACO is the standard 12-lead ECG. The conventional clinical criterion for acute myocardial ischemia is the presence of ischemia-related ST deviation (elevation or depression) [1]. However, acute myocardial ischemia may also cause alteration

of the myocardial depolarization resulting in “terminal QRS distortion” [4–7]. Prior studies have indicated that the amount of distortion is related to the severity of ischemia, and that it is an independent negative long-term prognostic factor in these patients [3,8–13]. Many attempts have been made to quantify this distortion by measuring QRS prolongation during ischemia [3,11,13–15]. In many patients this is, however challenging, since the end of the QRS is often indistinguishable because the distorted terminal QRS waveforms obscure the normally appearing “J point” that indicates the junction between QRS complex and ST segment.

Twenty-five years ago, Sclarovsky et al introduced an ECG method for grading the severity of ischemia following acute coronary occlusion: grade I – tall peaked T waves, grade I – ST segment elevation, and grade III – terminal QRS distortion [16]. However, this potentially important method failed to achieve clinical acceptance; because of the challenge of its accurate manual application [17], and because it is still only proven chronic prognostic value (i.e. correlation with larger infarct size and higher mortality). The acute diagnostic value of this method regarding reperfusion triage has yet to be documented [9,10]. Therefore, currently, there are no ECG methods for determination of the severity

[☆] Disclosures: None.

* Corresponding author at: Thoracic Center, Blekingesjukhuset, Karlskrona, 371 85, Karlskrona, Sweden. Tel.: +46 455731000.

E-mail address: michaelringborn@yahoo.com

of ischemia in patients with suspected ACO, and triage of the reperfusion therapy strategy is not considered.

Recently, a single-lead method for quantification of ischemic QRS prolongation has been proposed by Almer et al, in a study that included both experimental canine and clinical human populations [14]. There was a high correlation between the lack of collateral blood flow documented by radiolabeled microsphere counts and ischemic QRS prolongation in the canine population; and there were temporally and quantitatively similar ischemic QRS changes in patients receiving prolonged coronary angioplasty balloon inflation. There are, however, two key limitations to consider regarding the method used to quantify this ischemic QRS prolongation. It only considers a single ECG-lead, and it requires comparison with a baseline ECG recording.

It is the aim of this study to introduce an ECG method for quantification of ischemic QRS prolongation that considers all 12 standard leads, and does not require comparison with a baseline recording.

Methods

The rationale for the present study is that delayed activation within a severely ischemic region of myocardium, due to slowing of conduction, causes distortion in primarily the terminal aspect of the QRS waveform, and thus prolongs the QRS duration. This “ischemic QRS prolongation” is typically present in leads oriented parallel to the ischemic region, but is virtually absent in leads perpendicular to this region. This is demonstrated in Fig. 1, which shows the electrical axis of the heart in the transverse plane. The ECG complexes are the same as in Fig. 2, showing typical changes

associated with an occlusion of the left anterior descending artery (LAD). Leads that are relatively parallel to the ischemic region (V2–V4) show maximal ST deviation while leads that are relatively perpendicular to the ischemic region (V5 and V6) show minimal ST deviation. Analogously, terminal QRS distortion is present in the leads that are parallel to the ischemic region as a consequence of the slowed conduction. This regional slowing of conduction results in delayed activation of the severely ischemic area after the non-ischemic myocardium is already completely depolarized. Consequently, the only vector during this delayed depolarization, as displayed in Fig. 1, is oriented in the approximate direction toward V3 that therefore shows the maximum ST deviation. Leads that are perpendicular to this vector will be unable to show this late activity because their view is “from the side”.

A theoretical negative V3 lead, directly opposite of V3, would show changes mirroring V3, while both positive and negative leads perpendicular to the injury vector would show both minimal ST deviation and minimal terminal QRS distortion. Thus, leads that are perpendicular to an acutely ischemic region could serve as reference for both the millivolts of ST segment deviation and the milliseconds of terminal QRS complex distortion.

ECG measurements and method algorithm

The single lead method for estimating the QRS duration in the absence of a distinct J point is described in detail by Almer et al [14]. During ischemia, the lead with the largest ST segment deviation is determined. When no J point can be clearly distinguished, the QRS offset is defined as the point where a superimposed line descending from the peak of the R wave along 40% of its amplitude, between the R peak and

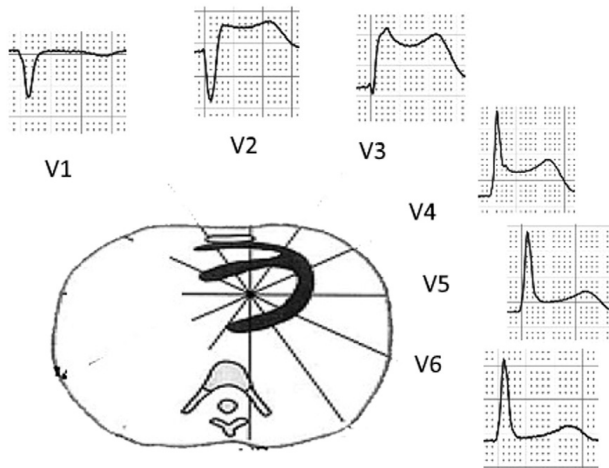


Fig. 1. Demonstration of the concept of parallel and perpendicular leads. Leads facing the ischemic region (V2–V4) show significant ST deviation and terminal QRS distortion. Leads that are perpendicular to this region show minimal ST deviation and terminal QRS distortion (reprinted and adapted from Pahlm-Webb with permission).

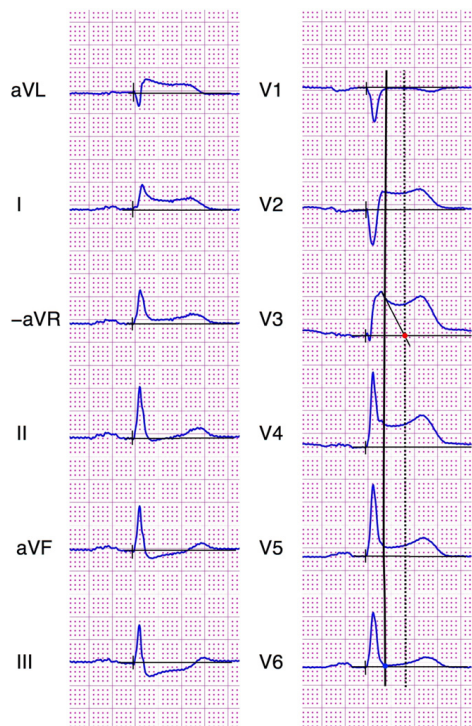


Fig. 2. Illustrates the application of the proposed method in a LAD occlusion. The bold line is drawn through the J point (blue dot) in the perpendicular lead (V6) and the dotted line is drawn through the estimated QRS offset (red dot) according to the Almer method in the lead with the maximal ST deviation (V3). The difference, in ms, between the QRS duration calculated in V3 and V6 is the ischemic QRS prolongation. The ischemic QRS prolongation is calculated to 90 ms or a ratio of 2.0.

the nadir of the ST-segment, intersects with the PR segment baseline (Fig. 3). Alternatively, when the final QRS waveform is an S wave, its offset is defined as the point where a superimposed line from its peak along 40% of its upslope intersects the PR segment baseline. If the changes in the lead with maximum ST elevation are so large as to prevent measurement, the closest adjacent lead is used instead (i.e. the lead with the 2nd largest ST deviation). Each value is measured as the average of measurements in 2 contiguous cardiac cycles.

The 12 lead method is presented in Fig. 2, as applied to the ECG of a patient with acute LAD occlusion caused by prolonged balloon PCI. The patient and the following example is part of the STAFF-III dataset of which a closer description can be seen elsewhere [18]. It consists of 102 patients referred for elective balloon PCI with prolonged occlusion, under continuous ECG recording, in Charleston, WV, USA in 1995 and 1996. All 12 leads are evaluated for ST deviation. The lead that shows the least ST deviation is considered to be perpendicular to the ischemic region. The

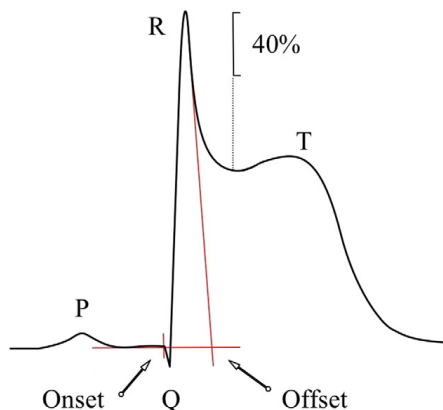


Fig. 3. Illustration of how the QRS offset is defined in the absence of a clear J point. The offset is defined as the point where a superimposed line along the peak of the R (or R' if present) wave and the first 40% of the R (or R' if present) wave downslope intersects the PR baseline. If there is an S wave, a superimposed line from the S wave nadir along the first 40% of the S wave upslope is used, and the intersection with the PR baseline defines the offset (adapted from Almer *et al.* [14]).

measured QRS duration in this lead from onset to J point is therefore considered to be the “non-ischemic QRS duration”. The lead that shows the most ST deviation is considered to be parallel to the ischemic region. Since there is no visible J point, the method of Almer [14] is applied to provide an estimated “ischemic QRS duration”. The difference between these measurements is considered the “ischemic QRS prolongation”. It is expressed in either ms; to the nearest 5 ms, or as a ratio which is defined as the “ischemic QRS duration” divided by the “non-ischemic QRS duration”.

Results

The example of application of the method in patients with LAD occlusion has been presented in Fig. 2, and an example of a patient with right coronary artery (RCA) occlusion is presented in Fig. 4. During the acute PCI balloon occlusions in each of the major coronary arteries, there are ischemic changes that obscure the J point, preventing precise measurement of QRS duration. However, these changes are viewed by different groups of leads when caused by acute occlusions of the different arteries.

In the example with LAD occlusion (Fig. 2), lead V3 with the maximal ST deviation was considered to be most parallel to the ischemic region, and the QRS duration was estimated to be 180 ms. In contrast, lead V6 with the minimal ST deviation, was considered to be most perpendicular to the ischemic region. Subtraction of its measured QRS duration of 90 ms yielded an ischemic QRS prolongation of 90 ms. Division of the “ischemic QRS duration” and the “non-ischemic QRS duration” yielded a ratio of 2.0

In the example with the RCA occlusion (Fig. 4), lead III with the maximal ST deviation was considered to be most

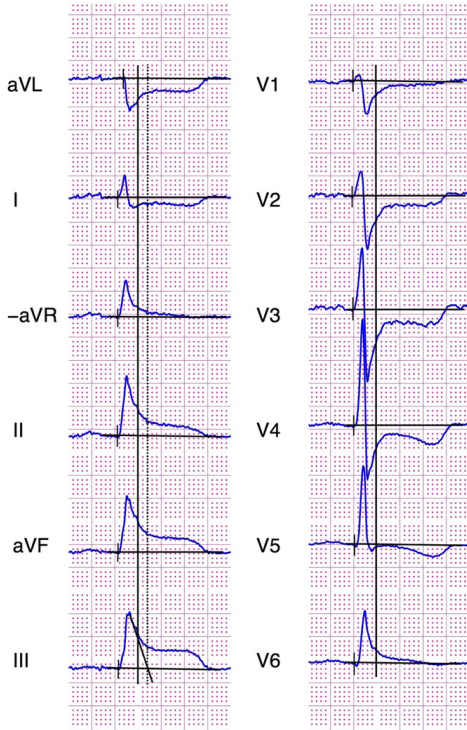


Fig. 4. Example of application of the method in a RCA occlusion. A bold line is drawn through the J point in the perpendicular lead (V5) and a dotted line is drawn through the estimated QRS offset according to the Almer method in the lead with the maximal ST deviation (III). Another bold line is drawn in the extremity leads at the estimated QRS offset calculated from lead V5 to illustrate the ischemic QRS prolongation as the time between the bold and dotted lines. The ischemic QRS prolongation is calculated to 40 ms or a ratio of 1.4.

parallel to the ischemic region and the QRS duration was estimated to be 130 ms. In contrast, lead V5 with the minimal ST deviation, was considered to be most perpendicular to the ischemic region. Subtraction of its measured QRS duration of 90 ms yielded an ischemic QRS prolongation of 40 ms. Division of the “ischemic QRS duration” and the “non-ischemic QRS duration” yielded a ratio of 1.4.

Fig. 5 illustrates the algorithm described above with a flow chart to evaluate the degree of QRS distortion. The lead with maximum and minimum ST deviation is identified and the difference in QRS duration is calculated. When no J point can be clearly distinguished the Almer method is applied.

Discussion

Several previous studies using different methods have shown ischemia-induced QRS changes in experimentally induced ischemia/infarction in animals, as well as in human

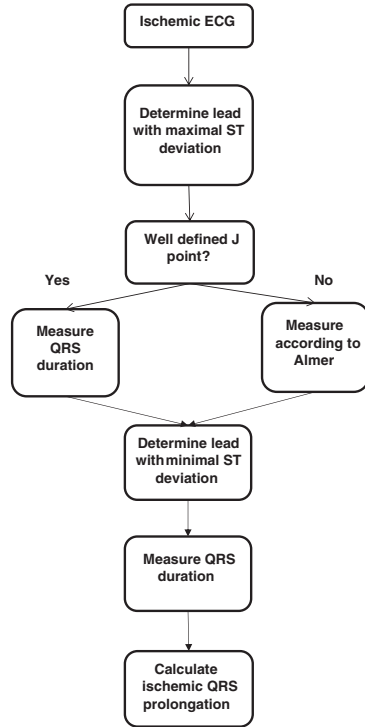


Fig. 5. Flow chart for application of the proposed method for quantification of the degree of severity of ischemia.

models of balloon-induced reversible ischemia [3–12]. These changes have furthermore been correlated to the severity of ischemia estimated by collateral flow and SPECT measurements. The previous and similar QRS prolongation method, using a single ECG lead, described by Almer et al has earlier been applied on an experimental animal population as well as in prolonged coronary balloon occlusion in man showing promising preliminary results [14]. There are however some differences in the exact application of our proposed method compared to the one proposed by Almer [14]. As ST deviation is the established method for identifying the ischemic area we have decided to use the lead with maximal ST deviation for measurement in contrast to the lead with maximal QRS prolongation which was used in the Almer study [1,14]. In contrast to the Almer method all 12 leads are considered and there is no need for a previous ECG for comparison.

The basis for using only the acute ECG to estimate QRS prolongation is that severe ischemia causes delayed activation in the ischemic region, which thus depolarizes after the rest of the myocardium has depolarized. This leaves the force moving toward the ischemic region the only remaining vector during late depolarization. Thus, QRS duration will be prolonged globally but this prolongation is

only visible in leads facing the ischemic region. Leads that are perpendicular to the ischemic region will show a shorter, incorrect, QRS duration that however is theoretically close to the baseline duration (in a non-ischemic situation) as these leads will be unable to detect the delayed activity in the ischemic region. The notion that a lead should be unable to detect a force moving perpendicular to it is consistent with vectorcardiography and should not be confused with QRS dispersion.

To bring this concept further and to be used in a clinical situation with ongoing ischemia and threatening infarction, the method needs to be robust, reproducible and shown to add clinical value in terms of outcome. Larger studies performed on QRS prolongation as well as evaluation of the Sclarovsky–Birnbaum (SB) ischemia grading system have shown that QRS changes in ST elevation myocardial infarction (STEMI) patients could potentially be used as a means of risk stratification [9,10,12,15]. Furthermore, the SB grading system has shown a relationship between terminal QRS distortion and larger infarcts as well as worse outcomes [9,10]. The present method adds the value of being independent of a distinct J point, and it also provides a gradual scale of QRS distortion, in contrast to the dichotomized SB grading scale. It therefore allows for a gradual estimation of severity in that a higher degree of ischemic QRS prolongation should imply more severe ischemia. As with the SB method, there is no need for previous ECGs as the ischemic QRS prolongation method only needs a snapshot ECG.

Possible clinical significance

Severely ischemic myocardium implies more rapid infarct development and thus likely worse clinical outcome after pPCI in patients with prolonged time to treatment [2]. Time is thus a more important factor in these individuals compared to those with less severe ischemic myocardium. It may be that patients with the most severe ischemia, and thus a higher degree of ischemic QRS prolongation, could benefit from alternative treatment, which could be administered already at the prehospital stage. The present method could offer a potential aid in deciding treatment strategy.

Limitations

There are a number of limitations to the presented method. Patients with very severe ischemia might have so pronounced terminal QRS distortion that they completely, or almost completely, lose the downslope of the R wave (commonly called tombstoning) making it impossible to apply the proposed method because of the lack of a QRS offset. However, most patients in this group would likely be classified as grade III ischemia according to the SB criteria and thus most of them would probably be classified as having “severe ischemia” even if the method presented is not applicable. Second, measurement on patients with a very small R wave could be difficult to achieve manually. However, this might still be possible if the method is automated.

Future directions

The method presented in this paper may offer the ability to estimate the severity of ischemia. However, this is still to be determined. Studies are currently underway with this in mind. One study assesses a group of patients undergoing elective balloon PCI for stable coronary artery disease where the relationship between severity by SPECT and the amount of ischemic QRS prolongation is being examined. Retrospective studies on the relationship between ischemic QRS prolongation and salvage by SPECT and cardiac magnetic resonance imaging (CMR) in STEMI patients are also planned. Further prospective studies would probably be needed to determine if the method could have merit as a tool for clinical decision-making. Manual measurement is time consuming and unpractical. For the method to be of clinical value it would have to be automated with a result given as a printout on the ECG.

Conclusion

This paper presents a 12-lead ECG method for estimating ischemic QRS prolongation as a means of identifying patients with severe ischemia who are liable to experience rapid infarction development. Using the proposed method, we are able to identify and quantify ischemic QRS prolongation independent of a distinct J point and without a prior baseline ECG. Further studies are needed, and are currently in progress, to validate the method.

References

- [1] O’Gara PT, Kushner FG, Ascheim DD, Casey DE, Chung MK, de Lemos JA, et al. 2013 ACCF/AHA guideline for the management of ST-elevation myocardial infarction: executive summary. *J Am Coll Cardiol* 2013;61:485–510, <http://dx.doi.org/10.1016/j.jacc.2012.11.018>.
- [2] Jennings RB, Wagner GS. Roles of collateral arterial flow and ischemic preconditioning in protection of acutely ischemic myocardium. *J Electrocardiol* 2014;47:491–9, <http://dx.doi.org/10.1016/j.jelectrocard.2014.04.015>.
- [3] Floyd JS, Maynard C, Weston P, Johanson P, Jennings RB, Wagner GS. Effects of ischemic preconditioning and arterial collateral flow on ST-segment elevation and QRS complex prolongation in a canine model of acute coronary occlusion. *J Electrocardiol* 2009;42:19–26, <http://dx.doi.org/10.1016/j.jelectrocard.2008.09.006>.
- [4] Cantor AA, Goldfarb B, Ilija R. QRS prolongation: a sensitive marker of ischemia during percutaneous transluminal coronary angioplasty. *Catheter Cardiovasc Interv* 2000;50:177–83, [http://dx.doi.org/10.1002/\(SICI\)1522-726X\(200006\)50:2<177::AID-CCD6>3.0.CO;2-H](http://dx.doi.org/10.1002/(SICI)1522-726X(200006)50:2<177::AID-CCD6>3.0.CO;2-H).
- [5] Surawicz B. Reversible QRS, changes during acute myocardial ischemia. *J Electrocardiol* 1998;31:209–20.
- [6] Surawicz B, Orr CM, Hermiller JB, Bell KD, Pinto RP. QRS changes during percutaneous transluminal coronary angioplasty and their possible mechanisms. *J Am Coll Cardiol* 1997;30:452–8, [http://dx.doi.org/10.1016/S0735-1097\(97\)00165-4](http://dx.doi.org/10.1016/S0735-1097(97)00165-4).
- [7] Bacharova L, Szathmary V, Mateasik A. QRS complex and ST segment manifestations of ventricular ischemia: the effect of regional slowing of ventricular activation. *J Electrocardiol* 2013;46:497–504, <http://dx.doi.org/10.1016/j.jelectrocard.2013.08.016>.
- [8] Bigi R, Mafri A, Colombo P, Gregori D, Corrada E, Alberti A, et al. Relation of terminal QRS distortion to left ventricular functional recovery and remodeling in acute myocardial infarction treated with

- primary angioplasty. *Am J Cardiol* 2005;96:1233–6, <http://dx.doi.org/10.1016/j.amjcard.2005.06.062>.
- [9] Birnbaum GD, Birnbaum I, Birnbaum Y. Twenty years of ECG grading of the severity of ischemia. *J Electrocardiol* 2014;47:546–55, <http://dx.doi.org/10.1016/j.jelectrocard.2014.02.003>.
- [10] Birnbaum Y, Sclarovsky S. The grades of ischemia on the presenting electrocardiogram of patients with ST elevation acute myocardial infarction. *J Electrocardiol* 2001;34:17–26, <http://dx.doi.org/10.1054/jelc.2001.28819> [Suppl.].
- [11] Weston P, Johanson P, Schwartz LM, Maynard C, Jennings RB, Wagner GS. The value of both ST-segment and QRS complex changes during acute coronary occlusion for prediction of reperfusion-induced myocardial salvage in a canine model. *J Electrocardiol* 2007;40:18–25, <http://dx.doi.org/10.1016/j.jelectrocard.2006.09.001>.
- [12] Wong CK, Gao W, Stewart RA, French JK, Aylward PEWH. Relationship of QRS duration at baseline and changes over 60 min after fibrinolysis to 30-day mortality with different locations of ST elevation myocardial infarction: results from the Hirulog and Early Reperfusion or Occlusion-2 trial. *Heart* 2009;95:276–82.
- [13] Romero D, Ringborn M, Laguna P, Pueyo E. Detection and quantification of acute myocardial ischemia by morphologic evaluation of QRS changes by an angle-based method. *J Electrocardiol* 2013;46:204–14, <http://dx.doi.org/10.1016/j.jelectrocard.2013.02.014>.
- [14] Almer J, Jennings RB, Maan AC, Ringborn M, Maynard CPO. Ischemic QRS prolongation as a biomarker of severe myocardial ischemia; 2015 [Submitted].
- [15] Ringborn M, Romero D, Pueyo E, Pahlm O, Wagner GS, Laguna P, et al. Evaluation of depolarization changes during acute myocardial ischemia by analysis of QRS slopes. *J Electrocardiol* 2011;44:416–24, <http://dx.doi.org/10.1016/j.jelectrocard.2011.03.005>.
- [16] Sclarovsky S, Mager A, Kusnec J, Rechavia E, Sagie A, Bassevich RSB. Electrocardiographic classification of acute myocardial ischemia. *Isr J Med Sci* 1990;26:525–31.
- [17] Billgren T, Birnbaum Y, Sgarbossa EB, Sejersten M, Hill NE, Engblom H, et al. Refinement and interobserver agreement for the electrocardiographic Sclarovsky-Birnbaum Ischemia Grading System. *J Electrocardiol* 2004;37:149–56, <http://dx.doi.org/10.1016/j.jelectrocard.2004.02.005>.
- [18] Laguna P, Sörmö L. ScienceDirect The STAFF III ECG database and its significance for methodological development and evaluation. *J Electrocardiol* 2014;47:408–17, <http://dx.doi.org/10.1016/j.jelectrocard.2014.04.018>.

Paper III



Ischemic QRS prolongation as a predictor of ventricular fibrillation in a canine model

Jakob Almer^a , Robert B. Jennings^b, Michael Ringborn^c and Henrik Engblom^a

^aDepartment of Clinical Physiology and Nuclear Medicine, Skåne University Hospital and Lund University, Lund, Sweden; ^bDuke University Medical Center, Durham, NC, USA; ^cThoracic Center, Blekingesjukhuset, Karlskrona, Sweden

ABSTRACT

Objectives. An acute coronary occlusion and its possible subsequent complications is one of the most common causes of death. One such complication is ventricular fibrillation (VF) due to myocardial ischemia. The severity of ischemia is related to the amount of coronary arterial collateral flow. In dog studies collateral flow has also been shown to be associated with QRS prolongation. The aim of this study was to investigate whether ischemic QRS prolongation (IQP) is associated with impending VF in an experimental acute ischemia dog model. **Methods.** Degree of IQP and occurrence of VF were measured in dogs ($n=21$) during coronary occlusion for 15 min and also during subsequent reperfusion (experiments conducted in 1984). **Results.** There was a significant difference in absolute IQP between dogs which developed VF during reperfusion (47 ± 29 ms, mean \pm SD) and those which did not (12 ± 10 ms; $p = .001$). **Conclusions.** IQP during acute coronary occlusion is associated with reperfusion VF in an experimental dog model and might therefore be a potential predictor of malignant arrhythmias in patients with acute coronary syndrome.

ARTICLE HISTORY

Received 22 March 2018
Revised 8 June 2018
Accepted 15 June 2018

KEYWORDS

Ventricular fibrillation; ischemia; electrocardiography; acute coronary syndrome

Introduction

Acute myocardial infarction (AMI) is one of the most frequent causes of death in the western world [1]. Early diagnosis of an acute AMI is based on the presence of acute ischemia-induced ST-segment elevation (STEMI) or its equivalent ST depression on the presenting ECG [2], due to an acute coronary occlusion (ACO). The severity of the ischemia is related to both metabolic preconditioning and the amount of coronary arterial collateral flow [3,4]. Treatment of STEMI is aimed at accomplishing coronary reperfusion as soon as possible, either by percutaneous coronary intervention (PCI) or by intravenous thrombolytic therapy, in order to maximize myocardial salvage [5]. One serious complication of acute ischemia is ventricular fibrillation (VF). VF can occur during ischemia and in conjunction with reperfusion therapy, although due to different pathophysiological mechanisms [6–11]. In both settings, however, these malignant arrhythmias can lead to sudden cardiac death [8]. Identifying patients susceptible for VF would therefore be of great importance.

Severe ischemia-induced changes in the myocardium may not only be manifested by ST-segment deviation, but also by changes of the QRS complex [12–14]. Previous studies have documented the association among increased QRS duration during ischemia, decreased coronary collateral flow and rapid rate of myocardial cell death [3,15,16]. In a recent study we found ischemic QRS prolongation (IQP) to be a

potential biomarker of severe myocardial ischemia [15], the method being recently tested by computer simulations [17]. Furthermore, transient ischemic QRS widening has been shown to predict impending VF and size of the myocardial injury in an experimental acute ischemia setting in pigs [18–20]. It has also been shown in humans that the magnitude of ST-segment elevation before PCI in STEMI independently predicts reperfusion VF [21].

The aim of this study was to test the hypothesis that IQP during the initial 15 min of ACO can serve as predictor for occurrence of VF within minutes following reperfusion in an experimental canine model.

Methods

Study population

All experiments involving the use of laboratory animals conform to the guidelines of the American Physiological Society and the standards in the Guide for the Care and Use of Laboratory Animals, DHEW Publ. No. NIH 85–23, revised 1985, and was approved by the institutional review board.

Data from 21 healthy mongrel dogs, previously included in studies of reperfusion effects in late ischemic injury originally published in 1985, were included in the present study [22]. All dogs underwent proximal occlusion of the left circumflex coronary artery (LCX) for 15 min.

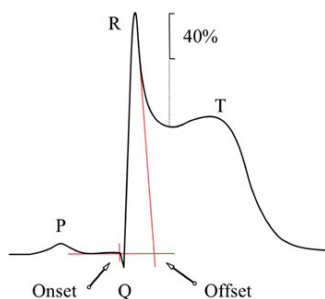


Figure 1. Depiction of ischemic QRS prolongation measurement method. During ischemia when no J-point could be clearly distinguished due to ST elevation, a line was drawn through the peak of the R (or R' if it was present) wave and along 40% of the downslope between the R peak and the nadir of the ST segment. Reprinted from Journal of Electrocardiology, 49/2, Almer et al., Ischemic QRS prolongation as a biomarker of severe myocardial ischemia, 139–147, Copyright (2016), with permission from Elsevier.

Surgical setup and ECG acquisition

All dogs were anesthetized with 30–40 mg/kg of sodium pentobarbital intravenously, intubated and ventilated as previously described in detail [22,23]. In short, a left thoracotomy was performed through the fourth intercostal space and the heart was suspended in a pericardial cradle. The LCX artery was identified and occluded for 15 min with a silk snare. Within the original experiment, investigating metabolic biomarkers in late ischemic injury, the dogs were divided into two groups, where the heart was excised at 3 or 20 min post-reperfusion. If the dog developed VF earlier than the planned time for excision it was excised immediately following total cardiac arrest. Using a Gould model 2400 recorder, ECG lead II was recorded continuously before, during the occlusion and also during reperfusion until the heart was excised.

The ischemic bed size was estimated in nine dogs (no more data were available) from either visual inspection of the heart directly after occlusion or by injecting a fluorescent dye, that was inspected postmortem by one observer (RBJ) [22]. Occurrence of ischemia-induced cyanosis on the heart surface was recorded and graded as small or large in extent, providing an estimate of the extent of ischemic epicardium. Bed size grades were defined as either covering the apex of the heart (large) or not (small). The fluorescent dye thioflavine S (TS; 1.0 ml/kg of a freshly centrifuged 4% solution in normal saline) was injected intravenously 10–15 s before excision of the heart. After excision, the heart was cooled, dissected and put under ultraviolet light to distinguish between non-ischemic or mildly ischemic (TS fluorescent) and severely or totally ischemic (non-fluorescent) areas. Ischemia bed size grades were defined as above. TS could not be used in dogs which developed VF.

ECG measurements

In acute STEMI, the terminal part of QRS complex is often distorted, without a clear demarcation between QRS and ST

segment. Thus, in this setting it is often very difficult to determine the location of QRS offset. Therefore, Almer et al. [15] developed a method to determine an estimate of the QRS offset, recently tested in computer simulations by Bacharova et al. [17]. ECG measurements within this study were performed using this method.

In short, QRS waveform measurements were obtained from ECG lead II at a paper speed of 25 mm/s and magnified $\times 2$ in a standard photocopier, that is, achieving 50 mm/s and 20 mm/mV. Before occlusion, measurement of baseline QRS duration, defined as the time between QRS onset and the J-point, was undertaken in all animals. During occlusion IQP was measured at 1 min intervals during first 5 min, the maximum value during this period was used in the data analysis.

IQP was measured by first recording the QRS duration using the J-point as offset if it could be clearly distinguished. When no J-point could be clearly distinguished due to ST elevation and terminal QRS distortion a line was drawn through the peak of the R (or R' if it was present) wave and along 40% of the downslope between the R peak and the nadir of the ST segment (Figure 1). The intersection of this line with the PR baseline was then used as offset. If there was an S wave associated with an ST-segment depression (basal lateral ischemia in LCX occlusions), a superimposed line from the S wave nadir along the first 40% of the S wave upslope was used and the intersection with the PR baseline marked the offset. Each value was measured as the average of measurements in two contiguous beats. The difference between the baseline QRS duration and the QRS duration during occlusion was calculated and referred to as absolute IQP (aIQP, measured to nearest 5 ms) and relative IQP (rIQP, normalized to baseline; Figure 1). Out of the five measurements (at 1 min intervals from occlusion), the measurement with the largest QRS duration, and thus aIQP, was used in the subsequent analysis. This QRS duration will be referred to as the max QRS duration from here on. Furthermore, the timing of the max QRS duration was recorded to the nearest minute post occlusion.

Timing and occurrence of VF was recorded to the nearest second after reperfusion. VF was defined as occurrence of bizarre, irregular, random waveforms, no clearly identifiable QRS complexes or P waves and/or wandering baseline continuing for more than 10 s without reverting to sinus rhythm.

All waveform measurements were manually performed by one observer (JA). Results were adjudicated with an experienced observer (GW) if uncertainties arose.

Statistical analysis

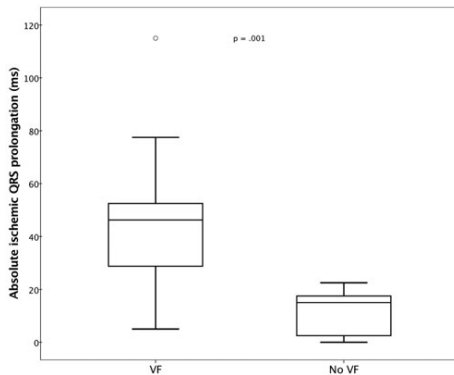
Graphical procedures and comparisons of mean to median as well as the relation of the SD to the mean were used to evaluate if data were normally distributed. IQP was not normally distributed and part of most analyses. For parameters that were not normally distributed, non-parametric tests were applied for statistical significance. Continuous variables are presented as mean \pm SD. Categorical data are presented

Table 1. Baseline characteristics.

Mean \pm SD (range)	Total (n = 21)	VF (n = 12)	No VF (n = 9)	P-value*
Pre-occlusion heart rate (bpm)	166 \pm 31 (124–260)	170 \pm 33 (130–260)	160 \pm 29 (124–222)	.434
Pre-occlusion blood pressure systolic/diastolic (mmHg)	166 \pm 29 (120–230)/ 111 \pm 2 (85–190)	159 \pm 22 (120–190)/ 114 \pm 29 (85–190)	174 \pm 35 (140–230)/ 108 \pm 17 (90–130)	.336/.775
Pre-occlusion QRS duration (ms)	45 \pm 4 (35–53)	44 \pm 3 (35–48)	47 \pm 4 (42–53)	.137
Max QRS duration (ms)	77 \pm 28 (42–155)	91 \pm 28 (50–155)	59 \pm 10 (42–73)	.004
Absolute IQP (ms)	32 \pm 28 (0–115)	47 \pm 29 (5–115)	12 \pm 10 (0–23)	.001
Relative IQP (%)	73 \pm 68 (0–288)	108 \pm 70 (11–288)	26 \pm 19 (0–45)	.001
Time to max IQP (min)	3.4 \pm 1.0 (2.0–5.0)	3.7 \pm 0.8 (3.0–5.0)	3.0 \pm 1.0 (2.0–4.0)	.181

IQP: ischemic QRS prolongation; VF: ventricular fibrillation.

*Mann-Whitney test.

**Figure 2.** Box plot of reperfusion VF and no VF groups.

as numbers. All statistical tests were two-sided and a *p*-value of $<.05$ was considered to indicate statistical significance. An receiver operating characteristic (ROC) analysis was performed to evaluate optimum cut-off value of IQP, using the Youden method. Sensitivity, specificity and area under the curve (AUC) were analyzed. SPSS version 19.0, SPSS version 23.0 and MATLAB version R2013a were used for the statistical analyses.

Results

The characteristics of the 21 dogs included in the study are shown in Table 1. Baseline QRS duration, max QRS duration and aIQP were 45 ± 4 , 77 ± 28 and 32 ± 28 ms, respectively. The maximum IQP was reached after 3.4 ± 1.0 min of occlusion. The IQP did not decrease from the maximum level, having reached a plateau, until reperfusion was accomplished at 15 min.

Twelve dogs (57%) developed VF at 20 ± 11 s post-reperfusion. Mean aIQP was 47 ± 29 ms and differed significantly ($p = .001$) from the nine dogs that did not develop VF, 12 ± 10 ms (Table 1 and Figure 2).

Of the eight dogs in which ischemic bed size was recorded, two had a large bed size and six had a small bed size. None of the dogs with a small bed size developed VF. Out of the dogs with a large bed size one developed VF. There was no significant difference in mean aIQP between these groups.

The ROC analysis produced an optimum cut-off value of 21 ms with sensitivity of 92% and specificity of 89%. The AUC was 0.94 (95% CI 0.83–1.00; Figure 4).

Time of excision, 3 or 20 min post-reperfusion, had no effect on the recorded results since all dogs which experienced VF developed their arrhythmia within 36 s after reperfusion.

Figure 3 shows example of ECGs of two dogs, one which subsequently developed reperfusion VF and one which did not. The one which developed VF (top) also showed significant IQP.

Discussion

The present study shows a significant difference between dogs developing VF during reperfusion and those that did not, as regards acute IQP. Furthermore, in the included ROC analysis an AUC value of 0.94 was obtained with an optimum cut-off value of 21 ms with sensitivity of 92% and specificity of 89%. Thus, within the current study, predicting reperfusion VF already at 3.4 ± 1.0 min into occlusion is potentially possible.

Thus, an early QRS prolongation due to acute myocardial ischemia may have the potential to predict impending reperfusion VF, which is in accordance with the findings of Demidova et al. in an experimental pig model of myocardial infarction [18,19,21]. Earlier studies have also found that similar patterns to the ones found in our population positively predict VF in humans, although not appreciated as QRS prolongation [24]. Furthermore, IQP has been shown to correlate with collateral flow in a canine model [15,23,25]. Dogs with >5 ms of IQP exhibited significantly lower collateral flow compared to dogs with ≤ 5 ms of IQP [15]. Hence, the increased risk of developing VF in acute ischemic heart disease might be related to more severe myocardial ischemia due to lower coronary collateral flow.

Translating the current results to a human population is, however, not necessarily straightforward. Within the study there were controlled experiments with total occlusion of the LCX in the dog. In a clinical setting this may differ widely where the initial thrombus may occlude the entire lumen of a vessel but dissolve and/or add thrombus material continuously causing spontaneous reperfusion and/or reocclusion. Although a spontaneous reperfusion in the acute phase of an AMI could be similar to the experimental setup, many more factors affect a clinical situation such as vessel spasms, previous heart disease and so on. Furthermore, Hedström et al. describes the difference in infarct evolution,

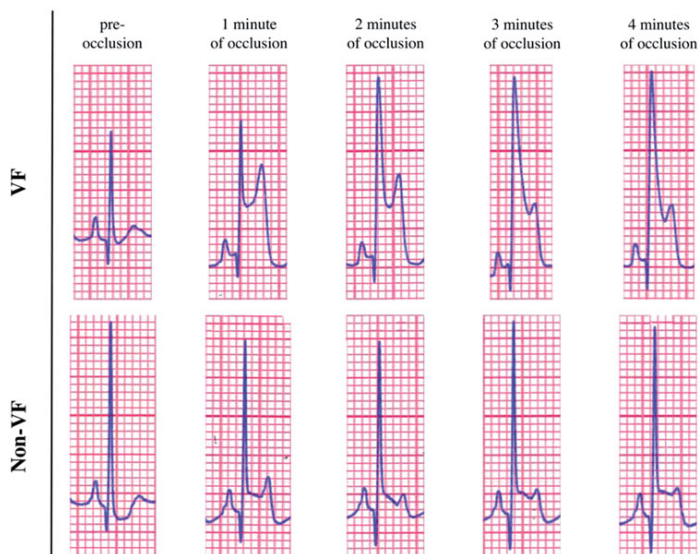


Figure 3. Example ECG of lead II in two dogs before and at 1, 2, 3 and 4 min into occlusion. The dog at the top later develops VF whereas the one at the bottom does not. The one at the top develops ischemic QRS prolongation during the first minutes of occlusion.

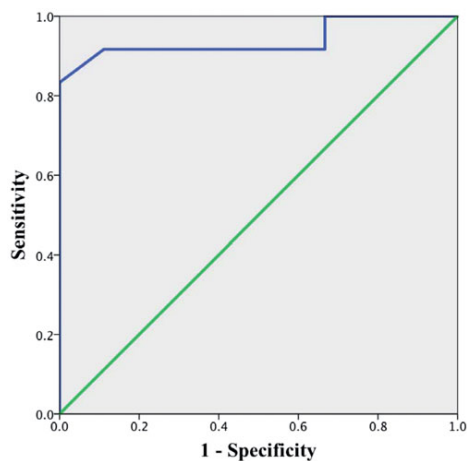


Figure 4. ROC curve (blue line) of IQP indicating VF or not. Green line indicates a reference AUC of 0.5.

using MRI, between dog and human, where the time to reach 50% of myocardium at risk is about 59% longer in humans than dogs [26]. Therefore, 15 min of occlusion probably corresponds to a longer time period in a human clinical setting. Although the current results have little implication in a clinical situation, it does, however, showcase IQP as a potential ECG marker.

Ischemic bed size was estimated in a subset within the current study. The results indicate that dogs with larger ischemic beds had longer QRS prolongation (albeit non-significant due to the coarse data recording). Also, none of the dogs with small bed size developed VF while one out of two in the large bed size group did.

In the experiment by Demidova et al. [18,20] myocardial infarction was induced through coronary artery occlusion lasting 40 min in an experimental pig model. Within this timeframe, two separate peaks of QRS widening was observed. These peaks occurred at 3.7 ± 1.6 and 19.1 ± 4.0 min into occlusion, the first similar in timing to the findings in the current study (3.7 ± 0.8 min). However, within the present study, the observers noted that the IQP developed into a plateau, after the maximum value had been reached, until reperfusion. This is dissimilar to the findings by Demidova et al. where the QRS widening peaked in order to reduce before the next peak. There are distinct differences between the experimental models; however, foremost is that of different animals used (dog vs. pig) that can explain the discrepancies but obstruct the translation of results. Furthermore, the current study was designed to study ischemia only, and therefore duration of ischemia was set to 15 min in order to avoid infarct development. In the study by Demidova et al. the duration of ischemia was 40 min in order for the animals to develop infarction [18]. It might be that biphasic QRS prolongation reflects both the initial ischemia and the start of infarct development at approximately 20 min.

Within the present study, ST-segment elevation was not considered since only one lead was available and no global ST-segment elevation could be appreciated. However, Weston et al. reported in a dog model that for a given magnitude of STE, the presence of concurrent QRS prolongation was associated with less myocardial salvage [25]. Furthermore, Demidova et al. found that the magnitude of ST-segment elevation before PCI for STEMI independently predicts reperfusion VF [21]. Thus, evaluating ST-segment elevation together with IQP in patients with STEMI might provide additional diagnostic information.

Limitations

The current study should be viewed in the light of some limitations. First, an animal model with small sample size was used. To what extent QRS prolongation can be used to predict AMI patients at risk of malignant arrhythmias is not known. Second, occlusion of only the LCX was investigated. Furthermore, only one ECG lead (lead II) was recorded and assessed. Different results may have been obtained if additional arteries and/or leads were assessed. However, within this study there are no means of optimizing the experiment setup more than 30 years later. Third, IQP measurements were made manually. Development of automated or semi-automated methods for IQP measurements would be desirable and necessary for clinical feasibility. Also a 12-lead ECG-method for quantifying ischemia-induced QRS prolongation would be paramount and has actually been presented in a recent study by Elmberg et al. based on the current method [27]. Fourth, in the current study only the first 15 min of coronary occlusion and a various degree of ischemia were evaluated. Studies in STEMI patients regarding development and temporal evolution of QRS prolongation during the first hours of ACO as well as its correlation with myocardial salvage are needed in order to elucidate whether the findings in the present study are similar to findings in a clinical setting in humans. Fifth, ischemic bed size was estimated within the current study based on visual inspection of cyanosis on the heart surface. The coarseness of the grading is a major limitation and the data should be viewed in the light of this.

Conclusion

There was a significant difference in IQP between dogs developing VF after reperfusion of an ACO as compared to those who did not. Thus, an early QRS prolongation due to acute myocardial ischemia may have the potential to predict impending reperfusion VF.

Acknowledgements

The authors would like to acknowledge the great contribution in all aspects of this manuscript, especially its very conception, to the late Dr. Galen Wagner. Dr. Wagner passed away on 13 July 2016 and the author team misses his expertise, guidance and energy very deeply.

Disclosure statement

No potential conflict of interest was reported by the authors.

Funding

This work was supported by the Swedish Research Council (Vetenskapsrådet); the Swedish Heart and Lung Foundation (Hjärt-Lungfonden); the Region of Scania; the Medical Faculty of Lund University; the American Heart Association, Durham, North Carolina, USA [account 5-21628] and by the National Heart, Lung and Blood Institute of the National Institutes of Health (grant number HL 23138 and HL 27416).

ORCID

Jakob Almer  <http://orcid.org/0000-0003-0462-0410>

References

- [1] Lopez AD, Mathers CD, Ezzati M, et al. Global and regional burden of disease and risk factors, 2001: systematic analysis of population health data. *Lancet*. 2006;367:1747–1757.
- [2] Hathaway WR, Peterson ED, Wagner GS, et al. Prognostic significance of the initial electrocardiogram in patients with acute myocardial infarction. GUSTO-I Investigators. Global Utilization of Streptokinase and t-PA for Occluded Coronary Arteries. *JAMA*. 1998;279:387–391.
- [3] Jennings RB, Wagner GS. Roles of collateral arterial flow and ischemic preconditioning in protection of acutely ischemic myocardium. *J Electrocardiol*. 2014;47:491–499.
- [4] Jennings RB, Sommers H, Smyth G, et al. Myocardial necrosis induced by temporary occlusion of a coronary artery in the dog. *Arch Pathol*. 1960;70:68–78.
- [5] Reed GW, Rossi JE, Cannon CP. Acute myocardial infarction. *Lancet*. 2017;389:197–210.
- [6] Luqman N, Sung RJ, Wang C-L, et al. Myocardial ischemia and ventricular fibrillation: pathophysiology and clinical implications. *Int J Cardiol*. 2007;119:283–290.
- [7] Manning AS, Hearse DJ. Reperfusion-induced arrhythmias: mechanisms and prevention. *J Mol Cell Cardiol*. 1984;16:497–518.
- [8] Paranskaya L, Akin I, Chatterjee T, et al. Ventrikuläre tachykardie und plötzlicher herztod nach primärer PCI-reperfusionstherapie. Einfluss auf die primärprävention des plötzlichen herztods. *Herzschrittmachertherapie und Elektrophysiologie*. 2011;22:243–248.
- [9] Boissel JP, Castaigne A, Mercier C, et al. Ventricular fibrillation following administration of thrombolytic treatment. The EMIP experience. *European Myocardial Infarction Project*. *Eur Heart J* 1996;17:213–221.
- [10] Henriques JPS, Gheeraert PJ, Ottervanger JP, et al. Ventricular fibrillation in acute myocardial infarction before and during primary PCI. *Int J Cardiol*. 2005;105:262–266.
- [11] Curtis MJ, Macleod BA, Walker MJ. Models for the study of arrhythmias in myocardial ischaemia and infarction: the use of the rat. *J Mol Cell Cardiol*. 1987;19:399–419.
- [12] Surawicz B, Orr CM, Hermiller JB, et al. QRS changes during percutaneous transluminal coronary angioplasty and their possible mechanisms. *J Am Coll Cardiol*. 1997;30:452–458.
- [13] Balci B. Tombstoning ST-elevation myocardial infarction. *Curr Cardiol Rev*. 2009;5:273–278.
- [14] Di Diego JM, Antzelevitch C. Cellular basis for ST-segment changes observed during ischemia. *J Electrocardiol*. 2003;36:1–5.
- [15] Almer J, Jennings RB, Maan AC, et al. Ischemic QRS prolongation as a biomarker of severe myocardial ischemia. *J*


- Electrocardiol. 2016;49:139–147. Available from: <http://www.ncbi.nlm.nih.gov/pubmed/26810927>.
- [16] Garcia-Rubira JC, Nuñez-Gil I, Garcia-Borbolla R, et al. Distortion of the terminal portion of the QRS is associated with poor collateral flow before and poor myocardial perfusion after percutaneous revascularization for myocardial infarction. *Coron Artery Dis.* 2008;19:389–393.
- [17] Bacharova L, Halkias I. The identification of the QRS complex offset in the presence of ST segment deviation. *J Electrocardiol.* 2016;49:977–979.
- [18] Demidova MM, Martín-Yebra A, van der Pals J, et al. Transient and rapid QRS-widening associated with a J-wave pattern predicts impending ventricular fibrillation in experimental myocardial infarction. *Heart Rhythm.* 2014;11:1195–1201.
- [19] Mart A, Demidova MM, Platonov P, et al. Increase of QRS duration as a predictor of impending ventricular fibrillation during coronary artery occlusion. *Comput Cardiol.* 2010. 2013;133–136.
- [20] Demidova MM, Martín-Yebra A, Koul S, et al. QRS broadening due to terminal distortion is associated with the size of myocardial injury in experimental myocardial infarction. *J Electrocardiol.* 2016;49:300–306.
- [21] Demidova MM, Carlson J, Erlinge D, et al. Predictors of ventricular fibrillation at reperfusion in patients with acute ST-elevation myocardial infarction treated by primary percutaneous coronary intervention. *Am J Cardiol.* [Internet]. 2015;115:417–422.
- [22] Jennings RB, Schaper J, Hill ML, et al. Effect of reperfusion late in the phase of reversible ischemic injury. Changes in cell volume, electrolytes, metabolites, and ultrastructure. *Circ Res.* 1985;56:262–278.
- [23] Floyd JS, Maynard C, Weston P, et al. Effects of ischemic preconditioning and arterial collateral flow on ST-segment elevation and QRS complex prolongation in a canine model of acute coronary occlusion. *J Electrocardiol.* 2009;42:19–26.
- [24] Aizawa Y, Jastrzebski M, Ozawa T, et al. Characteristics of electrocardiographic repolarization in acute myocardial infarction complicated by ventricular fibrillation. *J Electrocardiol.* 2012;45:252–259.
- [25] Weston P, Johanson P, Schwartz LM, et al. The value of both ST-segment and QRS complex changes during acute coronary occlusion for prediction of reperfusion-induced myocardial salvage in a canine model. *J Electrocardiol.* 2007;40:18–25.
- [26] Hedström E, Engblom H, Frogner F, et al. Infarct evolution in man studied in patients with first-time coronary occlusion in comparison to different species – implications for assessment of myocardial salvage. *J Cardiovasc Magn Reson.* 2009;11:38.
- [27] Elmberg V, Almer J, Pahlm O, et al. A 12-lead ECG-method for quantifying ischemia-induced QRS prolongation to estimate the severity of the acute myocardial event. *J Electrocardiol.* 2016;49:272–277.

Paper IV



ORIGINAL ARTICLE

Ischemic QRS prolongation as a biomarker of myocardial injury in STEMI patients

Jakob Almer¹  | Viktor Elmberg² | Josef Bränsvik¹ | David Nordlund¹ | Ardavan Khoshnood³ | Michael Ringborn⁴ | Marcus Carlsson¹ | Ulf Ekelund³ | Henrik Engblom¹

¹Department of Clinical Physiology and Nuclear Medicine, Skåne University Hospital and Lund University, Lund, Sweden

²Department of Clinical Physiology, Blekingesjukhuset, Karlskrona, Sweden

³Department of Emergency Medicine, Skåne University Hospital and Lund University, Lund, Sweden

⁴Thoracic Center, Blekingesjukhuset, Karlskrona, Sweden

Correspondence

Henrik Engblom, Department of Clinical Physiology and Nuclear Medicine, Skåne University Hospital, Lund, Sweden.
Email: henrik.engblom@med.lu.se

Funding information

This work was supported by independent research grants from the Swedish Heart-Lung Foundation, Swedish Research Council, Region Skåne (Sweden), Skåne University Hospital, Lund University Medical faculty.

Abstract

Background: Patients with acute coronary occlusion (ACO) may not only have ischemia-related ST-segment changes but also changes in the QRS complex. It has recently been shown in dogs that a greater ischemic QRS prolongation (IQP) during ACO is related to lower collateral flow. This suggests that greater IQP could indicate more severe ischemia and thereby more rapid infarct development. Therefore, the purpose was to evaluate the relationship between IQP and measures of myocardial injury in patients presenting with acute ST-elevation myocardial infarction (STEMI).

Methods: Seventy-seven patients with first-time STEMI were retrospectively included from the recently published SOCCER trial. All patients underwent a cardiac magnetic resonance (CMR) examination 2–6 days after the acute event. Infarct size (IS), myocardium at risk (MaR), and myocardial salvage index (MSI) were assessed and related to IQP. IQP measures assessed were; computer-generated QRS duration, QRS duration at maximum ST deviation, absolute IQP and relative IQP, all derived from a pre-PCI, 12-lead ECG.

Results: Median absolute IQP was 10 ms (range 0–115 ms). There were no statistically significant correlations between measures of IQP and any of the CMR measures of myocardial injury (absolute IQP vs IS, $r = 0.03$, $p = 0.80$; MaR, $r = -0.01$, $p = 0.89$; MSI, $r = -0.05$, $p = 0.68$).

Conclusions: Unlike previous experimental studies, the IQP was limited in patients presenting at the emergency room with first-time STEMI and no correlation was found between IQP and CMR variables of myocardial injury in these patients. Therefore, IQP does not seem to be a suitable biomarker for triaging patients in this clinical context.

KEYWORDS

acute coronary occlusion, electrocardiography, ischemia, QRS

1 | INTRODUCTION

Ischemic heart disease is one of the leading causes of death in the western world (Lopez, Mathers, Ezzati, Jamison, & Murray, 2006). Acute myocardial infarction (AMI) usually results from an acute

coronary occlusion (ACO), requiring immediate revascularization in order to minimize infarct size (Reed, Rossi, & Cannon, 2017). Electrocardiography (ECG) is the most widely used method for triaging patients with suspected AMI in the emergency room as well as in pre-hospital settings. Ischemia-related ST-segment deviation on the

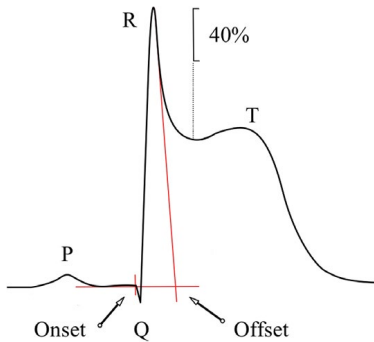


FIGURE 1 Depiction of ischemic QRS prolongation measurement method. During ischemia, when no J-point could be clearly distinguished due to ST-elevation, a line was drawn through the peak of the R (or R' if it was present) wave and along 40% of the downslope between the R peak and the nadir of the ST segment. Reprinted from Almer et al. (2016), copyright (2016), with permission from Elsevier

presenting 12-lead ECG accompanied by symptoms and release of biochemical markers of myocardial injury, such as cardiac Troponin T (cTnT), constitute the diagnostic foundation for AMI (Kumar & Cannon, 2009).

Several studies have shown that acute myocardial ischemia is not only manifested as ST-segment deviation on the ECG, but can also affect the QRS complex in situations with severe ischemia, usually seen as terminal QRS distortion (Balci, 2009; Surawicz, Orr, Hermiller, Bell, & Pinto, 1997). Garcia-Rubira et al. have shown a relationship between terminal QRS distortion and poor collateral flow, using the Sclarovsky-Birnbaum ischemia severity grading system where grade 3 of ischemia (G3I) is associated with terminal QRS distortion (Birnbaum, Birnbaum, & Birnbaum, 2014; Garcia-Rubira et al., 2008). Recently, terminal QRS distortion, assessed as ischemic QRS prolongation (IQP) was shown to be related to lower collateral flow in a dog model of acute myocardial ischemia (Almer et al., 2016). This suggests a relationship between ischemia-related IQP and severity of ischemia and, potentially, the speed at which the infarction develops in the ischemic myocardium. To what extent these findings translate to patients in a clinical setting is yet to be determined.

Cardiovascular magnetic resonance imaging (CMR) is currently considered the reference standard for assessment of myocardium at risk (MaR), final infarct size (IS), and myocardial salvage index (MSI) in the setting of ACO. Previous studies in STEMI patients have shown that G3I is associated with larger IS (acute and 4 months post STEMI), larger MaR, lower MSI and more severe microvascular obstruction. (Hassell et al., 2016; Rommel et al., 2016; Valle-Caballero et al., 2016; Weaver et al., 2011) Furthermore, low collateral flow, and thereby more severe ischemia, has been correlated to lower MSI and more rapid infarct development on CMR (Hedström et al.,

2009). Thus, IQP might enable identification of STEMI patients with severe ischemia and at risk of rapid infarct development.

Therefore, the purpose of the current study was to evaluate how IQP and Sclarovsky Birnbaum ischemia grade is related to measures of myocardial injury, such as IS, MaR, MSI and left ventricular function as assessed by CMR in patients presenting with first-time acute STEMI.

2 | METHODS

2.1 | Study population

Patients included in this retrospective study were originally a part of the randomized controlled SOCCER (The Supplemental Oxygen in Catheterized Coronary Emergency Reperfusion) trial. This trial was conducted at Skåne University Hospital, Sweden and was approved by the regional ethics committee. Oral informed consent was initially obtained from each patient in the ambulance and later completed in writing after PCI (Khoshnood et al., 2018).

The SOCCER population consisted of 160 normoxic (O_2 -saturation $\geq 94\%$) STEMI patients who underwent primary PCI and randomized to either standard oxygen therapy or no supplemental oxygen in the ambulance. A total of 95 patients underwent CMR 2–6 days after the PCI. Patients with a previous AMI or inability to make the decision to participate were excluded (Khoshnood et al., 2018).

Inclusion criteria in the current study were diagnostic CMR images and STEMI or STEMI equivalent criteria met (Martin et al., 2007; Wagner et al., 2009).

2.2 | ECG acquisition

Details regarding the ECG recordings have previously been described (Khoshnood et al., 2018). Briefly, while resting in a supine position, a 10 s, 12-lead ECG was acquired for each patient in the ambulance, at admission to the hospital prior to PCI and at discharge. For the dataset in the present study, digital ECGs were collected for all patients from the computerized patient records of Region Skåne (Melior; Siemens, Germany) and from the SWEDEHEART quality registries RIKS-HIA or SCAAR. If no ECG from the ambulance was available, the first ECG (prior to PCI) recorded at arrival to hospital was used for analysis. The signals were digitized at a sampling rate of 1 kHz, with an amplitude resolution of $0.6 \mu V$.

2.3 | ECG analysis

The acute ECG in the ambulance or first ECG after hospital admission before PCI was analyzed for IQP. The computer-generated QRS duration was noted for each ECG. All IQP measurements were made according to a single 12 lead ECG method (Elmberg et al., 2016).

In short, manual measurements were made from print outs of median beats of the ECG at a paper speed of 50 mm/s and gain of 10 mm/mV. The lead with the maximum ST-deviation as well as the

lead with the least ST deviation was determined. The latter was used as the reference lead. QRS duration (QRSd) was calculated for both leads. The difference between the QRSd measurements was calculated with a resulting QRS prolongation, referred to as aIQP (absolute IQP, in ms) and rIQP (relative IQP), normalized to QRSd at the reference lead. In addition, the QRSd in the reference lead was also measured on the discharge ECG and compared with the acute ECG.

If no distinct J point was present due to terminal distortion of the QRS complex, the QRS duration was estimated by superimposing a line descending from the peak of the R wave and following 40% of its amplitude (Almer et al., 2016). The estimated J point was defined as the intersection point of the superimposed line and the isoelectric line (Figure 1). If the final QRS waveform was an S wave, the same method was used but the line was superimposed from the peak of the S wave.

Measurements were made by two observers (JA, VE) blinded to the CMR data. In case of disagreement in the analysis, the differences were adjudicated in consensus together with a third observer (HE).

The Sclarovsky-Birnbaum Ischemia Grade was also determined from the acute ECG using the algorithm of the refined grading system described by Billgren et al. (Billgren et al., 2004). In short, each ECG was analyzed and assigned an ischemia grade from 1–3 where grade 3 of ischemia (G3) is associated with terminal QRS distortion. The algorithm has previously been described in detail (Billgren et al., 2004).

For estimation of the acuteness of the ischemic ECG changes, the ECGs were also analyzed using the Anderson-Wilkins (AW) acuteness score, which has previously been described in detail (Heden et al., 2003). In short, each standard lead (except -aVR) with ≥ 0.1 mV ST elevation in the precordial leads, ≥ 0.05 mV in the limb leads, or abnormally tall T waves, were considered. An acuteness score (1–4) was assigned to each lead based on the presence or absence of a tall T wave or an abnormal Q wave, where 1 is least acute and 4 most acute. The final AW acuteness score was then calculated as the average score of the included leads.

2.4 | CMR image acquisition

The magnetic resonance image acquisition has been described earlier in detail (Khoshnood et al., 2018). In short, acquisition of imaging data was done with a Philips 1.5T Achieva or a Siemens 1.5T Avanto scanner.

First, scout images were acquired to locate the heart. For visualization of MaR, multi-slice and multi-phase contrast-enhanced (CE)-SSFP images were acquired covering the entire left ventricle. The CE-SSFP images were acquired approximately 5 min after intravenous administration of 0.2 mmol/kg of a gadolinium-based extracellular contrast agent (Dotarem, Gothia Medical, Billdal, Sweden). The slice thickness was 8 mm with no slice gap. In-plane resolution was typically 1.5×1.5 mm and the temporal resolution for the CE-SSFP images was 20–30 frames per cardiac cycle. For infarct visualization, late gadolinium enhancement (LGE) images corresponding to the CE-SSFP images were acquired approximately 15 min after injection of gadolinium. The LGE-images were acquired using an inversion-recovery gradient-recalled echo sequence with a slice thickness of 8 mm with no slice gap. In-plane resolution was typically 1.5×1.5 mm. Inversion time was manually adjusted to null the signal from viable myocardium.

2.5 | CMR image analysis

All quantitative CMR analysis was performed on short-axis images using the software Segment v.1.9 (<http://segment.heiberg.se>). MaR was calculated using contrast-enhanced (CE)-SSFP short-axis images for both scanners. This technique has previously been validated both experimentally and in the clinical settings (Nordlund et al., 2017; Sörensson et al., 2010). Endo- and epicardial borders were manually delineated in end-diastole (ED) and end-systole (ES) in all the CE-SSFP short-axis images. Areas with increased signal intensity were manually delineated as previously described (Sörensson et al., 2010). Infarct size was quantified from the LGE images using an automated computer algorithm taking partial volume effects into consideration (Heiberg et al., 2008). MaR and IS were expressed as a percentage of

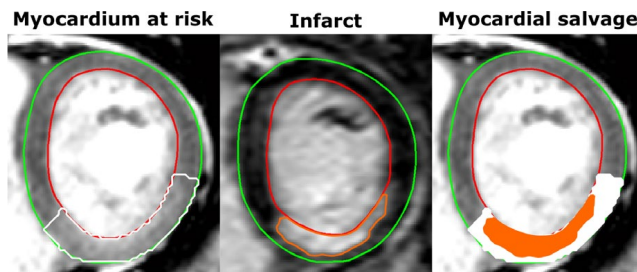


FIGURE 2 Co-localized mid-ventricular left ventricular slices showing myocardium at risk, infarction and myocardial salvage in a patient after myocardial injury caused by occlusion-reperfusion of the right coronary artery. Green lines delineate epicardium, red lines endocardium, white line myocardium at risk, and orange line infarction. In the image to the right, the infarct delineation has been superimposed upon the myocardium at risk delineation where salvaged myocardium is indicated in white

the left ventricular myocardium and the MSI was quantified as $(1-IS/MaR) \times 100\%$. Figure 2 shows an example of MaR, IS and MSI in a patient with an infarction in the right coronary artery (RCA) vessel territory.

For assessment of left ventricle ejection fraction (LVEF), endo- and epicardial borders were manually delineated in ED and ES in all the CE-SSFP short-axis images. LVEF (%) was calculated as $(100 \times [ED \text{ volume} - ES \text{ volume}] / ED \text{ volume})$.

2.6 | Statistical analysis

Visual evaluation of distribution as well as comparisons of mean to median was used to evaluate if data were normally distributed. For parameters not normally distributed, non-parametric tests were applied. Continuous data are expressed as median (range) and categorical variables as proportions. For correlations of IQP to data from CMR, Spearman's rank correlation coefficient was calculated. When adjusting for timing variables and AW-score, multivariate analysis was used. When comparing groups, the Mann-Whitney *U* test was used. All statistical tests were 2-tailed and a *p*-value of <0.05 was considered to indicate statistical significance. SPSS version 23.0 for Macintosh was used for the statistical analyses.

3 | RESULTS

Ninety-five patients from the SOCCER study population, with CMR examinations of diagnostic quality were subject for inclusion and out of those, 77 patients met STEMI criteria and were ultimately included in the study. Patient characteristics are described in Table 1.

Figure 3 shows example ECGs of patient without (a) and with (b) significant IQP. Median aIQP was 10 (0–115) ms (Table 2). No significant correlations were found between any CMR variable of myocardial injury and computer-generated QRSD, QRSD at max STD or aIQP (Table 3). QRS duration in the reference lead was similar on the acute ECG as on the discharge ECG recorded at 3.3 (1.6–15.2) days from PCI (80 ms [60–120 ms] vs 80 ms [50–100 ms], $p = 0.526$). Anderson-Wilkins score did not correlate to any IQP measure or CMR variable of myocardial injury. Adjusting for the acuteness of the ischemia according to the AW score did not change the results. Adjusting for time from pain onset to ECG or time from ECG to PCI did not affect the results either.

Sixty-seven patients (87%) had a Sclarovsky-Birnbaum ischemia grade of 2 (G2I) and nine patients (12%) had G3I. One patient had only ST-depressions could therefore not be assigned any ischemia grade (Billgren et al., 2004). There was no significant difference between the G2I and G3I groups regarding any measure of IQP or any of the CMR variables for myocardial injury (Table 4).

The J point was distinct in 48 patients and QRSD at max ST-deviation did not differ when using the J point as offset compared to the Almer method offset in these patients (94 [75–190 ms] vs 95 [77–200 ms]; $p = 0.305$).

TABLE 1 Baseline characteristics

	n	Median (Range) or n (%)
Age (years)	77	66 (33–86)
Gender (female)	77	27 (35)
Smoking	77	
Smoker		28 (37)
Ex-smoker		27 (36)
Never smoked		21 (28)
Co-morbidities	77	
Heart failure		0 (0)
Hypertension		29 (38)
Diabetes		10 (13)
CVI		3 (4)
Ischemic heart disease		1 (1)
Atrial fibrillation		1 (1)
CABG		0 (0)
Culprit artery (angiography)	75	
LAD		38 (51)
LCX		5 (7)
RCA		32 (43)
Time from pain onset to ECG (min)	68	70 (6–305)
Time from ECG to PCI (min)	77	94 (63–205)

Note. CABG: coronary artery bypass grafting; CVI: cerebrovascular injury; LAD: left anterior descending artery; LCX: left circumflex artery; RCA: right coronary artery.

4 | DISCUSSION

No correlations were found between IQP and CMR variables of myocardial injury in patients experiencing first-time STEMI. Furthermore, patients with G3I did not differ from G2I with regard to CMR markers of myocardial injury or IQP.

Several measures of the severity of ischemia in ACO have previously been suggested, such as the Sclarovsky-Birnbaum Ischemia Severity Grading System, (Birnbaum et al., 2014) and the morphology criteria of “tombstoning”, presented by Guo et al. (Guo, Yap, Chen, Huang, & Camm, 2000). QRS “tombstoning” morphology has been reported to correlate to mortality, in-hospital cardiogenic shock, ventricular tachycardia and ventricular fibrillation, in patients with anterior AMI (Balci, 2009). Furthermore, Sclarovsky-Birnbaum G3I has been correlated to IS (acute and at 4 months post STEMI), impaired myocardial salvage, and reperfusion injury (Birnbaum et al., 2014; Hassell et al., 2016; Rommel et al., 2016). Thus, although markers of terminal QRS distortion have been shown to be related to myocardial injury, IQP or G3I show no such correlation in the current study. Almer et al. (Almer et al., 2016) have previously shown a mean aIQP of 49 ± 57 ms (mean \pm SD), in patients with a controlled experimental total coronary occlusion, compared to the median of 10 ms within the current study. This could potentially be explained

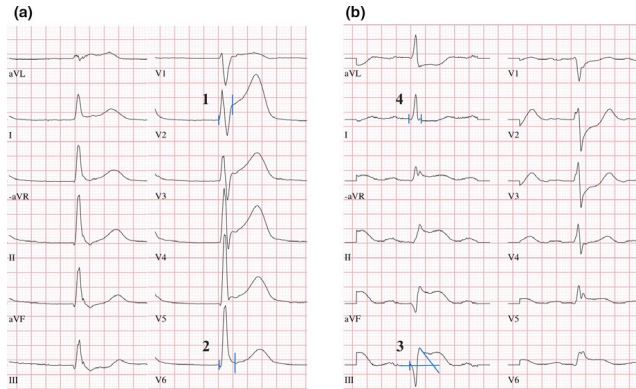


FIGURE 3 Electrocardiography examples from a patient with a LAD occlusion (a) and a patient with an RCA occlusion (b). (a) Twelve-lead ECG with maximum ST-deviation in lead V2 (1) of 0.525 mV. Since there is a distinguished J-point, it is used as offset, resulting in a QRS duration at maximum ST deviation of 90 ms. Lead V6 (2) was used as a reference, showing a QRS duration of 85 ms, resulting in an absolute ischemic QRS prolongation of 5 ms. (b) Twelve-lead ECG with maximum ST-deviation in lead III (3) of 0.425 mV. Since no clear j point can be determined, the intersect method for QRS duration was applied, resulting in a QRS duration at maximum ST deviation of 150 ms. Lead I (4) was used as a reference, showing a QRS duration of 82 ms, resulting in an absolute ischemic QRS prolongation of 65 ms

TABLE 2 Main variables

	n	Median (range)
MaR/LV mass (%)	77	31 (8–57)
IS (%)	77	15 (0–43)
MSI (%)	77	47 (3–100)
LVEF (%)	76	48 (29–73)
Computer-generated QRS duration (ms)	74	95 (76–152)
Reference QRS duration (ms)	77	80 (60–120)
QRS duration at max ST-deviation (ms)	77	95 (75–200)
Absolute IQP (ms)	77	10 (0–115)
Anderson-Wilkins acuteness score (1–4)	77	3.0 (1.0–4.0)

Note. IQP: ischemic QRS prolongation; IS: infarct size; LV: left ventricular; LVEF: left ventricular ejection fraction; MaR: myocardium at risk; MSI: myocardial salvage index.

TABLE 3 Spearman correlations for aIQP

	Correlation coefficient	p-value
MaR/LV mass (%)	−0.02	0.89
IS (%)	0.03	0.80
MSI (%)	−0.05	0.68
LVEF (%)	−0.16	0.34

Note. aIQP: absolute ischemic QRS prolongation; IS: infarct size; LV: left ventricular; LVEF: left ventricular ejection fraction; MaR: myocardium at risk; MSI: myocardial salvage index.

TABLE 4 Mann-Whitney test for Sclarovsky-Birnbaum ischemia grade 2 vs 3

	p-value
Computer-generated QRS duration	0.32
QRS duration at max ST-deviation	0.17
Absolute IQP	0.14
MaR	0.79
IS	0.46
MSI	0.24
LVEF	0.42

Note. IQP: ischemic QRS prolongation; MaR: myocardium at risk; IS: infarct size; MSI: myocardial salvage index; LVEF: left ventricular ejection fraction.

by less severe ischemia in the current study population. In comparison, a 2016 study by Rommel et al. (Rommel et al., 2016) found that G3I was correlated to IS, impaired MSI, and reperfusion injury in a STEMI population. The Rommel cohort consisted of 572 patients of which 186 (32%) had G3I, compared to 9 patients (12%) in the current study. Thus, the study population in the present study seems to differ with regards to the frequency of ischemia-related terminal QRS changes.

The findings in present study suggest that IQP is of limited use in the clinical context of ACO. It would, however, be of clinical importance to investigate if IQP could be used as an indicator of severe ischemia in the pre-hospital setting, when the patient is earlier in the ischemic injury process, which more resembles the experimental situation where IQP has been shown to be useful (Almer et al., 2016).

4.1 | Limitations

The results must be viewed in the light of several limitations. First, the small sample size could mean that the study was too underpowered to detect any correlation between IQP and CMR markers. Second, the ECG waveforms change as the infarct evolve which complicates the interpretation of the analysis. There are several factors that can have an effect on the infarct evolution; opening and closing of the culprit artery because of vasospasm, (Lanza, Careri, & Crea, 2011) lysing of the thrombus at the obstruction point, downstream embolic obstruction and hypotension impacting flow in the culprit artery but also in other diseased but non-obstructed arteries which may be suppliers of collaterals. Thus, an ECG obtained at a certain time point pre-PCI in this dynamic pathophysiological evolutionary process might not reflect the overall disease state and lead to misinterpretation of the severity of ischemia. Third, although there was a maximum time of 6 hr between pain onset and the analyzed ECG, this period varied among the patients. Thus, if the ECG was recorded late in the infarct evolution process, it is possible that severe ischemia, initially causing significant IQP, has resulted in infarction and less IQP at the time of the recording. In order to try to compensate for this, the AW acuteness score was assessed but did not change the results. Fourth, time from ECG to PCI varied. Adjusting the correlation between IQP and MSI with this time did, however, not change the results. Fifth, two methods were used for estimating the QRS complex offset, either with a distinct J point or using the "Almer method". As shown in simulation studies, the end of depolarization can be shifted to the ST segment even when the J point is distinct (Bacharova, Szathmary, & Mateasik, 2013). However, QRS duration at max ST-deviation did not differ between the two methods in the present study.

5 | CONCLUSION

Unlike previous experimental studies, there was only a small IQP in patients presenting at the emergency room with first-time STEMI and no correlation was found between IQP and CMR variables of myocardial injury in these patients. Therefore, IQP does not seem to be a suitable biomarker for triaging patients in this clinical context.

ORCID

Jakob Almer  <http://orcid.org/0000-0003-0462-0410>

REFERENCES

- Almer, J., Jennings, R. B., Maan, A. C., Ringborn, M., Maynard, C., Pahlm, O., ... Engblom, H. (2016). Ischemic QRS prolongation as a biomarker of severe myocardial ischemia. *Journal of Electrocardiology*, 49(2), 139–147. <https://doi.org/10.1016/j.jelectrocard.2015.12.010>
- Bacharova, L., Szathmary, V., & Mateasik, A. (2013). QRS complex and ST segment manifestations of ventricular ischemia: The effect of regional slowing of ventricular activation. *Journal of Electrocardiology*, 46(6), 497–504. <https://doi.org/10.1016/j.jelectrocard.2013.08.016>
- Balci, B. (2009). Tombstoning ST-elevation myocardial infarction. *Current Cardiology Reviews*, 5(4), 273–278. <https://doi.org/10.2174/157340309789317869>
- Bilgiren, T., Birnbaum, Y., Sgarbossa, E. B., Sejersten, M., Hill, N. E., Engblom, H., ... Wagner, G. S. (2004). Refinement and interobserver agreement for the electrocardiographic Sclarovsky-Birnbaum Ischemia Grading System. *Journal of Electrocardiology*, 37(3), 149–156. <https://doi.org/10.1016/j.jelectrocard.2004.02.005>
- Birnbaum, G. D., Birnbaum, I., & Birnbaum, Y. (2014). Twenty years of ECG grading of the severity of ischemia. *Journal of Electrocardiology*, 47(4), 546–555. <https://doi.org/10.1016/j.jelectrocard.2014.02.003>
- Elmberg, V., Almer, J., Pahlm, O., Wagner, G. S., Engblom, H., & Ringborn, M. (2016). A 12-lead ECG-method for quantifying ischemia-induced QRS prolongation to estimate the severity of the acute myocardial event. *Journal of Electrocardiology*, 49(3), 272–277. <https://doi.org/10.1016/j.jelectrocard.2016.02.001>
- García-Rubira, J. C., Nuñez-Gil, I., García-Borbolla, R., Manzano, M. C., Fernandez-Ortiz, A., Cobos, M. A., ... Macaya, C. (2008). Distortion of the terminal portion of the QRS is associated with poor collateral flow before and poor myocardial perfusion after percutaneous revascularization for myocardial infarction. *Coronary Artery Disease*, 19(6), 389–393. <https://doi.org/10.1097/MCA.0b013e328300d4bb>
- Guo, X. H., Yap, Y. G., Chen, L. J., Huang, J., & Camm, A. J. (2000). Correlation of coronary angiography with "tombstoning" electrocardiographic pattern in patients after acute myocardial infarction. *Clinical Cardiology*, 23(5), 347–352. <https://doi.org/10.1002/clc.4960230508>
- Hassell, M. E. C. J., Delewi, R., Lexis, C. P. H., Smulders, M. W., Hirsch, A., Wagner, G., ... Nijveldt, R. (2016). The relationship between terminal QRS distortion on initial ECG and final infarct size at 4 months in conventional ST-segment elevation myocardial infarction patients. *Journal of Electrocardiology*, 49(3), 292–299. <https://doi.org/10.1016/j.jelectrocard.2016.03.009>
- Heden, B., Ripa, R., Persson, E., Song, Q., Maynard, C., Leibbrandt, P., ... Wagner, G. S. (2003). A modified Anderson-Wilkins electrocardiographic acuteness score for anterior or inferior myocardial infarction. *American Heart Journal*, 146(5), 797–803. [https://doi.org/10.1016/S0002-8703\(03\)00404-6](https://doi.org/10.1016/S0002-8703(03)00404-6) [pii]
- Hedström, E., Engblom, H., Frogner, F., Aström-Olsson, K., Ohlin, H., Jovinge, S., & Arheden, H. (2009). Infarct evolution in man studied in patients with first-time coronary occlusion in comparison to different species - implications for assessment of myocardial salvage. *Journal of Cardiovascular Magnetic Resonance*, 11(1), 38. <https://doi.org/10.1186/1532-429X-11-38>
- Heiberg, E., Ugander, M., Engblom, H., Götborg, M., Olivecrona, G. K., Erlinge, D., & Arheden, H. (2008). Automated quantification of myocardial infarction from MR images by accounting for partial volume effects: Animal, phantom, and human study. *Radiology*, 246(2), 581–588. <https://doi.org/10.1148/radiol.2461062164>
- Khoshnood, A., Carlsson, M., Akbarzadeh, M., Bhiladvala, P., Roijer, A., Nordlund, D., ... Ekelund, U. (2018). Effect of oxygen therapy on myocardial salvage in ST elevation myocardial infarction: The randomised SOCCER trial. *European Journal of Emergency Medicine*, 25(2), 78–84. <https://doi.org/10.1097/MEJ.0000000000000431>
- Kumar, A., & Cannon, C. P. (2009). Acute coronary syndromes: Diagnosis and management, part I. *Mayo Clinic Proceedings*, 84, 917–938. <https://doi.org/10.4065/84.10.917>
- Lanza, G. A., Careri, G., & Crea, F. (2011). Mechanisms of coronary artery spasm. *Circulation*, 124, 1774–1782. <https://doi.org/10.1161/CIRCULATIONAHA.111.037283>

- Lopez, A. D., Mathers, C. D., Ezzati, M., Jamison, D. T., & Murray, C. J. (2006). Global and regional burden of disease and risk factors, 2001: Systematic analysis of population health data. *Lancet*, 367(9524), 1747–1757. [https://doi.org/10.1016/S0140-6736\(06\)68770-9](https://doi.org/10.1016/S0140-6736(06)68770-9)
- Martin, T. N., Groenning, B. A., Murray, H. M., Steedman, T., Foster, J. E., Elliot, A. T., ... Wagner, G. S. (2007). ST-Segment deviation analysis of the admission 12-lead electrocardiogram as an aid to early diagnosis of acute myocardial infarction with a cardiac magnetic resonance imaging gold standard. *Journal of the American College of Cardiology*, 50(11), 1021–1028. <https://doi.org/10.1016/j.jacc.2007.04.090>
- Nordlund, D., Kanski, M., Jablonowski, R., Koul, S., Erlinge, D., Carlsson, M., ... Arheden, H. (2017). Experimental validation of contrast-enhanced SSFP cine CMR for quantification of myocardium at risk in acute myocardial infarction. *Journal of Cardiovascular Magnetic Resonance*, 19(1), 12. <https://doi.org/10.1186/s12968-017-0325-y>
- Reed, G. W., Rossi, J. E., & Cannon, C. P. (2017). Acute myocardial infarction. *Lancet*, 389(10065), 197–210. [https://doi.org/10.1016/S0140-6736\(16\)30677-8](https://doi.org/10.1016/S0140-6736(16)30677-8)
- Rommel, K.-P., Badarnih, H., Desch, S., Gutberlet, M., Schuler, G., Thiele, H., & Eitel, I. (2016). QRS complex distortion (Grade 3 ischaemia) as a predictor of myocardial damage assessed by cardiac magnetic resonance imaging and clinical prognosis in patients with ST-elevation myocardial infarction. *European Heart Journal Cardiovascular Imaging*, 17(2), 194–202. <https://doi.org/10.1093/ehjci/jev135>
- Sörensson, P., Heiberg, E., Saleh, N., Bouvier, F., Caidahl, K., Tornvall, P., ... Arheden, H. (2010). Assessment of myocardium at risk with contrast enhanced steady-state free precession cine cardiovascular magnetic resonance compared to single-photon emission computed tomography. *Journal of Cardiovascular Magnetic Resonance*, 12(1), 25. <https://doi.org/10.1186/1532-429X-12-25>
- Surawicz, B., Orr, C. M., Hermiller, J. B., Bell, K. D., & Pinto, R. P. (1997). QRS changes during percutaneous transluminal coronary angioplasty and their possible mechanisms. *Journal of the American College of Cardiology*, 30(2), 452–458. [https://doi.org/10.1016/S0735-1097\(97\)00165-4](https://doi.org/10.1016/S0735-1097(97)00165-4)
- Valle-Caballero, M. J., Fernández-Jiménez, R., Díaz-Munoz, R., Mateos, A., Rodríguez-Álvarez, M., Iglesias-Vázquez, J. A., ... Ibanez, B. (2016). QRS distortion in pre-reperfusion electrocardiogram is a bedside predictor of large myocardium at risk and infarct size (a METOCARD-CNIC trial substudy). *International Journal of Cardiology*, 202, 666–673. <https://doi.org/10.1016/j.ijcard.2015.09.117>
- Wagner, G. S., Macfarlane, P., Wellens, H., Josephson, M., Gorgels, A., Mirvis, D. M., ... Gettes, L. S. (2009). AHA/ACC/HRS Recommendations for the standardization and interpretation of the electrocardiogram, Part VI: Acute ischemia/infarction. *Journal of the American College of Cardiology*, 53(11), 1003–1011. <https://doi.org/10.1016/j.jacc.2008.12.016>
- Weaver, J. C., Rees, D., Prasan, A. M., Ramsay, D. D., Binnekamp, M. F., & McCrohon, J. A. (2011). Grade 3 ischemia on the admission electrocardiogram is associated with severe microvascular injury on cardiac magnetic resonance imaging after ST elevation myocardial infarction. *Journal of Electrocardiology*, 44(1), 49–57. <https://doi.org/10.1016/j.jelectrocard.2010.09.013>

How to cite this article: Almer J, Elmerg V, Bränsvik J, et al. Ischemic QRS prolongation as a biomarker of myocardial injury in STEMI patients. *Ann Noninvasive Electrocardiol*. 2018;e12601. <https://doi.org/10.1111/anec.12601>



Jakob Almer, MD, was born in 1989. He grew up in Ystad, Skåne, attended the International Baccalaureate at Malmö Borgarskola and later went to medical school at Lund University. He graduated in 2015 and currently works full-time as resident physician in Anaesthesiology and Intensive Care at Skåne University Hospital.

Jakob did not plan for a PhD but due to his interest in cardiac electrophysiology and the IQP concept, which was born out of a collaboration with Dr. Galen Wagner and Henrik Engblom, he grew into the idea. After doing 4 years full time research mostly during weekends and evenings while also working as a physician full

time, this is the result. The thesis is a proof of concept of the IQP method, with potential of predicting and preventing cardiac arrests.

Apart from his professional life, Jakob values family life above all. He lives in the middle of Skåne with his loving wife and two young children.